UiT
THE ARCTIC UNIVERSITY OF NORWAY

Department of Pharmacy, Faculty of Health Sciences

Development of a homologous gene replacement approach to study ciprofloxacin resistance in clinical *Escherichia coli* isolates

Sanne Ekroll Valla

Thesis for the degree Master of Pharmacy, May 2017

Supervisor: Nicole L. Podnecky, Ph.D.
Assistant supervisors: Professor Pål J. Johnsen, Ph.D
Elizabeth G. A. Fredheim, Ph.D

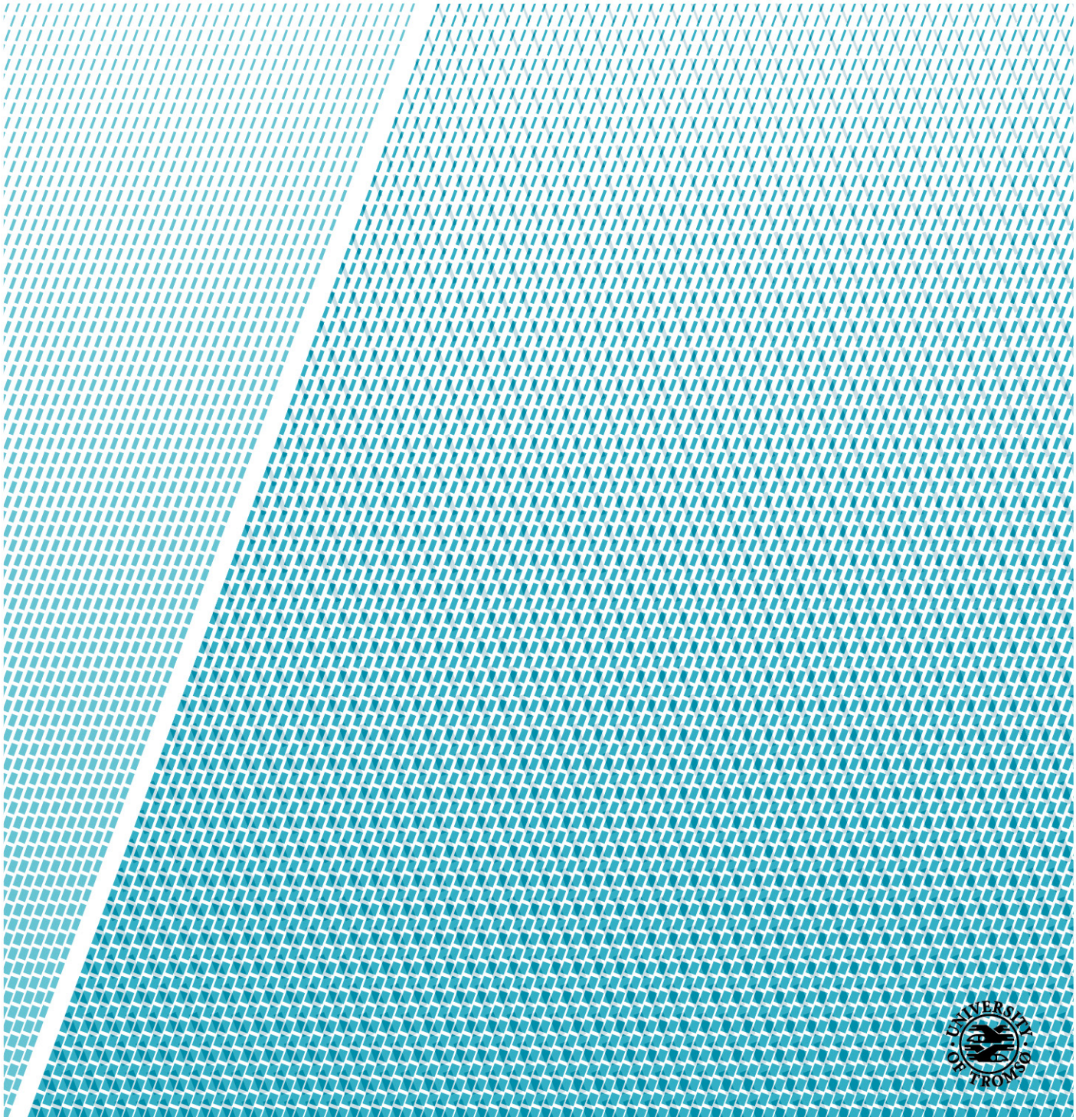

Abstract

Urinary tract infections are common amongst infectious diseases in humans, and often these infections are caused by uropathogenic *Escherichia coli*. Effective antimicrobial treatment of infections are medical achievements that should not be taken for granted, as antimicrobial resistance has developed and causes treatments to become ineffective. Further, resistance traits can be spread between unrelated bacteria through mechanisms such as conjugation, where plasmids (mobile genetic elements) are potential carriers of multidrug resistance traits.

Treatment strategies outside the production of novel antimicrobial drugs are being investigated. Collateral sensitivity is an example of a treatment strategy that specifically targets resistant bacteria. By gaining antimicrobial resistance to an initial drug, susceptibility towards other antimicrobials can increase due to the initial resistance.

The aim of this project was to develop a homologous gene replacement approach to introduce or repair defined mutations known to cause ciprofloxacin resistance in *Escherichia coli*. This would enable investigation of the effects specific resistance-causing mutations have on collateral susceptibility changes in different strain backgrounds. Methods of traditional cloning by ligation, as well as the more modern isothermal cloning method, were used to build constructs that would replace the original genomic target by homologous gene replacement.

While we were able to build gene constructs with defined mutations by isothermal cloning, moving these constructs into integrative plasmids for homologous gene replacement proved challenging. However, one construct was ligated into an integrative plasmid, but has yet to be transferred by conjugation to the clinical isolate of interest. Ultimately, we were able to design and optimize several cloning approaches to introduce or repair mutations, but further work is necessary to enable the efficient use of homologous gene replacement in the future.

Acknowledgements

I would like to thank all the members of the Microbial Pharmacology and Population Biology Research Group (MicroPop). It has been nine educational months while working with this project in the MicroPop laboratory, at the Department of Pharmacy, UiT.

I want to express my greatest gratitude to my supervisor Dr. Nicole L. Podnecky, for giving me excellent guidance throughout this project, both during laboratory work and during the writing of this thesis.

Also, I am grateful to my assistant supervisors, Pål J. Johnsen and Elizabeth G. A. Fredheim, for being available and supportive, and for giving me final feedback on this thesis.

Last, but not least, I appreciate my family and friends for all their support.

Sanne Ekroll Valla

Tromsø, 15th of May 2017

Table of contents

List of Tables and Figures ..... Feil! Bokmerke ikke definert.

List of Abbreviations ..... **VIII**

Chapter 1: Introduction **1**

1.1 Escherichia coli *1*

1.2 Urinary Tract Infections and Treatment *2*

1.3 Antimicrobial Agents *2*

1.3.1 Ciprofloxacin – Mechanism of Action 6

1.4 Antimicrobial Resistance *6*

1.4.1 Detecting Antimicrobial Resistance 7

1.4.2 Mechanisms of Antimicrobial Resistance 8

1.4.3 Ciprofloxacin-resistance 9

1.4.4 Antimicrobial Resistance Development 10

1.4.5 AMR – A Global Problem 12

1.5 Collateral Sensitivity *14*

1.5.1 Collateral Sensitivity in Ciprofloxacin Resistant Mutants 14

1.6 Homologous Gene Replacement *16*

1.7 Study Aims *18*

1.8 Hypothesis *18*

Chapter 2: Material and Methods **19**

2.1 Bacterial Strains *19*

2.2 Plasmids *19*

2.3 Media Preparation and Growth Techniques *20*

2.3.1 Solid Growth Media 20

2.3.2 Plating of Cells on Solid Growth Media 21

2.3.3 Liquid Growth Media 21

2.3.4 Preparation of Glycerol Freeze Stocks 22

2.4 Isolation of Genomic DNA *22*

2.5 Plasmid Isolation *23*

2.6 Quantification of DNA *24*

2.7 Restriction Endonuclease Digestion *24*

2.8 Polymerase Chain Reaction *25*

2.8.1 PCR Primer Design 27

2.9 Gel Electrophoresis *27*
2.10 Gel Extraction *28*
2.11 DNA Sequencing *29*
2.12 Molecular Cloning *30*
2.12.1 Zero Blunt® PCR Cloning 30
2.12.2 pGEM®-T Easy Cloning 32
2.12.3 Isothermal Assembly Cloning 34
2.12.4 Cloning with Restriction Endonucleases 36
2.13 Transformation of Plasmids into Chemically-Competent E. coli *37*
2.14 Conjugation (Bi-parental Mating) *38*
2.15 Antimicrobial Susceptibility Testing *39*
Chapter 3: Experimental Results and Discussion **41**
3.1 A HGR Approach to Introduce or Repair gyrA and parC Mutations *41*
3.2 Cloning and Troubleshooting *42*
3.2.1 Building Homologous Gene Replacement Constructs 42
3.2.2 Cloning *gyrA* and *parC* Constructs into pDS132 by ITAC 52
3.2.3 Molecular Cloning of *gyrA* and *parC* Constructs into pEX6K 60
3.3 Conjugation of pEX6K-derivatives into ECO-SENS Strains *65*
3.3.1 Susceptibility Testing of WT ECO-SENS Strains 66
Chapter 4: Concluding Remarks and Future Aspects **68**
References **69**
Attachments **1**

Table 1: Table of *E.coli* strains used in this project. 19
Table 2: Plasmid vectors and respective properties. 20
Table 3: Recipes for solid media. 21
Table 4: Recipe for restriction digests. 25
Table 5: PCR master mix for one 25 µL PCR. 26
Table 6: Sequencing reaction contents. 29
Table 7: Reaction recipe for ligation with pCR®-Blunt. 31
Table 8: Reaction recipe for ligation into pGEM® T-easy vector. 33
Table 9: ITAC master mix. 36
Table 10: Results from ITAC purification optimization. 58

Table A 1: Antimicrobials and chemicals added to growth media. 1
Table A 2: Table of plasmids constructed in this project 1
Table A 3: Primers (oligonucleotides) used in this project. 5
Table A 4: Restriction endonucleases and corresponding buffers. 6

Figure 1: Illustration of antimicrobial drug targets and mechanisms of resistance within a bacterium 3
Figure 2: Heat map of Ciprofloxacin mutants and Collateral Changes. 15
Figure 3: Illustration of Homologous Gene Replacement (HGR). 17
Figure 4: Plasmid map of pCR-Blunt (3512 bp). 30
Figure 5: Plasmid map of pGEM®-T Easy (3015bp). 32
Figure 6: Illustration of ITAC reaction. 35
Figure 7: Amount of MHB added to the 96-well plate in a 2-fold IC_{90} set up. 40
Figure 8: Flow chart of general outline in HGR approach. 42
Figure 9: Sequence comparison between *gyrA* and *parC* genes 43
Figure 10: Image of *gyrA* and *parC* genes. 44
Figure 11: Confirmation of pCR-Blunt-*gyrA* and pCR-Blunt-*parC* plasmids. 46
Figure 12: Image of pSV-1 to pSV-11 plasmids with gyrA/*parC* gene inserts 47
Figure 13: Image of pSV-19 to pSV-22 after *Eco*RI digest. 49
Figure 14: Image of pSV-23 after *Eco*RI digest. 51
Figure 15: Plasmid map of pDS132 (5286 bp). 52

Figure 16: Image of PCR products from plasmids pSV-13, pSV-19 and pSV-20, and pDS132 after digestion with *Xba*I. 53
Figure 17: Image of PCR products from plasmids pSV-15, pSV-21 and pSV-24, and pDS132 after digestion with *Xba*I. 54
Figure 18: Flow chart of attempts made to clone HGR constructs into pDS132 60
Figure 19: Plasmid map of pEX6K (7298 bp). 61
Figure 20: Image of pSV-25 to pSV-30 after digestion with *NotI* 63
Figure 21: Image of pSV-32, pEXKm5 and pEX6K after sequential digestion 65

Figure A 1: Smart Ladder *MW-1700-10* 7
Figure A 2: Image of pCR-Blunt-*gyrA* and pCR-Blunt-*parC* plasmids 7
Figure A 3: Image of pSV-13 to pSV-16 plasmids with *gyrA*/parC gene inserts 8
Figure A 4: Image of PCR products from plasmids pSV-11, pSV-2, pSV-3. 8
Figure A 5: Image of PCR products from plasmids pSV-11, pSV-2, pSV-3. 9
Figure A 6: Image of PCR products from plasmids pSV-5, pSV-7, and (repeated) pSV-2 9
Figure A 7: Image of PCR products from plasmids pSV-9. 10
Figure A 8: Image of PCR products from plasmids pSV-7 and pSV-9. 10
Figure A 9: Image of PCR products from plasmid pSV-8. 11
Figure A 10: Image of pDS132 after repeated digestion with *Xba*I. 11
Figure A 11: Image after electrophoresis of expanded *Xba*I digest 12
Figure A 12: Image of PCR products of pDS132. 12
Figure A 13: Sequence results from pSV-13, pSV-19 and pSV-20. 13
Figure A 14: Sequence results from pSV-15, pSV-21 and pSV-24. 14

List of Abbreviations

A	adenine
ad	to
AMP	ampicillin
bp	base pair(s)
C	cytosine
CHL	chloramphenicol
CIP	ciprofloxacin
DAP	diaminopimelic acid
dH_2O	distilled water
DHF	dihydrofolate
DHP	dihydropteroate
DNA	deoxyribonucleic acid
dNTP	deoxynucleotide
E. coli	*Escherichia coli*
e.g.	for example (*exempli gratia*)
EtBr	ethidium bromide
ETEC	entetotoxigenic *Escherichia coli*
EtOH	ethanol
EUCAST	European Committee on Antimicrobial Susceptibility Testing

fmet-tRNA	formylmethionyl-transfer RNA
G	guanine
HGR	homologous gene replacement
HGT	horizontal gene transfer
IPTG	isopropyl β–D-1-thiogalactopyranoside
kbp	kilo base pair(s) 1 kbp = 1000 bp
KM	kanamycin
LB	Luria Bertani broth
MIC	minimum inhibitory concentration
mM	millimolar
mRNA	messenger-RNA
NEB	New England Biolabs
ng	nanogram
^{R}	resistant
RNA	ribonucleic acid
rpm	revolutions per minute
S.O.C.	super optimal broth with catabolite repression
sec(s)	second(s)
T	thymidine
UPEC	uropathogenic *Escherichia coli*
UTI	urinary tract infection

V	volt
WT	wild type
XGal	5-bromo-4-chloro-3-indolyl-β-D-galactopyranoside
ZN	zeocin

Chapter 1: Introduction

1.1 *Escherichia coli*

Bacteria are broadly categorized into two groups, Gram positive bacteria and Gram negative bacteria. Gram positive bacteria have a cell wall consisting of a thick peptidoglycan layer, whereas Gram negative bacteria have a phospholipid bilayer membrane that surrounds a thinner peptidoglycan-containing cell wall. *E. coli* are Gram negative, unpigmented, rod-shaped bacteria, and are defined as facultative anaerobes, because they grow optimally in the presence of oxygen, but have the ability to survive and still grow without oxygen.

E. coli was discovered in 1885, and is a commonly studied microorganism. The genome of *E. coli* varies in size and the GC-content is approximately 50 % (1). There are about 4700 genes in the *E. coli* genome that originate from a gene pool with at least 10 000 different genes (after eliminating all transposable elements and prophages) (2). Of these genes, 2000 are found in all *E. coli*, representing the core genome. The remaining about 2700 genes of the accessory genome vary between different strains of *E. coli*. Among the 2700 accessory genes could be genes that for instance encode cellular changes that would make the bacterium resistant to certain antimicrobials.

E. coli exist as a mutualistic contributor in our intestinal bacterial flora. But in addition to being a part of the normal bacterial flora in humans and many animals, some strains of *E. coli* are considered pathogenic, having the ability to cause disease. Large genetic diversity and changes in the accessory genome contribute to the broad spectrum of diseases caused by *E. coli*, including diseases that can vary from asymptomatic bacteriuria, to urosepsis and meningitis (3). Pathogenic *E. coli* can be grouped into several different pathotypes that commonly cause infection, *e.g.* enterotoxigenic *E. coli* (ETEC) and uropathogenic *E. coli* (UPEC) (3).

1.2 Urinary Tract Infections and Treatment

Urinary tract infections (UTIs) are the most common infectious diseases in humans (4). They are most often caused by bacteria from the intestinal tract that enter the urethral opening and colonize the urinary tract (5). Uropathogenic *E. coli* (UPEC) is the most common cause of UTIs and is responsible for approximately 80% of uncomplicated UTIs (5). UTIs are categorized by severity and ascent of the infection up the urinary tract, ranging from asymptomatic bacteriuria (bacteria in the urine), to cystitis (infection in the bladder), to pyelonephritis (infection in the kidneys), and urosepsis (infection in blood). Women are more susceptible to UTIs than men; this is due to the shorter anatomic distance between the urethral tract and the anus, and the length of the urethral tract itself. Approximately 50% of all women will have a UTI during their lifetime, the majority are uncomplicated cystitis (5).

The recommended treatment for a UTI varies with the severity of the disease, but there are several antimicrobial agents that are commonly used. For adults in primary care in Norway, trimethoprim, nitrofurantoin or pivmecillinam is prescribed for three days in cases of cystitis, while trimethoprim/sulfamethoxazole combination or pivmecillinam is prescribed for seven to ten days for treatment of pyelonephritis (6, 7). Ciprofloxacin (CIP) can be used in cases of pyelonephritis when initial treatment fails. However, the guidelines for antimicrobial treatment in Norway vary between the primary care and hospitals, where CIP is not used to treat pyelonephritis in hospitalized patients (8).

Even though Norwegian guidelines for treatment of UTIs does not include CIP as first line treatment, CIP is frequently prescribed for other indications, such as lower respiratory tract infections and pneumonia (9). According to the Norwegian prescription registry (Reseptregisteret), 948 279 defined daily doses of fluoroquinolones were prescribed in Norway in 2010 (10).

1.3 Antimicrobial Agents

Antimicrobial agents are compounds that have the ability to kill or prevent the growth of microorganisms, such as bacteria. Antibiotics are naturally produced from microorganisms, for instance penicillin, which is produced by the fungi *Penicillium chrysogenum* (previously

known as *Penicillium notatum*) (11). Since antibiotics are also antimicrobials per definition, the term antimicrobial can be used when describing both naturally occurring and synthetically derived germicides.

When antimicrobial drugs are used to inhibit or kill bacteria during the treatment of an infection, for the benefit of the patient, that antimicrobial should have a minimal effect on host cells. Ideally, antimicrobials have selective toxicity, where for example a specific antimicrobial drug target site is present in bacteria but is not found in mammalian cells. The antimicrobial would thereby only affect bacterial cells. Antimicrobials can be divided into groups based on the essential cellular processes that the drugs target as described in the sections below. See Figure 1 for illustration of common antimicrobial drug targets (and common mechanisms of resistance, which will be described in Section 1.4).

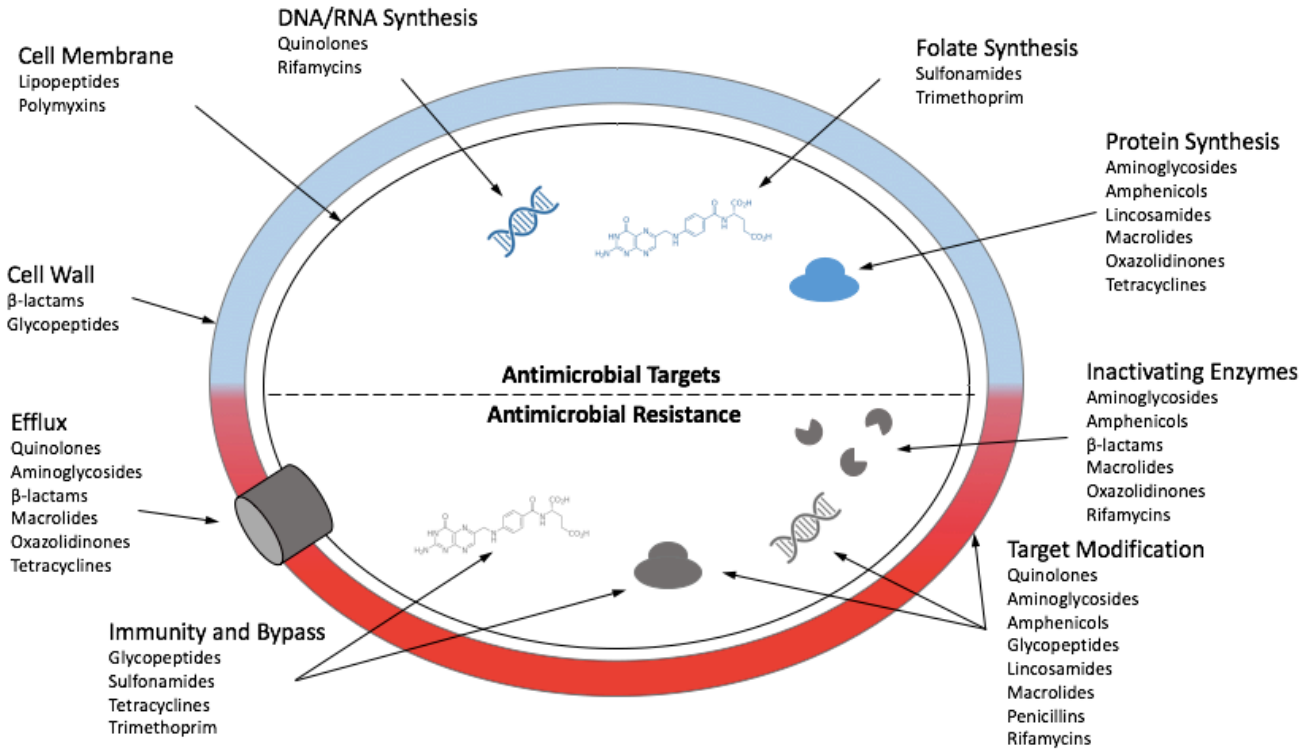

Figure 1: Illustration of antimicrobial drug targets and mechanisms of resistance within a bacterium. The relevant drug classes are listed below each target and resistance mechanism. Illustration based on paper by Wright, 2010 (12) and Walsh, 2000 (13).

Inhibition of cell wall synthesis

The function of the cell wall is to maintain the shape of the cell, and to delineate the cell from its outer environment while preserving osmotic pressure inside the cell (14). The cell wall of both Gram negative and Gram positive bacteria is composed of cross-linked peptidoglycan, which is a unique component in the bacterial cell wall (15). Synthesis of peptidoglycan molecules occurs in the cytoplasm. The peptidoglycan is then moved across the cytoplasmic membrane before assembly occurs by a transpeptidation reaction, where penicillin-binding proteins (PBPs) are responsible for the final steps of peptidoglycan crosslinking (15).

ß-lactam antimicrobials (*e.g.* penicillins, cephalosporins and monobactams) possess similarities to a portion of the peptidoglycan structure that is bound by PBPs. ß-lactams act as competitive binders to PBPs and make a PBP-ß-lactam complex that is more stable than the naturally-occurring PBP-peptigoglycan complex. As a result, the transpeptidation reaction is irreversibly inhibited and peptidoglycan synthesis stops (14).

Similarly, glycopeptides bind to the site of peptidoglycan that binds to PBPs, and thereby inhibit the formation of a PBP-peptidoglycan complex. In this way, glycopeptides prevent the incorporation of subunits to the growing peptidoglycan molecule. However, because of the size of glycopeptide molecules, Gram negative bacteria like *E. coli* are intrinsically resistant to glycopeptides (14), a phenomenon that will be discussed more in Section 1.4.

Inhibition of folate synthesis

Some components of bacterial folate biosynthesis are antimicrobial drug targets. However both prokaryotes and eukaryotes require folates and/or their cofactors for several important cellular and metabolic processes, including the synthesis of nucleotides, of which deoxyribonucleic acid (DNA) is build (16). Selective toxicity of antimicrobials towards the bacterial components of folate synthesis exists because folates are essential vitamins that humans do not produce on their own and must instead get from dietary intake, while bacteria have their own folate synthesis pathways (17).

Sulfamethoxazole specifically inhibits the activity of dihydropteroate (DHP) synthase, an enzyme responsible for the production of 7,8-dihydropteroate from DHP and p-aminobenzoic acid (18). Trimethoprim inhibits the activity of dihydrofolate (DHF) reductase, which reduces dihydrofolate to tetrahydrofolate (18). Sulfamethoxazole and trimethoprim are antimicrobial

drugs often used in combination because they target different components in the same folate synthesis pathway, giving a synergistic antimicrobial effect.

Inhibition of protein synthesis

The production of proteins is a necessary process for any living organism, and proteins can serve as *e.g.* drug receptors, transporter molecules and regulators of gene expression. In order to synthesize proteins, active genes are used as a template where RNA polymerases transcribe the information from the gene into messenger-RNA (mRNA). The mRNA is then bound by ribosomes and translated; where a ribosome reads the code of the mRNA, transfer RNA (tRNA) carry amino acids to the ribosome, and a specific amino acid chain is assembled by the ribosome (19).

Several components of protein synthesis in bacteria are drug targets for different groups of antimicrobials. The aminoglycosides, such as gentamicin, bind to specific proteins in the 30S ribosomal subunit. Further, they inhibit the binding of formylmethionyl-transfer RNA (fmet-tRNA) to the ribosome, which is essential for protein synthesis to begin (15). Tetracyclines also bind to the 30S ribosomal subunit and prevent aminoacyl tRNA to associate with the ribosome (20). Other antimicrobials, such as the amphenicols, lincosamides, oxazolidinones and macrolides, bind to the 50S ribosomal unit, inhibiting assembly of the amino acid chains (15).

Inhibition of nucleic acid synthesis

Nucleic acid synthesis includes assembling deoxyribonucleotides and ribonucleotides to form DNA and RNA, respectively. The production of new DNA occurs by making a copy of one of the strands from the original DNA sequence, and enzymatically adding the complementary nucleotide bases (19). Inhibitors of nucleic acid synthesis have the ability to stop the production of DNA prior to cell division and prevent the transcription of RNAs through different approaches. Rifamycins binds to the RNA polymerase, blocking the synthesis of messenger-RNA (mRNA) (15). The quinolones, such as ciprofloxacin, inhibits DNA replication by targeting topoisomerases, which will be discussed further in the next section, as ciprofloxacin is a central antimicrobial drug in this study.

1.3.1 Ciprofloxacin – Mechanism of Action

Ciprofloxacin (CIP) is a quinolone-class, synthetically-produced antimicrobial that is effective against a broad spectra of bacteria, which is reflected in its frequent use (21). CIP is an antimicrobial that inhibits DNA replication in bacteria by inhibition of specific topoisomerases, DNA gyrase (topoisomerase II) and topoisomerase IV (22). These topoisomerases are important for the correct unwinding of the DNA molecule before replication can proceed. Specifically, DNA gyrase is an enzyme that introduces negative superhelical turns into the positive superhelical DNA (22). DNA gyrase is composed of four proteins, two subunits of GyrA and two subunits of GyrB, which are encoded for by the *gyrA* and *gyrB* genes, respectively. Topoisomerase IV is an enzyme that removes the interlinking of daughter chromosomes, allowing segregation of the DNA into daughter cells at the end of cell division. Topoisomerase IV consists of two subunits of both ParC and ParE (22). CIP specifically blocks the activity of DNA gyrase and topoisomerase IV by stabilizing CIP-enzyme-DNA complexes, which results in conformational changes to both the enzymes and the DNA (22). The CIP-enzyme-DNA complexes are reversible, but as they result in breaks in the double stranded DNA, the effect of CIP is considered bactericidal, as it induces killing of the bacteria. The absence of functioning DNA gyrase and topoisomerase IV would then inhibit replication and DNA repair processes within the bacteria (23).

1.4 Antimicrobial Resistance

Antimicrobial resistance (AMR) is a phenomenon where a microbe has the ability to survive antimicrobial action, and is no longer susceptible or inhibited by the antimicrobial drug. Determination of susceptibility is needed in order to identify bacteria as either sensitive, intermediate or resistant to specific antimicrobial drugs. According to “Helsebiblioteket”, a clinical definition widely used is that a bacterial strain is resistant when tolerating a concentration of an antimicrobial drug that is higher than the highest achievable drug concentration at the infectious site, indicating a high risk of therapeutic failure (24).

Antimicrobial susceptibility can be expressed as the minimal drug concentration to inhibit visible bacterial growth, the minimum inhibitory concentration (MIC) (25). MIC values from

various bacterial populations of the same species can be used to inform clinical breakpoints – the specific drug concentrations where an isolate of this species usually is killed or growth is inhibited. Clinicians can use the clinical breakpoints to indicate dose sizes during antimicrobial drug treatment, but the breakpoints can also be used to determine if a strain is susceptible, intermediate or resistant when tested with antimicrobials in a laboratory.

The European Committee on Antimicrobial Susceptibility Testing (EUCAST) gathers MIC data from experiments done around the world. By collecting values from international studies, *e.g.* the ECO-SENS studies, they have produced graphs and tables displaying values of clinical breakpoints for specific strains in presence of antimicrobial drugs (26). From further analysis of this data they offer a public database with epidemiological cut-off (ECOFF) values which indicates the highest MIC value(s) within WT populations (27). This can be helpful for monitoring resistance development over large geographical areas.

1.4.1 Detecting Antimicrobial Resistance

There are several tests that can be performed on bacteria to determine their susceptibility towards antimicrobials. These include agar dilution, macro- and microbroth dilution, gradient strip diffusion (*e.g.* E-test®) and disk diffusion methods.

Agar dilution is set up by making agar plates containing specific antimicrobial drug concentrations along a two-fold scale. Bacteria are then applied to the antimicrobial containing solid agar, and the MIC is the concentration in the plate where the drug inhibits bacterial growth (25). Similar to the agar dilution method, the macrobroth dilution is set up by making a gradient of antimicrobial drug concentrations, but in liquid broth instead of solid agar (25). An advantage to the agar dilution method is that several strains can be tested on one plate, while only a single strain can be added to a liquid culture. In the microbroth dilution method, a tray with typically 96 wells of ~200 µL is filled with broth containing antimicrobial(s), again at a range of drug concentrations. Using the tray of wells enables testing several strains on one tray, but the set up can also be several antimicrobial drugs that gets tested with one bacterial strain, or one antimicrobial drug at a very wide range of concentrations.

Also for testing the susceptibility towards antimicrobials, a bacterial strain can be spread on an agar plate, and disks or strips containing antimicrobial drugs can be added to the plate. For the gradient strip diffusion test, a plastic/paper strip containing an antimicrobial drug is applied to the plate with bacteria (25). The strip contains a drug-gradient that diffuses into the agar, and a scale is marked on the upper surface of the strip, making it possible to read the MIC where the bacteria stops to grow. Similarly, in the disk diffusion test, a paper disk containing the antimicrobial drug is applied to a plate containing bacteria. The disk has a specific drug concentration which creates a gradient in the agar as it diffuses into the medium (25). The disk diffusion method does not result in a MIC value, but inhibition of growth is analyzed by measuring the diameter of the inhibition zone (area around the disk where bacteria do not grow), relative to the time drug has diffused. The disk diffusion test can always be used as a qualitative measure of whether the bacteria is sensitive, intermediate or resistant, but also an approximate MIC can be calculated based on the result of the disk diffusion test (25).

1.4.2 Mechanisms of Antimicrobial Resistance

Some antimicrobial agents are naturally ineffective against particular bacteria; hence the bacteria are intrinsically resistant to the antimicrobial. An example is where Gram negative bacteria are intrinsically resistant to glycopeptides, since the glycopeptide-molecules are too large to efficiently move through the outer phospholipid membrane and reach its target, the peptidoglycan (28). Alternatively, some bacteria naturally lack the antimicrobial drug target completely, and therefore are not affected by the antimicrobial drug. This is the scenario with *E. coli* and the lipopeptide drug daptomycin, where *E. coli* lacks the drug target site in the cytoplasmic membrane (29).

Contrary to intrinsic resistance, resistance can be acquired by bacteria, making previously useful antimicrobials ineffective. Common mechanisms of AMR can be grouped in three major categories; specific target mutations, enzymatic inactivation and general mechanisms, *e.g.* permeability modification (13). Specific mutations that alter the drug target, preventing the antimicrobial agent from binding or affecting the target, can cause resistance. Mutations can also occur in the promoter of a target, leading to an overexpression of the target, demanding an increase in antimicrobial molecules to be effective.

Some bacteria possess genes encoding specific proteins that can enzymatically modify or inactivate an antimicrobial agent; for example bacteria that produce the ß-lactam degrading enzyme, ß-lactamase (15). Finally, altering the membrane permeability, and thereby reducing the amount of drug that reach the cytoplasm, can cause resistance (13). This could happen either by reducing the uptake of drug into the cell, or by increasing the elimination of drug through active efflux. See Figure 1, for illustration of common antimicrobial targets and resistance mechanisms.

1.4.3 Ciprofloxacin-resistance

Resistance to CIP occurs in bacteria through two of the mechanisms mentioned above; alterations in the drug target and alterations in the membrane permeability (22). Mutations that encode for alterations to the drug targets, DNA gyrase and topoisomerase IV, are frequently observed. Mutations in *gyrA* are generally reported more often than in *gyrB*, while *parC* mutations have been found in clinical isolates of *E. coli* with high level of resistance and are more common than *parE* mutations (22). Often topoisomerase IV acts as a primary drug target in Gram positive bacteria, and DNA gyrase acts as the primary drug target in Gram negative bacteria. In *E. coli*, the DNA gyrase is more sensitive to quinolones than the topoisomerase IV, and mutations to DNA gyrase is common in CIP resistant *E. coli* (22).

To have an antimicrobial effect, quinolones must enter the cytoplasm of the bacterium to reach DNA gyrase and topoisomerase. Quinolones enter through the cell membrane either through porins or by passive diffusion, which demands a high level of hydrophobicity in the drug (21). In *E. coli* and other Gram negative bacteria, there have been reported alterations in the number of porins in the outer membrane and increased expression of efflux pumps (22). This leads to reduced cytoplasmic concentrations of CIP, and decreased interaction between the antimicrobial drug and the drug targets.

Efflux pumps, located on the cell membrane, can extrude CIP from the cell through energy-demanding, active transport. Several efflux pumps have been characterized that efflux quinolones both in Gram positive and Gram negative bacteria (21). Previously reported mutations in *E. coli* have been shown to result in increased expression of efflux pumps like AcrAB-TolC, AcrEF-TolC, MdtK and EmrAB (30), (31). Efflux pumps are related to

multidrug resistance because efflux is not restricted to secretion of specific substrates. On the contrary, one efflux pump can be responsible for secretion of several antimicrobial drugs. For instance, the AcrAB-TolC efflux pump is known to efflux quinolones like CIP, but also other antimicrobials like tetracyclines, amphenicols, β-lactams and macrolides (30) (31).

For CIP-resistant *E. coli*, individual mutations can increase the MIC by a factor of 2-20, but no single mutation alone can make the MIC rise above the clinical breakpoint (1 mg/L) (32). Resistance to CIP in *E. coli* is therefore a multistep process.

1.4.4 Antimicrobial Resistance Development

Bacteria that are fit and virulent can continue to colonize, grow and divide. However, the presence of antimicrobials puts pressure on bacteria by inhibiting essential cellular processes. To overcome this antimicrobial stress, there are several mechanisms that bacteria use to alter their genome and improve their likelihood of survival. Bacteria can obtain mutations in the already existing genetic material and/or acquire new genetic material by horizontal transfer between bacteria (33).

A mutation is an alteration in the DNA, and a point mutation is a mutation where the alteration happens in a single base (34). Point mutations can be induced by mutagens, agents that are known to increase the mutation rate, or they can occur spontaneously. Mutations typically occur due to errors made during DNA replication. Normally, DNA polymerases have proofreading functions that greatly reduce the occurrence of point mutations. Point mutations include base substitutions (replacement of bases), base additions, and base deletions; and they can result in beneficial, neutral or harmful effects for bacteria (34).

The functional consequences of base substitutions are either that the mutation changes a codon for an amino acid into another codon for the same amino acid (silent or synonymous mutation), that the mutated codon encodes a different amino acid (missense mutation), or that the mutated codon is a stop codon (nonsense mutation) (34). Base additions and deletions occur less frequently than base substitutions, but these mutations cause frameshifts that will result in an altered gene product (34).

Mutations resulting in a loss of protein function for the bacteria occur more often than mutations resulting in the gain of function (34). This illustrates the ability of bacteria to get rid of non-essential functions, and thereby increase fitness.

When mutations occur in genes that are relevant for antimicrobial effect they could result in AMR. Mutation(s) in *e.g.* a gene that encodes for an antimicrobial target could result in an altered target making the bacteria more resistant to the antimicrobial. DNA mutations causing AMR may not occur simultaneously with exposure to an antimicrobial agent. In fact, mutations in genes that cause AMR can be present in bacteria without the bacteria ever being exposed to any antimicrobials in clinical use (*e.g.* penicillin-resistant strains of bacteria were detected before penicillin was introduced as a treatment (35)). Random mutations causing AMR are selected for by the presence of antimicrobials, and could then be maintained by bacteria.

1.4.4.1 The Spread of Resistance

Since the reproduction of bacteria occurs by division of one bacterial cell into two individual and identical cells, bacterial growth is considered to be exponential. A bacterium containing a resistance gene would "spread" the resistance trait by replicating; but in addition to this vertical gene transfer, transferring genes horizontally is possible amongst bacteria.

Horizontal gene transfer (HGT) includes several genetic mechanisms that enable bacteria to receive and integrate new segments of DNA obtained from other bacteria. This enables the spread and exchange of resistance genes at a tremendous pace. The main mechanisms of HGT include transduction, transformation and conjugation of DNA and mobile genetic elements, such as plasmids (3).

Through transduction, the transfer of DNA occurs via bacteriophages, viruses that are able to carry bacterial DNA. Bacteriophages infect host bacterial cells and are reproduced within the host. The bacteriophages package bacterial DNA, as well as their own, into capsids. The host cell eventually lyses, which enables the bacteriophages to infect new bacteria and transfer the bacterial DNA to a new host (3).

Transformation is the uptake and integration of free DNA-segments that are available from the environment around a recipient cell. The ability of *E. coli* to receive DNA by natural transformation is dependent on conditions in the environment, where successful transformation has been shown to be restricted to aquatic and calcareous habitats (36). *E. coli* can be made competent for transformation in the laboratory by treating the cells with chemicals like calcium chloride and heat shocking the cells, or by creating pores in the cell membrane using electrical pulses.

Plasmids are small DNA molecules that exist within a bacterial cell but are separate from the rest of the chromosomal DNA. Plasmids replicate independently of the chromosomal DNA, and are capable of containing one or even several antimicrobial resistance genes, which can easily spread to many, unrelated bacteria (37). Mobile genetic elements, such as plasmids, are typically transferred by conjugation. Conjugative plasmids contain an origin of transfer, the *oriT*, which enables their transfer by conjugation. (33). Some plasmids have the ability to move between bacterial hosts that are distantly related.

Conjugation is a process where DNA is transferred through direct contact between the donor and the recipient bacterial cell (38). The contact between the cells is by a pilus, produced by the donor cell, that attaches to the recipient cell and pulls it close. The double stranded DNA to be transferred is nicked at the *oriT*, and a single strand is received by the recipient through the pilus, which is followed by synthesis of the complementary strand in both the donor and recipient (38). After conjugation, both the donor and recipient carry the transferred DNA, and the recipient also gains the ability to produce pili and thereby becomes a donor as well. In addition to plasmids, other mobile genetic elements exist, and some are also capable of conjugation, but these are not relevant for this project.

1.4.5 AMR – A Global Problem

Multidrug resistant bacteria have evolved and are an enormous threat to modern medicine. To keep antimicrobial treatment effective as AMR has emerged, a shift towards the use of more broad-spectrum antimicrobials has been seen, at least in high-income countries (35). But as the latest generations of antimicrobials and broad-spectrum antimicrobials are increasingly ineffective due to AMR, we could be left with no effective antimicrobial drug treatments to

kill multidrug resistant bacteria, which can evolve further to become pan-resistant, or untreatable. Major surgery, organ transplantation, and treatment of premature babies are some of the medical achievements that would not be available without the ability to successfully treat bacterial infections (35).

Continued overuse of antimicrobials over the last decades, both in the community, in hospitals, and in livestock animal farming and aquaculture, have contributed by putting evolutionary pressure on microorganisms to develop and maintain AMR (35). Antimicrobials are overused as prophylactics for prevention of infectious diseases in livestock farming and in aquaculture (39). This treatment method allows for animals to live under poor hygienic conditions but at the same time stay free of disease, and the constant antimicrobial pressure selects for AMR emergence in bacteria both within and around the animals (39). Also, in countries like India and China, antimicrobial contamination from drug production factories is a serious concern (40). Stricter manufacturing regulations could prevent antimicrobial waste from being dumped and spread in the environment.

The pharmaceutical industry has not been able to develop enough novel antimicrobials needed to keep up with the rate of resistance development (35). Though novel antimicrobials are difficult to discover and develop, there are other strategies to extend the lifespan of the currently available and effective antimicrobial drugs. Improved guidelines for antimicrobial drug therapy and resistance surveillance have been established (41) and treatment approaches that could potentially reduce the selection for AMR are being explored in laboratories. Treatment approaches that have been tested in clinical trials include antimicrobial drug combinations, and drug cycling (42) (43).

Another approach is to look for ways to specifically target resistant bacteria. For example, bacteria that have developed AMR to one specific antimicrobial drug have been shown to exhibit increased sensitivity towards other, unrelated antimicrobials as a result of the initial resistance. This phenomenon is known as collateral sensitivity (44). Choosing treatment based on collateral sensitivity could be an approach to effectively kill resistant bacterial populations as they evolve during treatment of an infection.

1.5 Collateral Sensitivity

Collateral sensitivity was first discussed by W. Szybalski and V. Bryson in 1952 in a study on cross resistance profiles of *E. coli* (44). They discovered that a resistant strain can show not only lower and equal, but also higher levels of susceptibility towards other antimicrobials not previously introduced to the strain. Cases where a resistant strain obtained increased sensitivity towards an antimicrobial, compared to the WT strain, were described as collateral sensitivity. If bacteria evolve to gain AMR during antimicrobial treatment of an infection, the treatment might be greatly improved by switching the therapy to a drug that the resistant strain is collaterally sensitive towards. The collaterally sensitive strain would then either be killed by the second drug, or could develop AMR to the second drug, in which case the strain would be reciprocally sensitive to the initial drug that was used (45)

Maps of collateral networks have been made that show the collateral changes in sensitivity or resistance to a wide range of antimicrobials, resulting from an initial resistance to a specific antimicrobial (45) (46). The networks of collateral changes can be used to predict which antimicrobial(s) would be more effective in case a resistant pathogen evolves during the initial treatment of infection, and could suggest the secondary therapeutic choice. Based on these findings, new treatment strategies could emerge to improve some of the current guidelines for combination- and cycling therapy. The concept of collateral sensitivity could be helpful both to inform antimicrobial choice in the clinic and possibly reduce the need for development of novel antimicrobials.

1.5.1 Collateral Sensitivity in Ciprofloxacin Resistant Mutants

The collateral effects on antimicrobial susceptibility have been tested by members of the Microbial Pharmacology and Population Biology (MicroPop) research group (Podnecky et al., unpublished findings). Figure 2 shows a heat map of ten different CIP^R strains and the fold changes in susceptibility to 16 different antimicrobial drugs. Their results showed that the collateral effects of the K56-2 CIP-resistant (CIP^R) strain, differ from the K56-70 and K56-78 CIP^R strains. K56-2 CIP^R showed generally a lower frequency of collateral susceptibility changes to the tested drugs, than what is seen in the other nine CIP^R strains.

K56-70 CIP^R was similar to the majority of strains tested, while the K56-78 CIP^R strain showed both high frequency and the highest levels of cross-resistance of the strains. The CIP^R strains were whole genome sequenced to identify mutations that may cause CIP^R. Interestingly, each of the K56-2 CIP^R, K56-70 CIP^R and K56-78 CIP^R strains had the same amino acid substitution in GyrA, where the serine at position 83 was replaced with a leucine (S83L). This mutation is commonly observed in strains resistant to CIP (22). The K56-2 CIP^R strain also had a second mutation in GyrA, where glutamic acid replaced the alanine at position 119 (A119E), as well as a mutation in ParC, where glycine at position 78 was replaced by aspartic acid (G78D). Thus, the K56-2 CIP^R strain had mutations to both CIP drug targets, GyrA and ParC. Whereas, in addition to the GyrA S83L mutation, the K56-70 CIP^R and K56-78 CIP^R stains had mutations that affect efflux pump expression. Both strains had mutations to the *rpoB* and *marR* genes, which affect expression of the MdtK and AcrAB-TolC efflux pumps, respectively (30). Additionally, the K56-78 CIP^R strain had a mutation in *acrR*, which another regulator of the AcrAB-TolC efflux pump.

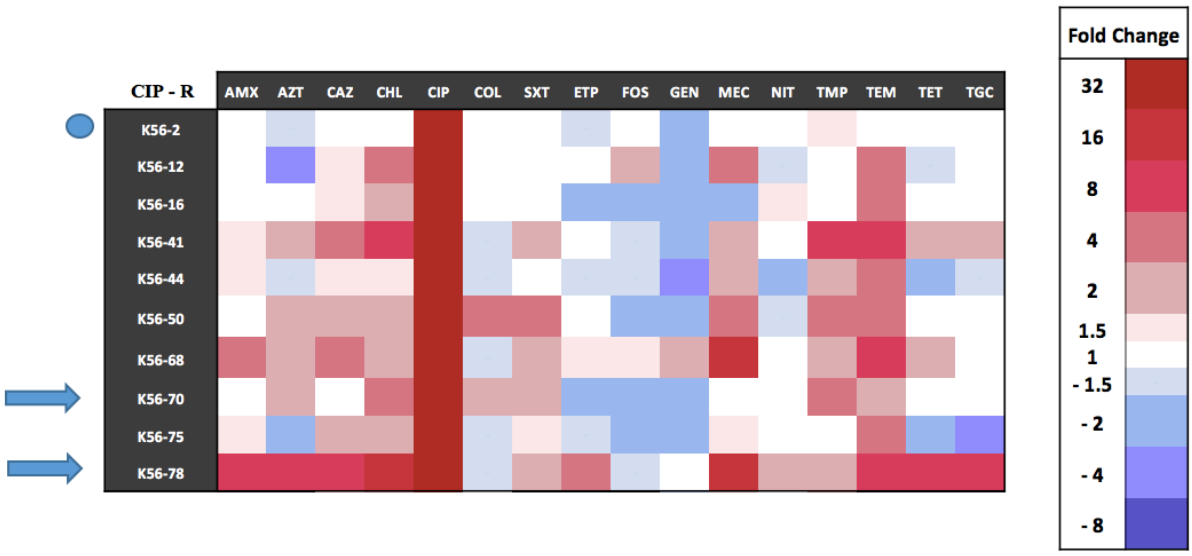

Figure 2: Heat map of Ciprofloxacin mutants and Collateral Changes. The K56-2 CIP^R strain (blue dot) shows differences in susceptibility to the K56-70 and K56-78 CIP^R strains (blue arrows). Illustration is based on previous work done in the MicroPop lab where cross-resistance (red color) and collateral sensitivity (blue color) effects were observed. Abbreviations of antimicrobial drugs: AMX; amoxicillin, AZT; azithromycin, CAZ; ceftazidime, CHL; chloramphenicol, CIP; ciprofloxacin, COL; colistin, SXT; sulphamethoxazole/trimethoprim, ETP; erythromycin, FOS; fosfomycin, GEN; gentamicin, MEC; mecillinam, NIT; nitrofurantoin, TMP; trimethoprim, TEM; temocillin, TET; tetracycline, TGC; tigecycline,

1.6 Homologous Gene Replacement

Gene replacement by homologous recombination, or homologous gene replacement (HGR), can be used to genetically engineer bacteria, altering the genetic material to introduce a specific mutation or to insert or delete sections of DNA. The desired DNA construct, *e.g.* an experimentally modified gene containing defined mutations (also referred to as the HGR construct), is often inserted, or cloned, onto a integrative DNA vector that is used to move the HGR construct into the bacteria (47). The typical vectors used are plasmids, mobile genetic elements that carry genes and other genetic material (as described in Section 1.4.4.1). Through HGR methods, the desired construct, carried by the integrative vector, can be exchanged with a DNA segment in the bacterial chromosome, allowing the substitution of targeted genes with gene copies containing defined mutations (47). Gene replacement methods are used to investigate the specific effect of a gene or mutation, such as whether AMR to a certain antimicrobial and collateral effect changes towards other antimicrobials are due to specific mutations.

In order for HGR to be successful, the DNA segments to be exchanged (the HGR construct and the genomic target) must have a high degree of similarity, or homology. Laboratory techniques allow for DNA modification of the construct, and short pieces of DNA can be added to an already isolated DNA fragment using PCR amplification or other molecular cloning approaches. In this way, regions of DNA that are homologous to the DNA surrounding the genomic target (homologous flanks) are added to the construct. Additionally, the bacteria must contain specific proteins that enable homologous recombination, amongst these proteins is RecA, which pairs homologous DNA segments and promotes the recombination event.

The “in-out” method can be used for HGR in *E. coli* (47). In this method, the desired DNA construct is cloned into a conjugative and non-replicative integrative plasmid; *e.g.* the pEX6K plasmid (Figure 19). In addition to the desired construct, the integrative plasmid carries various genes that serve as selection- and counter-selection markers. For pEX6K, these include a kanamycin-resistance gene (*npt*II) as a selection marker and *sacB*, a gene that encodes levansucrase production as a counter-selection marker (47).

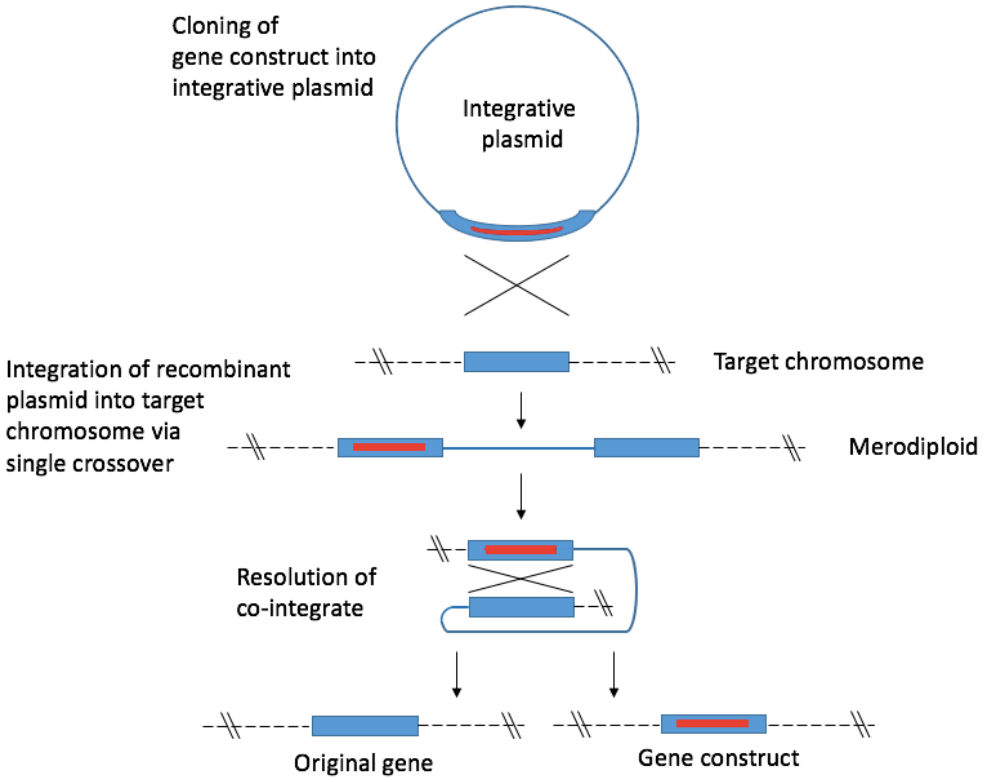

Figure 3: Illustration of Homologous Gene Replacement (HGR). The desired HGR construct is cloned onto an integrative plasmid. Homologous recombination (crossover event) occurs at one of the homologous flanking regions. Antimicrobial resistance selection causes maintenance of the plasmid integrate, creating merodiploids that contain both the HGR construct and the original genomic target. Resolution of the merodiploid (co-integrate) occurs by a second recombination event, where in one of two cases the original DNA genomic target is expelled together with the rest of the plasmid, leaving the desired construct in the chromosome. Illustration based on paper by Madyagol et al.,2011. (47).

The lack of a compatible origin of replication in pEX6K forces bacteria that do not encode the *pir* gene (necessary for the R6K origin of replication, present on the pEX6K) to integrate the whole plasmid into the chromosome when exposed to kanamycin. This plasmid integration is mediated by homologous recombination at one of the homologous flanking regions. By selecting on kanamycin, the plasmid is maintained in the genome. With the integration of the plasmid DNA, the genome contains both the original genomic target and the desired HGR construct, making it a merodiploid (partial diploid). Additionally, the merodiploids contain the entire plasmid backbone and specifically, the *sacB* gene. *sacB* produces levansucrase, an enzyme that degrades sucrose and produces levans – fructose polymers of high molecular weight that are lethal to Gram negative bacteria (47). When exposed to sucrose, the counter-selection forces the merodiploid to either mutate or get rid of the *sacB* gene, but because of the homologous regions in the DNA, another homologous recombination event typically

occurs. In the second recombination event, in one of two cases the recombination occurs at the second homologous region and the original genomic target is expelled together with the plasmid backbone. The plasmid is then recircularized, and the desired HGR construct is left in the chromosome. See Figure 3.

1.7 Study Aims

The aim of this project is to investigate the collateral differences in antimicrobial susceptibility between different strains of *E. coli* containing the same CIP-resistant (CIP^R) mutation in *gyrA* and/or *parC*. We aim to develop an HGR approach to introduce or repair defined point mutations known to cause CIP resistance. HGR constructs of the *gyrA* and *parC* genes from the K56-70 WT and K56-78 WT strains containing the CIP resistance mutations from K56-2 CIP^R, will be used to replace the original K56-70 WT and K56-78 WT genes, by homologous gene replacement. These cloned mutants will be studied by comparing the antimicrobial susceptibilities to those of the laboratory-selected mutants K56-70 CIP^R and K56-78 CIP^R. This will allow us to investigate what effects the resistance mutations have on collateral changes in antimicrobial susceptibility.

1.8 Hypothesis

My hypothesis is that when the K56-70 WT and K56-78 WT strains obtain the $gyrA_{(S83L\ A119E)}$ or $parC_{(G78D)}$ CIP resistance mutations from the K56-2 CIP^R strain, the manipulated K56-70 and K56-78 mutants will become CIP resistant, and will also adopt the collateral changes that were observed in the K56-2 CIP^R strain.

Chapter 2: Material and Methods

2.1 Bacterial Strains

The clinical isolates used in this project are from community acquired UTIs in women, which have been collected and studied in the ECO-SENS project (48) (49).

Table 1: Table of *E.coli* strains used in this project.

Clinical Isolates (ECO-SENS	Year	Country	Phylogroup	ST
K56-2	2000	Greece	B2	73
K56-70	2007-2008	Sweden	B2	550
K56-78	2007-2008	UK	D	1235

Laboratory Strains	Genotype	Source
DH5-α	F^- λ^- *ilvG*$^-$ *rfb-50 rph-1* RP4-2-Tc::[ΔMu1::*aac*(3)IV-Δ*aphA*-Δnic35-ΔMu2::zeo] Δ*dapA*::(*erm-pir*) Δ*recA*	Ferrières et al., 2010 (50)
MFD*pir*	F^- *endA1 glnV44 thi-1 recA1 relA1 gyrA96 deoR nupG purB20* ϕ80d*lacZ*ΔM15 Δ(*lacZYA-argF*)U169, hsdR17($r_K^- m_K^+$), λ^-	Messing, J., 1983 (51)

2.2 Plasmids

Vectors are used to carry genetic material. In this project, plasmid vectors were used, that were suitable for cloning with laboratory-modified genes. All plasmids used in this project are listed in Table 2.

Table 2: Plasmid vectors and respective properties.

Plasmid	Properties	Size (bp)	Source
pCR®-Blunt	pUC *oriV* P_{lac} *lacZ*α *ccdB* KM^R ZN^R	3512	Invitrogen (California, USA)
pGEM®-T Easy	f1 ori *lacZ* AMP^R	3015	Promega (Wisconsin, USA)
pDS132	R6K *oriV oriT* CHL^R	5286	Philippe et al., 2004 (52)
pEX6K	R6K *oriT sacB* KM^R	7298	M.C. Di Luca, unpublished

2.3 Media Preparation and Growth Techniques

All cultivation of bacteria in this project included growth of the bacteria in ambient air at 37°C overnight, unless otherwise specified.

2.3.1 Solid Growth Media

Generally, media for solid cultivation was prepared by mixing nutrient-rich powders, *e.g.* Luria Bertani (LB) broth powder, with agar and distilled water (dH_2O) in a Pyrex bottle. The recipes used in this project are listed in Table 3. Solutions were then sterilized by autoclaving at 121 °C for 20 minutes. Media was cooled to about 50 °C on a magnetic stirrer, then poured into Petri plates. After solidification at room temperature, the plates were stored at 4 °C. When necessary, chemicals such as antimicrobial drug(s) were added to the media just before pouring the plates. See Table A 1 in Attachments for antimicrobials and respective concentrations used in preparation of selective media in this project.

Table 3: Recipes for solid media.

Media	Contents	dH_2O added
LB-Agar	20 g LB Broth (Sigma Aldrich, Missouri, USA) 12 g Select Agar (Sigma Aldrich)	800 mL
YT $Sucrose_{5\%}$	8 g Tryptone (Becton, Dickinson and Company, New Jersey, USA) 8 g Yeast Extract (Becton, Dickinson and Company) 12,8 g Select Agar (Sigma Aldrich) 120 g Sucrose (Sigma Aldrich)	800 mL

2.3.2 Plating of Cells on Solid Growth Media

Spread plating was used to get even growth across an entire plate. When spread, bacterial solutions were pipetted onto plates with solid media and a sterile plastic T-shaped spreader was used to spread the cells evenly on the whole surface of the plate, before inverting the plate and leaving it for incubation.

To purify bacterial isolates, the "streak for isolation" method was used to obtain single colonies. A sterile plastic loop was used to touch *e.g.* a colony growing on a plate or collect a small amount from a freeze culture. The bacteria-containing loop was used to streak the bacteria onto a plate by rapidly moving the loop back and forth, covering about one third of the plate (zone one). A new loop was used to streak from the inoculated area of zone one, onto approximately another third of the plate (zone two). The loop was then turned over and the clean side was used to streak from zone two onto the rest of the plate (zone three) in a zig zag pattern.

2.3.3 Liquid Growth Media

For preparation of liquid media used to grow overnight cultures, 5 mL of liquid LB (general lab supply) was added to a round bottom tube with a vented cap. If the media contained

additional chemicals, such as antimicrobial drug(s), this was added to the media just before inoculation. See Table A 1 in Attachments for antimicrobials and respective concentrations used in preparation of selective media in this project. The bacteria added to the media was either from a glycerol freeze stock, or a single colony picked from an overnight culture growing on solid media. Liquid cultures were placed in a shaking incubator at 225 revolutions per minute (rpm).

2.3.4 Preparation of Glycerol Freeze Stocks

0,5 mL of an 80% glycerol solution was added to a screw capped cryotube. 1,5 mL of a liquid overnight culture of the desired bacteria was mixed with the glycerol to give a 2 mL freeze stock with a final glycerol concentration of 20%. Freeze stocks were stored at -75 °C. In this project, freeze stocks were made after every successful transformation of genetic material into a recipient strain.

2.4 Isolation of Genomic DNA

For isolation of genomic DNA from *E. coli*, the GenElute Bacterial Genomic DNA Kit (Sigma Aldrich, Missouri, USA) was used according to the manufacturer's guidelines. A 5 mL liquid culture with the desired bacteria was grown overnight. 1,5 mL of the liquid culture was centrifuged for two minutes to form a pellet of the bacterial cells. The supernatant was discarded, and the pellet was re-suspended thoroughly in 200 µL of lysozyme (100 mg/mL) before incubation at 37 °C for 30 minutes. To degrade RNA, 20 µL of RNase A (10 µg/mL) was added, followed by incubation at room temperature for two minutes. 20 µL of proteinase K (20 mg/mL) and 200 µL of lysis solution C was then added. The sample was vortexed for about 15 seconds (secs) and incubated for 10 minutes at 55 °C. This resulted in lysis of the cells and degradation of proteins.

The columns provided in the kit were prepared by adding 500 µL of column preparation solution and centrifuging for one minute. To prepare the DNA to bind to the column, the DNA was dehydrated by adding 200 µL of 95-100% ethanol (EtOH), followed by vortexing

of the sample. The entire sample was then transferred to the column, and centrifuged for one minute. The DNA that had bound to the column was washed twice by adding 500 µL wash solution, followed by centrifugation steps of one and three minutes (respectively). After the second wash, the column was centrifuged for one additional minute, to make sure all of the residual EtOH was removed. The column was then placed in a clean collection tube and 100 µL of Tris-buffer (10 millimolar (mM)), was added to the center of the column and incubated at room temperature for five minutes. The DNA and buffer were eluted into the clean collection tube by centrifugation for one minute. All centrifugation steps were carried out at 13 000 rpm. Genomic DNA was stored at 4 °C.

2.5 Plasmid Isolation

Plasmid DNA was isolated from bacterial cells using the GeneJET® Plasmid MiniPrep Kit (Thermo Fisher Scientific, Waltham, USA), following the manufacturer's guidelines. Typically, a 3,5-5 mL liquid culture of the cells containing the plasmid of interest was grown overnight in LB, with an antimicrobial drug added for selective pressure (Table A 1). The cell suspension was pelleted and re-suspended in 250 µL resuspension buffer; then the cells were lysed with 250 µL lysis buffer. The lysate was neutralized by addition of 350 µL neutralization solution, and the cell debris was pelleted during a 5-minute centrifugation step. The supernatant containing the plasmid DNA was applied to a silica column, and was then centrifuged for one minute, binding the DNA to the column. After adherence to the column, 500 µL of the EtOH-containing wash buffer was added to remove remaining impurities from the DNA sample and centrifuged for one minute. The wash step was repeated a second time, and then the empty column was centrifuged for an additional one minute to remove any residual EtOH. The pure DNA was eluted into a sterile tube with a small volume, typically 30 µL, of elution buffer. All centrifugation steps were carried out at 13 000 rpm. Plasmid DNA was stored at -20 °C.

In some cases, we suspected bacteria contained a low copy number of plasmids, which resulted in low plasmid yields after isolation. In these cases, six replicates of 5 mL liquid cultures were prepared, and treated as single plasmid isolations through cell lysis, neutralization and pelleting of the cellular debris. The supernatant of the six replicates were

then bound onto one silica column, and the plasmid isolation was completed as described above.

In some occasions during this project, the kit was not available in the lab, and in those cases the Monarch® Plasmid Miniprep Kit (New England Biolabs (NEB), Massachusetts, USA) was used, according to the manufacturers protocol.

2.6 Quantification of DNA

For quantitating DNA in this project, the NanoDrop™ 1000 Spectrophotometer (Thermo Fisher Scientific) was used, an instrument that is based on UV/VIS spectrophotometry. After nulling the instrument with sterile Milli-Q water, 1,5 μL of a DNA sample was placed between the two pedestals on the instrument. A xenon flash lamp illuminated the sample and a spectrometer analyzed the light that passed though. According to Beer's law, the concentration of the analytic agent in a sample is proportional to the absorbance of light. Before analyzing DNA samples, the instrument was initialized by adding the sample background to the instrument as a blank. The sample background was typically elution buffer. In this way, only the absorbance of light by the analytic agent itself, in this case the DNA, was accounted for when determining the concentration.

The spectrometer takes measurement at several wavelengths (ranging from 220-750 nm), which assesses the purity of the sample. Contaminants, like proteins or phenols, will absorb strongly around 280 nm while DNA is detected at 260 nm. The purity of a DNA sample is measured as the ratio of absorbance at 260 nm and 280 nm, the 260/280 ratio. For pure samples this value should range from about 1,8-2,2, where lower values indicate impurity.

2.7 Restriction Endonuclease Digestion

After insertion of a DNA segment into a plasmid vector by ligation, the plasmids were cut with restriction endonucleases, which are enzymes that cut double-stranded DNA at specific recognition sites. The resulting DNA digest sizes could indicate the content of the plasmid,

and tell whether a segment had been inserted or not, and sometimes the orientation of the insert.

DNA digests were setup according to the recipe in Table 4, and were incubated at the appropriate temperature, typically 37°C, for one hour. The DNA fragments after digestion were analyzed by electrophoresis (Section 2.9), and the sizes of the fragments were used confirm successful ligation of the DNA segments. See Table A 4 in Attachments for restriction endonucleases and the corresponding buffers used in this project.

Table 4: Recipe for restriction digests.

Reagents	Amount/volume
Plasmid	800 ng
Restriction enzyme	1-2 µL
Buffer	2 µL
Sterile Milli-Q Water	Ad 20 µL

In some cases, sequential digests were set up, where several endonucleases were added one after another to one digestion reaction that was incubated at different temperatures for each enzyme.

Restriction endonucleases were also used for cloning itself, see Section 2.12.4.

2.8 Polymerase Chain Reaction

Polymerase chain reaction (PCR) is a method to amplify a specific piece of DNA. The method is based on using the piece of DNA to be amplified, also known as the amplicon, as a template for the production of new DNA copies, in a reaction that includes specific enzymatic reagents and temperature shifts.

After a mixture of the needed reagents, often called a PCR master mix, is prepared, the reaction occurs repeatedly in cycles using a thermal cycler, which allows rapid and controlled shifts of temperature. At temperatures around 93-98 °C, double stranded DNA reversibly denatures into two single, complementary strands. At lower temperatures, when the template DNA is still present as two single strands, short segments of DNA that are complementary to specific sites of the single strands, can anneal. These short DNA segments are known as primers, and will anneal to complementary single stranded DNA at temperatures around 50 °C (or 5 °C below the specific primer's melting temperature). A set of two primers is necessary, binding both strands of the amplicon. After primer binding the temperature rises to 68-72 °C, so that the DNA polymerase enzyme can generate a new copy of DNA. The DNA polymerase incorporates deoxynucleotides (dNTPs) that are complementary to the single strand, thereby synthesizing a new double stranded piece of DNA. After the synthesis of the new DNA, the temperature is again risen to 93-98 °C, making also the newly synthesized DNA available as single stranded templates. This makes the reaction exponential.

All the reagents used to make a master mix of one PCR reaction are listed in Table 5. The following thermal steps were used: initial denaturation at 98 °C for 30 secs followed by 30 cycles (98 °C for 10 sec; 59,7-64 °C for 30 sec; 72 °C for 30 secs per kilo base pair (kbp) of amplicon) and a final extension at 72 °C for 10 minutes.

Table 5: PCR master mix for one 25 µL PCR.

Reagents	Stock Concentration	Volume	Final Concentration
5X Phusion High Fidelity buffer	5X	5 µL	1X
dNTP	10 mM	0,5 µL	0,2 mM
Forward Primer	10 µM	1 µL	0,4 µM
Reverse Primer	10 µM	1 µL	0,4 µM
Phusion High Fidelity DNA polymerase	2000 U/mL	0,5 µL	1 U/reaction
DNA template		1-1,5 µL	
Sterile Milli-Q Water		Ad 25 µL	

2.8.1 PCR Primer Design

A primer is a short sequence of nucleotides that is needed to amplify specific DNA segments during PCR. The freeware program Primer3 (53) was used to design the primers, but some of the standard parameters were specified in order to optimize the primers.

The primers, preferably between 18 and 23 bases in size, were not to contain four or more of the same nucleotide in a row. The melting temperature of the primer should be between 57 and 62 °C, and a content of the bases guanine (G) and cytosine (C) of around 50% was optimal. Also, the 3´ ends were to include a G or a C base, which made the primer bind tightly to the C or G base in the complementary strand. Having a G or a C at the 3´ end is known as a GC-clamp, and this is preferable because there are three hydrogen bonds between a G and a C base, whereas there are only two hydrogen bonds between a thymidine (T) and an adenine (A). A GC-clamp aids the DNA polymerase to begin adding the bases needed to make a complete double strand.

The primers were always designed to be complementary to parts of the desired amplicon(s), but in cases where PCR products were used for cloning by ITAC, primers were designed to also include a 5´ region (30 bp) complementary to the overlapping parts of the fragments to be cloned. (See Section 2.12.3) All primers are listed in the oligonucleotide Table A 3 in Attachments.

2.9 Gel Electrophoresis

For analysis of DNA fragments in this project, gel electrophoresis was used. The method is based on loading a DNA sample on a gel, and then providing electrical current which makes the negatively charged DNA wander from a negatively charged pole to one of positive charge. To keep the DNA samples from floating up and out of the gel, a loading buffer that weighs down the samples was always added. Different fragments of DNA were separated from each other by size, since smaller fragments travel easier through the gel matrix than larger ones. Different gels can be used for this purpose, but in this project only agarose gels were used.

In order to visualize the DNA on the gel, ethidium bromide (EtBr) was added to the gel, which intercalates between base pairs in the DNA. EtBr is visualized by exciting it with UV-light, this is a way to monitor the DNA segments as they move across the gel. A DNA ladder, a mixture of DNA fragments of known sizes and concentrations, was added to every gel as a comparison to the samples. Figure A 1 in Attachments shows the DNA ladder used, SmartLadder MW-1700-10 (Erogentec, Seraing, Belgium).

Typically, a 1% agarose gel was made with 0,5 or 1 g agarose powder (Invitrogen) solubilized in 50 or 100 mL, respectively, of 1X Tris-acetate-EDTA (TAE) buffer at the boiling temperature of the buffer. Occasionally, when analyzing PCR products of small size, a 2% agarose gel was prepared to increase the separation of small DNA fragments through the gel. Before casting, the gel-solution was supplemented with EtBr to a concentration of 0,3 µg/mL. Both 1% and 2% agarose gels were run at 100 volt (V) for one hour.

2.10 Gel Extraction

In order to keep and continue working with DNA samples that have been analyzed by gel electrophoresis, DNA was extracted from the agarose gel. The QIAquick® Gel Extraction Kit (Qiagen, Hilden, Germany) was used.

The gel extraction procedure included cutting the desired DNA band out from the agarose gel and dissolving the gel slice in 3 volumes equivalents of a pH-adjusted buffer at 50 °C. Isopropanol (100%) (one volume equivalent) was then added to the dissolved sample. The sample was applied to a silica column followed by one minute of centrifugation. DNA binding of the sample to the column occurred at a pH ≤ 7,5. 750 µL wash buffer was then added to remove other components from the column. The wash buffer and contaminants were removed by centrifuging the sample twice, and finally the purified DNA was eluted from the column using 30 µL of elution buffer that had been preheated to 42 °C. After addition of the buffer, the sample was incubated at room temperature for five minutes before centrifugation for one minute to elute DNA.

In some occasions during this project, there was doubt about the efficacy of this gel extraction kit, and in those cases the Monarch® DNA Gel Extraction Kit (NEB) was used according to the manufacturer's protocol.

2.11 DNA Sequencing

With DNA sequencing, the order of nucleotides within a DNA fragment is determined. In this project, Sanger sequencing with the BigDye® Terminator v3.1 Cycle Sequencing Kit (Thermo Fisher Scientific) was used.

To prepare the DNA to be sequenced, a 20 µL sample (Table 6) of the template DNA, primer(s) to amplify the template, BigDye v3.1, 5X buffer and sterile Milli Q water, was run in a ThermoCycler for the following reaction: 96 °C for 1 min, followed by 25 cycles of 96 °C for 10 secs; 50 °C for 5 secs; 60 °C for 2 minutes. After preparation, the samples were sent to be sequenced at the Medical Genetics Department at the University Hospital of North Norway. The results were analyzed using the Sequencher DNA Sequence Analysis Software (Gene Codes Corporation, Michigan, USA).

Table 6: Sequencing reaction contents.

Reagents	Amount
DNA template	500 ng
Primer(s)	3,2 pmol
5X Big Dye Sequencing Buffer	4 µL
Big Dye v3.1	1 µL
Sterile Milli-Q water	Ad 20 µL

2.12 Molecular Cloning

2.12.1 Zero Blunt® PCR Cloning

The pCR®-Blunt plasmid vector from the Zero Blunt® PCR Cloning Kit (Invitrogen) was used for subcloning of DNA fragments. Successful insertion of a DNA fragment into the pCR®-Blunt plasmid (Figure 4) disrupts expression of the lethal *lacZα-ccd*B gene fusion, which results in death of transformants containing the plasmid without a DNA insert. See Table 2, for description of pCR®-Blunt plasmid features.

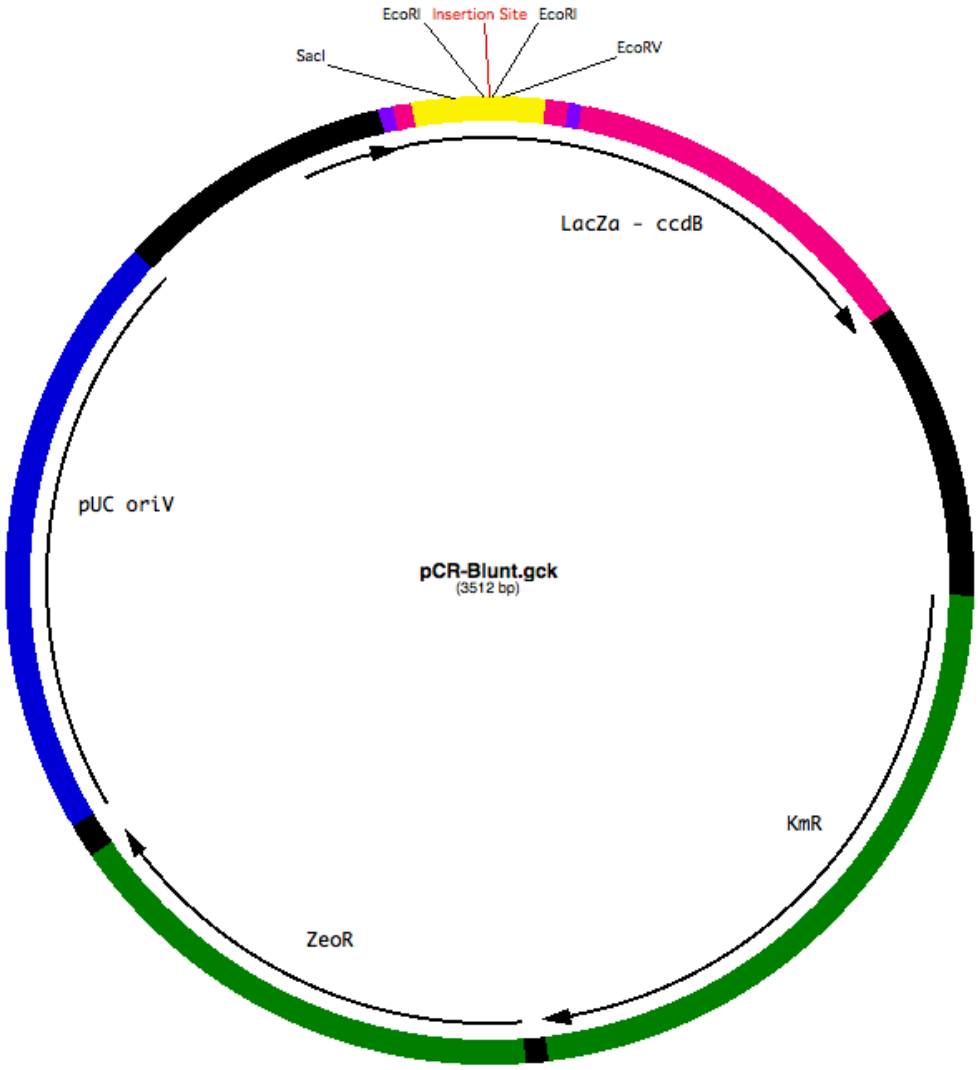

Figure 4: Plasmid map of pCR-Blunt (3512 bp). Properties and restriction sites used in this project are indicated.

The 10 µL ligation reaction consisted of the pCR®-Blunt plasmid, the blunt ended PCR product to insert, DNA ligase to fuse the fragments together, in addition to buffer and water. See Table 7.

Table 7: Reaction recipe for ligation with pCR®-Blunt.

Reagents	Amount
pCR Blunt® (25 ng)	1 µL
Blunt PCR product	1-5 µL
5X ExpressLink™ T4 Ligase Buffer	2 µL
Sterile Milli-Q water	Ad 9 µL
5X ExpressLink™ T4 DNA Ligase (5 U/µL)	1 µL

A 1:10 molar ratio of vector:insert was used. The amount of PCR product DNA added in the ligation reaction was calculated according to the following equation provided by the manufacturer:

$$\text{x ng insert} = \frac{(10)(y \text{ bp PCR product})(25 \text{ ng linearized pCR®}-\text{Blunt})}{(3500 \text{ bp pCR®}-\text{Blunt})}$$

The ligation reaction was incubated at room temperature for one hour, then stored at 4 °C overnight and transformed into chemically competent *E. coli* DH5-α the following day (Section 2.13).

2.12.2 pGEM®-T Easy Cloning

The pGEM®-T Easy vector (Figure 5) from the pGEM®-T Easy Cloning Kit (Promega) is a linearized plasmid with an additional T base on both 3´ ends, also known as T-overhangs. DNA fragments with T-overhangs in the 3´ ends can be ligated with DNA fragments containing an additional A base, so called A-overhangs, in the 5´ ends. For attachments of the fragments, DNA ligase makes covalent phosphodiester bonds between the hydroxyl and phosphoryl ends of the DNA fragments and hydrogen bonds are generated between the T and A nucleotides, thereby creating a new base pair (54). Hence, for successful ligation into the pGEM®-T Easy vector, the inserts must contain an A-overhang in the 5´ ends (see next section). See Table 2 for pGEM®-T Easy plasmid properties.

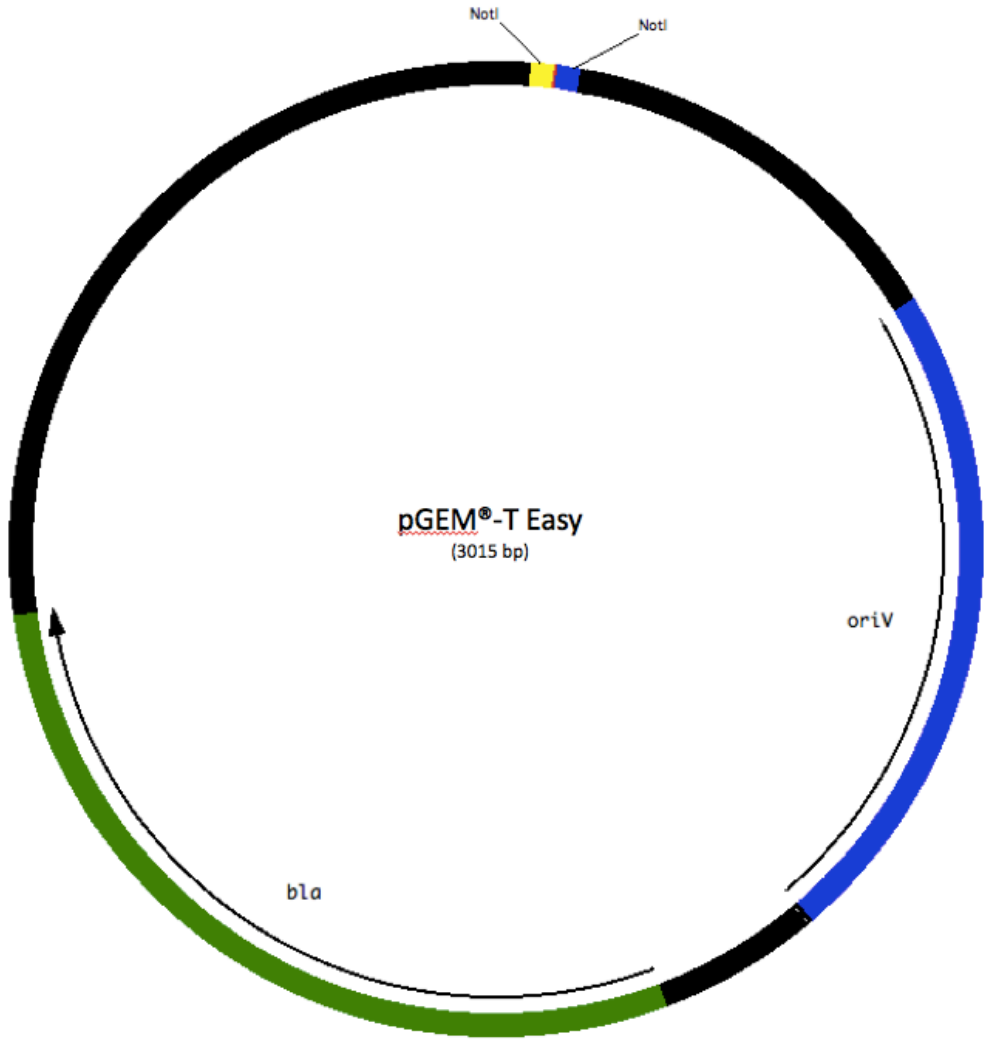

Figure 5: Plasmid map of pGEM®-T Easy (3015bp). Properties and restriction sites used in this project are indicated.

A 10 µL ligation reaction (Table 8) was used to fuse the pGEM®-T Easy vector with the constructs that contain an A-overhang. After incubation at room temperature for one hour, the reaction solution was stored at 4 °C overnight, and transformed into chemically competent *E. coli* DH5-α the following day (Section 2.13). When plated on LB and 5-bromo-4-chloro-3-indolyl-β-D-galactopyranoside (XGal) and isopropyl β–D-1-thiogalactopyranoside (IPTG), transformants containing plasmids with the inserted sequence will be white. Transformants carrying an empty vector will be pigmented blue (known as blue/white screening).

Table 8: Reaction recipe for ligation into pGEM® T-easy vector.

Reagents	Amount
pGEM®-T Easy Vector (50 ng)	1 µL
A-tailed PCR product	3 µL
2X Rapid Ligation Buffer	5 µL
T4 DNA Ligase (3 U/µL)	1 µL
Sterile Milli-Q water	Ad 10 µL

2.12.2.1 Synthesizing 5' A-overhangs

To create an A-overhang on the 5´ ends of blunt-ended PCR products, A-nucleotides had to be attached to the ends. In this project, a 10 µL reaction was set up by mixing 5 µL of the 2X DreamTaq™ master mix, containing the DreamTaq™ polymerase (Thermo Fisher Scientific), with 3 µL PCR product and dATPs to a final concentration of 0,2 mM. The sample was incubated at 70 °C for 30 minutes, which allowed the polymerase to modify the DNA ends and attach the A-overhang. DNA polymerases with good proofreading functions, such as the Phusion High-Fidelity DNA polymerase (used for PCR amplification in this study), will see the unpaired A as an error in DNA replication, and will remove the A overhang.

2.12.3 Isothermal Assembly Cloning

Isothermal Assembly Cloning (ITAC), also known as Gibson Assembly cloning, is a single-step method of molecular cloning that combines DNA fragments that contain overlapping regions (55). In contrast to traditional cloning, the shape of the fragment ends is irrelevant for ITAC. However, for the fragments to be successfully combined, the ends must contain identical, or so called overlapping, regions of 15-80 bases, see Figure 6.

ITAC involves several steps to process and combine the DNA fragments. First the 5´ T5 exonuclease digests into the 5´ ends of both the double stranded insert and vector. This enzyme is only active after adding the DNA fragments to the master mix and until the incubation at 50 °C, which inactivates the exonuclease. The exonuclease digestion creates single stranded 3’ overhangs. Exposing the single stranded DNA allows the complementary ends of the DNA fragments to anneal. The High Fidelity DNA polymerase then incorporates dNTPs to fill in the gaps that might have occurred, before ligation by T4 DNA ligase, which creates one intact double stranded construct (Figure 6).

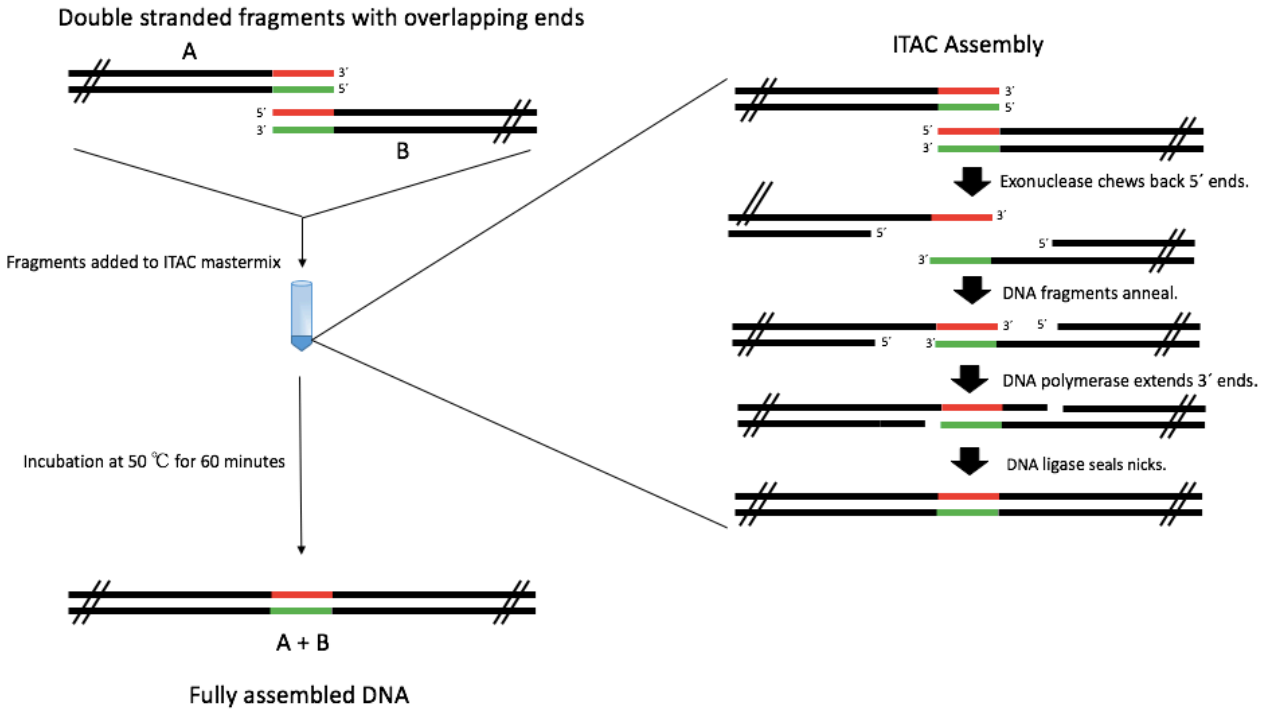

Figure 6: Illustration of ITAC reaction. Two double stranded DNA fragments with identical (overlapping) regions are added to the ITAC master mix followed by an isothermal reaction at 50°C. The thermosensitive enzyme exonuclease digests on 5´ ends, making complementary single stranded 3´ overhangs in the fragments. Exonuclease gets inactivated and the fragments anneal where polymerase fills the gaps. Finally, DNA ligase attaches the fragments. Illustration is based on paper by Gibson et al., 2009 (55) and protocol description from NEB (56).

The DNA fragments to be combined (vector and insert) were amplified by PCR. PCR primers for ITAC were designed with regions that were complementary to the desired amplicon (about 20 bases) and also complementary to the DNA fragment that it would be combined with (30 bases). The amplified segments therefore contained an addition of 30 bases on the 5´ end of the final PCR products, representing the overlapping region.

A total volume of 5 µL of the two PCR products were added to 15 µL of the ITAC master mix (Table 9), which contains the following enzymes: 5´ T5 exonuclease, DNA polymerase and DNA ligase. Reactions were incubated at 50 °C in a thermocycler for one hour. ITAC reactions were then transformed into chemically-competent *E. coli* with appropriate selection for the newly assembled plasmid.

Table 9: ITAC master mix. Aliquots of 15 µL ITAC master mix was used for one reaction.

Reagents	Stock Concentration	Volume	Final Concentration
5X ITAC Buffer	5X	320 µL	1,33 X
T5 Exonuclease	10 U/µL	0,64 µL	6,4 U
Phusion DNA polymerase	2 U/µL	20,0 µL	40 U
Taq DNA Ligase	40 U/µL	160,0 µL	6400 U
Sterile Milli-Q Water		Ad 1200 µL	

2.12.3.1 Drop Dialysis

DNA samples were purified using sterile Milli-Q water by a method known as drop dialysis. The DNA sample was spotted onto the surface of a filter-paper with 0,05 micrometer (µm) pores, that was floating on the water. Typically, an empty petri plate was used for this purpose, and the sample was incubated at room temperature for 20 minutes. The goal was the removal of excess salts and other leftover substances remaining from previous reactions, such as the ITAC master mix.

2.12.4 Cloning with Restriction Endonucleases

DNA digestion of both vector and insert DNA with the same or compatible restriction endonucleases leave ends of the fragments that are complementary to each other, and can be cloned together by DNA ligation. However, this method requires a dephosphorylation step, preventing the plasmid from recircularizing without the desired insert, see next Section. (See Section 2.7 for restriction endonucleases used in plasmid identification.)

A 20 µL reaction containing 1 µL T4 DNA ligase (Promega), 5X Ligation buffer (4 µL), vector and insert DNA, and sterile Milli-Q water, was incubated at room temperature for one hour. After incubation, the sample was stored overnight at 4 °C before transformation into chemically competent *E. coli* DH5-α.

A molecular ratio of 1:1 represents a scenario where there is one vector for every one insert. The ratios between vector and insert were calculated based on the following equation:

$$\frac{(6{,}02 \text{ x } 10^{23})\ (\text{DNA (ng/µL) x}10^{-9})}{(\text{Size (bp)})\ (660)} = \text{copy number/µL}$$

$$\frac{\text{copy number/µL}}{(6{,}02 \text{ x } 10^{23})\ (10^{15})} = \text{fentamoles/µL}$$

Copy number/µL represents how many copies of the vector or insert is in one µL of DNA sample. For the ligations, 15 fentamoles of the vector and 45 fentamoles of the insert (1:3 molar ratio) was used.

2.12.4.1 DNA Dephosphorylation

Linearized plasmids digested with a restriction endonuclease, were dephosphorylated to prevent the plasmid from recircularizing, since dephosphorylated ends cannot be ligated together by DNA ligase.

1,5 units (U) of shrimp alkaline phosphatase (rSAP) was added to the previous restriction endonuclease digestion reaction, and incubated at 37 °C for 30 minutes. To deactivate the rSAP, the sample was heated to 65 °C for 5 minutes.

2.13 Transformation of Plasmids into Chemically-Competent *E. coli*

Following the manipulation of plasmids, the DNA was transformed into chemically competent *E. coli* cells for storage and future work. Bacterial cells (DH5α or MFD*pir* -Table 1) were prepared to enable DNA uptake by transformation according to a method described by Inoue, Nojima and Okayama (57) and stored at -75°C by Nicole Podnecky.

A 200 µL vial of chemically-competent cells was slowly thawed on ice, then added to the plasmid-containing solution to a total volume of 210-220 µL. The sample was incubated on ice for 30 minutes, then heat-shocked at 42 °C for 45 secs, followed by further incubation on ice for two minutes. To assist the bacterial cells' recovery, super optimal broth with catabolite repression (S.O.C.), was added to the cells to a total volume of 1 mL, and the cells were then placed in a shaking incubator (150 rpm) at 37 °C for one hour. After recovery, the bacterial suspension was spread plated on appropriate selective media.

All pCR®-Blunt and pGEM®-T Easy plasmid derivatives were transformed into the *E. coli* DH5-α strain, and all pDS132 or pEX6K plasmid derivatives were transformed into the *E.coli* MFD*pir* conjugation strain, since the *pir* gene is required for maintenance of plasmids carrying the R6K origin of replication. Diaminopimelic adic (DAP) was added to the S.O.C. at a concentration of 400 µg/mL, for the transformations into the MFD*pir* strain.

For the DH5-α strain, 100 µL of the transformation reaction was plated on one plate, and the rest of the reaction was plated on a second plate, whereas the entire reaction was plated on one plate for the MFD*pir* strain. This was due to the lower competence and growth capacity of the MFD*pir* strain. All plates were incubated over night at 37 °C, but some were left to incubate for another night when no transformants had initially grown. After every successful plasmid transformation, four single isolated colonies were picked from the plate and inoculated into selective liquid overnight cultures. A portion of a liquid culture was used to make glycerol freeze stocks (Section 2.3.4), and the rest was typically used for plasmid isolation (Section 2.5).

2.14 Conjugation (Bi-parental Mating)

Plasmids containing an *oriT* can be transferred to other strains by conjugation from the *E. coli* MFD*pir* conjugation donor strain. This strain carries the conjugation machinery RP4, and can therefore serve as a plasmid donor. In addition, the MFD*pir* strain is a DAP auxotroph and cannot produce DAP itself. The absence of DAP in the media can therefore be used as a counter-selection, as the MFD*pir* strain would not be able to survive.

A liquid culture of MFD*pir* containing a conjugagive plasmid, and the recipient strain, were grown overnight. 1 mL of each culture was put in separate sterile tubes and centrifuged at 12.000 rpm for 30 secs. The supernatant was discarded and the cells were resuspended in 1 mL of 10 mM $MgSO_4$ before centrifugation for 30 secs to wash the cells. This wash step was repeated two times, before resuspending the cells in 200 µL $MgSO_4$. 50 µL of both the MFD*pir* donor and the recipient strain was mixed and spotted on a LB DAP (400 µg/mL) plate that had been preheated to 37 °C. Also, 30 µL of both the "parent strains" (donor and recipient) was spotted on the same plate as controls. After incubation overnight at 37 °C, the three cell spots were scraped from the plate using a sterile plastic loop. The cells were resuspended in 500 µL of LB and washed with 1 mL of LB three times to remove any residual DAP. After resuspending in 1 mL LB, the three cell solutions were spread on individual plates with selective pressure according to the plasmid-encoded resistance gene(s) (see Table A 1 in Attachments for table of chemicals/drugs added to media). After incubation overnight at 37 °C, only the mated cells that received the plasmid would be able to survive the selective pressure. The MFD*pir* strain will not survive without presence of DAP, which is not added to the selective plates, and the recipient strain is lacking the AMR to survive the selection.

2.15 Antimicrobial Susceptibility Testing

A microbroth dilution assay (IC_{90}) was used to determine the susceptibility of the ECO-SENS strains (Table 1) to kanamycin. The strains of interest were struck from a glycerol freeze stock onto an LB plate. After incubation overnight at 37°C, 0,5 McFarlands (~$1{,}5x10^8$ cells) were prepared by suspending the bacteria in 0,85% sterile saline. The 0,5 McFarland solutions were diluted 1:1000 (5 µL:5 mL) in Mueller Hinton Broth (MHB). A 96 well plate was filled with MHB as indicated in Figure 7 below.

	1	2	3	4	5	6	7	8	9	10	11	12
A	100 µl		100 µl	100 µl	100 µl	100 µl	100 µl	100 µl	100 µl	100 µl	100 µl	200 µl
B	100 µl		100 µl	100 µl	100 µl	100 µl	100 µl	100 µl	100 µl	100 µl	100 µl	200 µl
C	100 µl		100 µl	100 µl	100 µl	100 µl	100 µl	100 µl	100 µl	100 µl	100 µl	200 µl
D	100 µl		100 µl	100 µl	100 µl	100 µl	100 µl	100 µl	100 µl	100 µl	100 µl	200 µl
E	100 µl		100 µl	100 µl	100 µl	100 µl	100 µl	100 µl	100 µl	100 µl	100 µl	200 µl
F	100 µl		100 µl	100 µl	100 µl	100 µl	100 µl	100 µl	100 µl	100 µl	100 µl	200 µl
G	100 µl		100 µl	100 µl	100 µl	100 µl	100 µl	100 µl	100 µl	100 µl	100 µl	200 µl
H	100 µl		100 µl	100 µl	100 µl	100 µl	100 µl	100 µl	100 µl	100 µl	100 µl	200 µl

Figure 7: Amount of MHB added to the 96-well plate in a 2-fold IC_{90} set up.

Antimicrobial working stocks were mixed in MHB to double the highest concentration tested. 200 µL of the antimicrobial working stock was added in column 2. Using a multi-channel pipette, 100 µL of the antimicrobial was transferred from column 2 to column 3, where the antimicrobial was mixed (by pipetting up and down 15 times) with the MHB already added to column 3. 100 µL was then transferred from column 3 to column 4, mixed, and so on until column 11. 100 µL was taken out from column 11 and discarded after mixing.

One bacterial strain was added per row, across columns 1-11. The ATCC 25922 strain was added to every plate as the quality control strain, to ensure the antimicrobial stocks used were at the correct concentration. Column 12 served as a negative control, with no antimicrobial and no bacteria added. Column 1 served as a positive control, with only MHB and bacteria added. Rows A and H were not used due to an increased risk of evaporation from these wells.

After incubation in a shaking incubator at 37 °C and 700 rpm for 18 hours, the optical density at 600 nm (OD_{600}) was measured by a plate reader. To determine the drug concentration which inhibited 90% of the growth (IC_{90}), the OD_{600} value of a sample was compared to the OD_{600} value of a positive control, according to the following equation:

$$\%\ \text{Inhibiton} = \left(1 - \frac{\text{OD}_{600}\ \text{drug treated} - \text{OD}_{600}\ \text{negative control}}{\text{OD}_{600}\ \text{positive control} - \text{OD}_{600}\ \text{negative control}}\right) \times 100$$

The final IC_{90} value was the lowest antimicrobial concentration at which ≥ 90% inhibition was observed.

Chapter 3: Experimental Results and Discussion

HGR is a valuable tool to manipulate the genome of bacterial strains, as described in Section 1.6. Using HGR, specific genetic elements are introduced and replace a strain's original genomic target. Genetic elements to introduce could for instance be genes that contain AMR-causing mutations, and then by comparing the antimicrobial susceptibility of the original to the engineered strains, the effect of the mutations can be evaluated. Conversely, the genetic element could be a WT gene, and HGR can be used to repair, or replace, a mutated genomic target. With either approach, HGR enables the evaluation of effects caused by specific mutation(s). The aim of this project was to develop an HGR approach to introduce or repair defined mutations in the ciprofloxacin drug target genes, *gyrA* and *parC* of clinical *E. coli* isolates.

3.1 A HGR Approach to Introduce or Repair *gyrA* and *parC* Mutations

We outlined an approach to design HGR constructs of *gyrA*/*parC* containing the $gyrA_{(S83L\ A119E)}$ or $parC_{(G78D)}$ mutations from the K56-2 CIP^R strain, and replace the WT *gyrA* and *parC* genes in the K56-70 and K56-78 WT strains (See Figure 8 for illustration of the general outline in our HGR approach). The effects of these mutations could be evaluated by antimicrobial susceptibility testing. Changes in antimicrobial susceptibilities and potential collateral changes between the engineered mutants and the selected laboratory-mutants K56-70 CIP^R and K56-78 CIP^R, could then be compared. We also planned a similar approach to repair the specific point mutations in K56-2 CIP^R, by replacing the mutated *gyrA* and *parC* genes with HGR constructs of the K56-2 WT *gyrA*/*parC*. This would allow us to determine if CIP resistance and the collateral susceptibility effects seen in K56-2 CIP^R are indeed caused by the defined mutations alone.

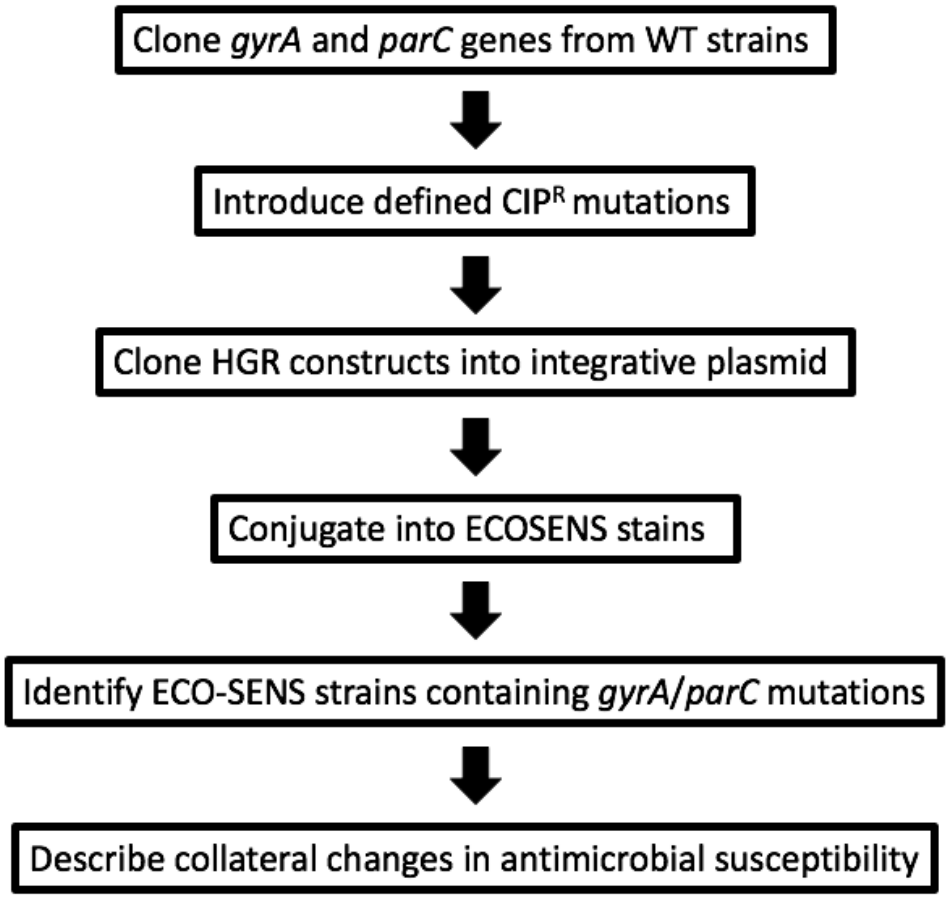

Figure 8: Flow chart of general outline in HGR approach.

3.2 Cloning and Troubleshooting

3.2.1 Building Homologous Gene Replacement Constructs

3.2.1.1 Primer Design for *gyrA* and *parC* regions

Our initial goal was to design single *gyrA* and *parC* constructs that were suitable for HGR across multiple strains. We used Sequencher software to compare DNA sequences of the *gyrA* and *parC* gene regions in the K56-2, K56-70 and K56-78 strains (Figure 9). A consensus

sequence, representing the most frequent nucleotide at each position, was generated and we identified many differences between the strains. The K56-78 in particular had many mutations in the *gyrA* gene (blue dots in panel A of Figure 9), but mutations that we observed in the *gyrA* and *parC* genes were synonymous (did not change the amino acid sequence of these proteins), with the exception of the S83L and A119E mutations in *gyrA* and the G78D mutation in *parC* of the K56-2 CIP strain.

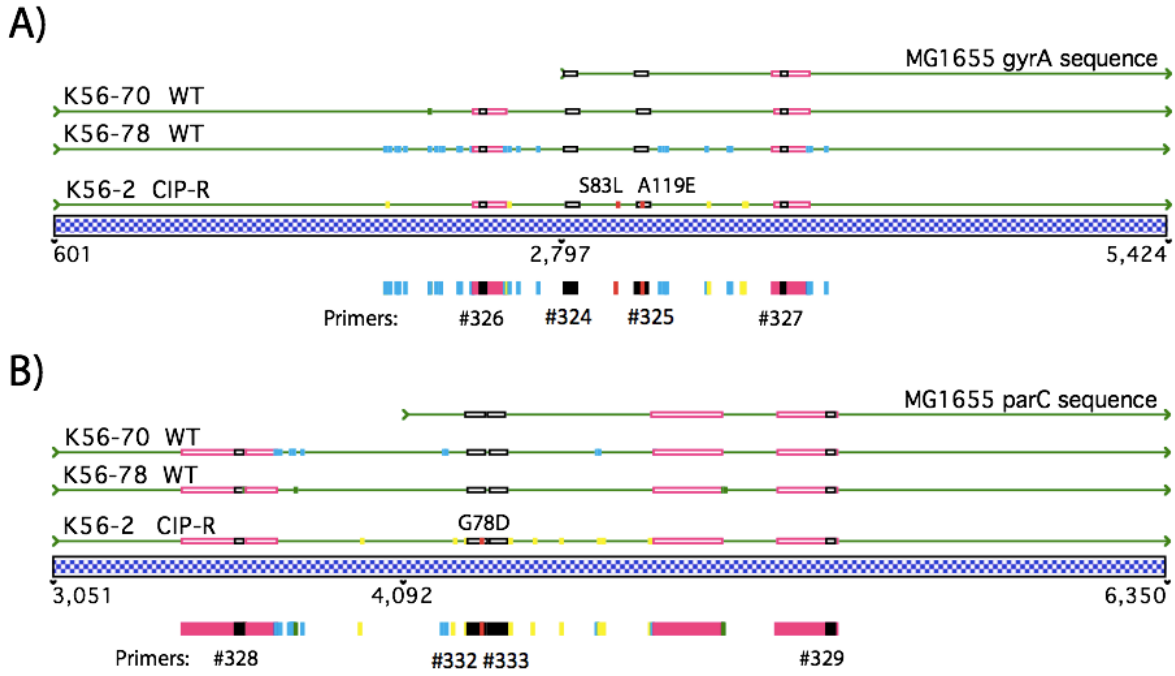

Figure 9: Sequence comparison between *gyrA* and *parC* genes from K56-70 WT, K56-78 WT, K56-2 CIP^R and MG1655. (A) *gyrA*$_{(S83L\ A119E)}$ and (B) *parC*$_{(G78D)}$ mutations in K56-2 CIP^R are marked in red. The consensus sequence of the 3 strains is represented by the blue checkered bar. Yellow, green and blue dots represent sites of variation between the strains as compared to the consensus sequence. Regions conserved across all three strains are marked in pink and PCR primers that were designed are shown in black.

In order to preserve the sequence of each strain, we had to build strain-specific HGR constructs. We identified conserved regions for all the strains, and primers were designed within the conserved regions so that the same primer set could be used to amplify the HGR construct for all of the strains. We designed primers to amplify large regions of *gyrA* and *parC* (#326 & #327 and #328 & #329, respectively) to serve as the HGR construct backbone. We also designed primers to amplify a short region of *gyrA* and *parC* that contained only the

mutation(s) of interest (#324 & #325 and #332 & #333, respectively), which would be used to introduce the mutations into each strain-specific HGR construct.

All primers (oligonucleotides) are listed in **Table A 3** in Attachments.

3.2.1.2 PCR Amplification and Zero Blunt® PCR Cloning of *gyrA and parC*

Portions of the *gyrA* and *parC* genes from our selected strains were cloned into the PCR Blunt plasmid vector. First, genomic DNA was isolated in duplicate from the K56-2 CIP^R, K56-2 WT, K56-70 WT and K56-78 WT ECO-SENS strains, resulting in DNA concentrations between 88,16 and 213,17 ng/µL. The duplicate with the highest DNA concentration was used to PCR amplify the *gyrA* and *parC* genes from the genomic DNA (Section 2.8). Primers #326 & #327 and #328 & #329 were used for this purpose. The size and purity of the resulting *gyrA* (1321 bp) and *parC* (1772 bp) PCR products were analyzed by gel electrophoresis (Figure 10), see Section 2.9.

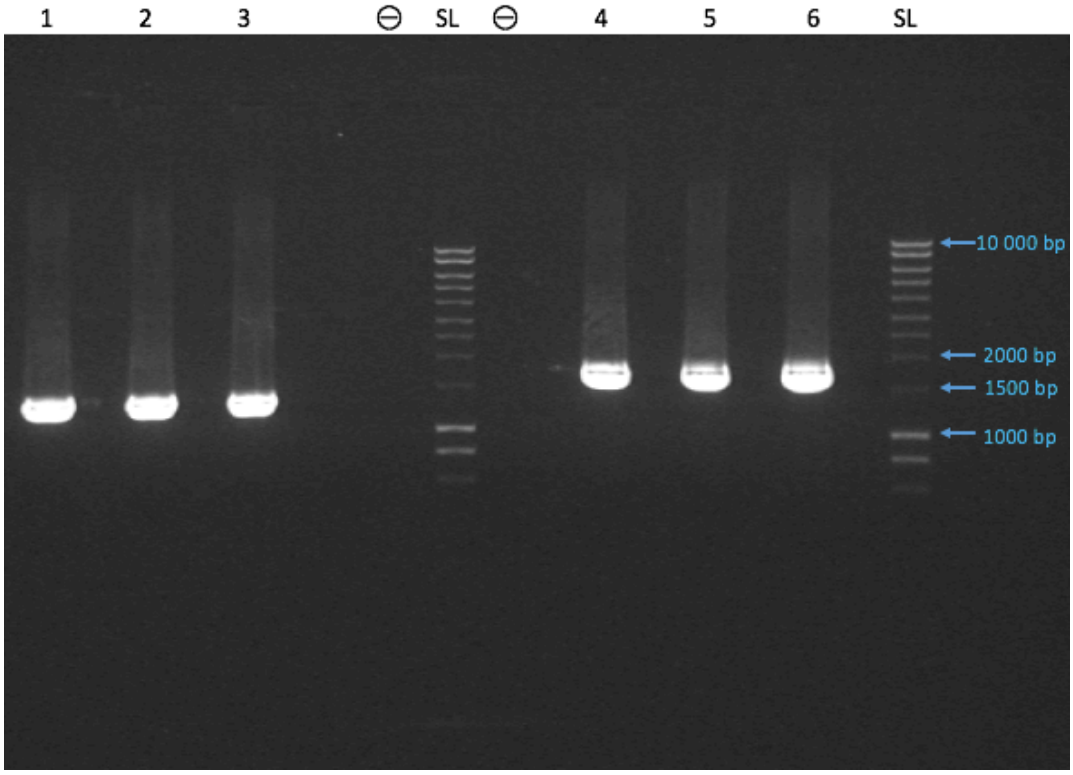

Figure 10: Image of *gyrA* and *parC* genes. (1% agarose gel.) **Lane descriptions.** 1: *gyrA* from K56-2 CIP^R, 2: *gyrA* from K56-70 WT, 3: *gyrA* from K56-78 WT, 4: *parC* from K56-2 CIP^R, 5: *parC* from K56-70 WT, 6: *parC* from K56-78 WT. (−): negative (PCR master mix), SL; SmartLadder.

The PCR products from each strain looked correct both in size and that no additional bands were present. Each DNA band were excised from the agarose gel, and the DNA was extracted using the QIAquick Gel Extraction Kit. This yielded blunt-ended DNA products with concentrations between 25,28 and 55,2 ng/µL, appropriate for ligation into the pCR®-Blunt plasmid vector (Section 2.12.1). See Figure 4 for plasmid map of pCR-Blunt.

The *gyrA* and *parC* PCR products from the K56-2 CIP^R, K56-2 WT, K56-70 WT and K56-78 WT strains, were ligated into the pCR®-Blunt plasmid. Transformation of the ligations resulted in pCR-Blunt-*gyrA* and pCR-Blunt-*parC* DH5-α transformants that grew on LB kanamycin 50 µg/mL (KM_{50}) plates (see Section 2.13). Four single colonies from each ligation were grown in liquid culture (LB KM_{50}) and glycerol freeze stocks were made. Plasmid DNA was isolated from these cultures (Section 2.5), resulting in DNA yields between 140,7 and 357,9 ng/µL.

Correct and single insertion of the *gyrA* and *parC* segments, as well as the orientation of the insert, were investigated by endonuclease digestion of the plasmids. The pCR-Blunt-*gyrA* and pCR-Blunt-*parC* plasmids were cut with the restriction endonucleases *Sac*I and *Eco*RV, respectively (Section 2.7). The *gyrA* and *parC* segments could have been inserted in one of two ways, resulting in different fragment sizes. For *Sac*I digestion, expected sizes were either 4392 bp + 441 bp (orientation #1), or 3876 bp + 966 bp (orientation #2). For *Eco*RV, the expected fragment sizes were either 4516 bp + 669 bp (orientation #1) or 4149 bp + 1135 bp (orientation #2). Fragments of 3512 bp in size indicated an empty pCR®-Blunt vector.

The pCR-Blunt-*gyrA* and pCR-Blunt-*parC* plasmid digestions were consistent with the expected fragment sizes and both orientations were observed (Figure 11) with the exception of pCR-Blunt-*parC*-K56-2-WT clone #1 and #3, where *Eco*RV-digestion did not result in the expected fragment sizes (Figure A 2 in Attachments). The plasmids pSV-1 to pSV-16 were selected for further work (Table A 2 in Attachments).

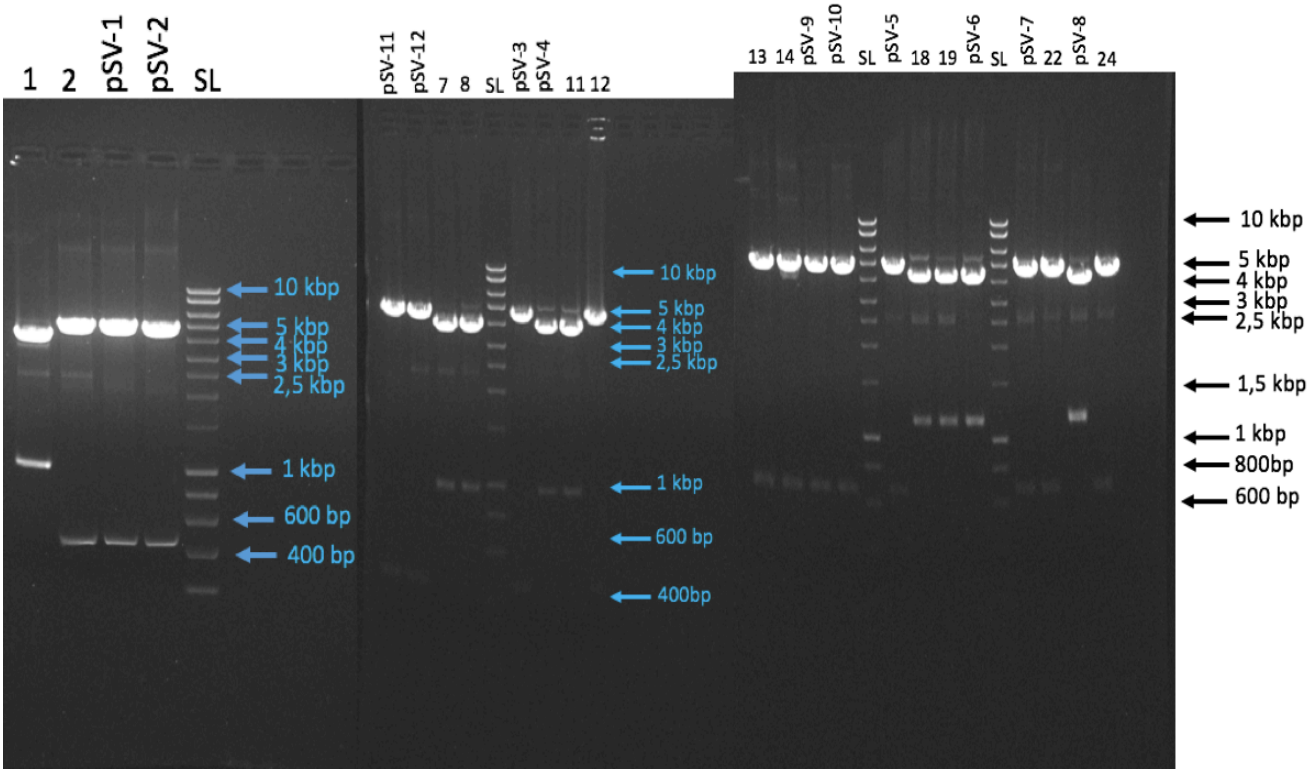

Figure 11: Confirmation of pCR-Blunt-*gyrA* and pCR-Blunt-*parC* plasmids.
Gel images of pCR-Blunt-*gyrA* and pCR-Blunt-*parC* plasmids with gene inserts rom K56-2 CIP^{R}, K56-70 WT and K56-78 WT, after digestion with *Sac*I (plasmid w/*gyrA*) and *Eco*RV (plasmid w/*parC*) on a 1% agarose gel. All digests were consistent with expected fragment sizes. **Lane descriptions.** 1: pCR-Blunt-K56-70-WT-*gyrA* clone #1 orientation 1. 2: pCR-Blunt-K56-70-WT-*gyrA* clone #2, orientation 2. 7, 8: pCR-Blunt-K56-2-CIP^{R}-*gyrA*$_{(S83L\ A119E)}$ clone #3 and #4, orientation 2. 11: pCR-Blunt-K56-78-WT-*gyrA* clone #3, orientation 2. 12: pCR-Blunt-K56-78-WT-*gyrA* #4, orientation 1. 13, 14: pCR-Blunt-K56-2-CIP^{R}-*parC*$_{(G78D)}$ clone #1 and #2, orientation 2. 18, 19: pCR-Blunt-K56-70-WT-*parC* clone #2 and #3, orientation 2. 22, 24: pCR-Blunt-K56-78-WT-*parC* clone #2 and #4, orientation 2. SL; Smart Ladder.

To further test the plasmids, pSV-1 to pSV-16 were cut with the restriction endonuclease *Eco*RI. *Eco*RI should cut the pCR-Blunt plasmid within the multiple cloning site (Figure 4, plasmid map), but not cut the *gyrA* and *parC* inserts. The expected fragment sizes after the digest were 3500 bp + 1333 bp for pCR-Blunt-*gyrA*, and 3500 bp + 1784 bp for pCR-Blunt-*parC*. All digests were consistent with the expected fragment sizes. See Figure 12 for gel image of pSV-1 to pSV-11 and Figure A 3 in Attachments for pSV-13 to pSV-16.

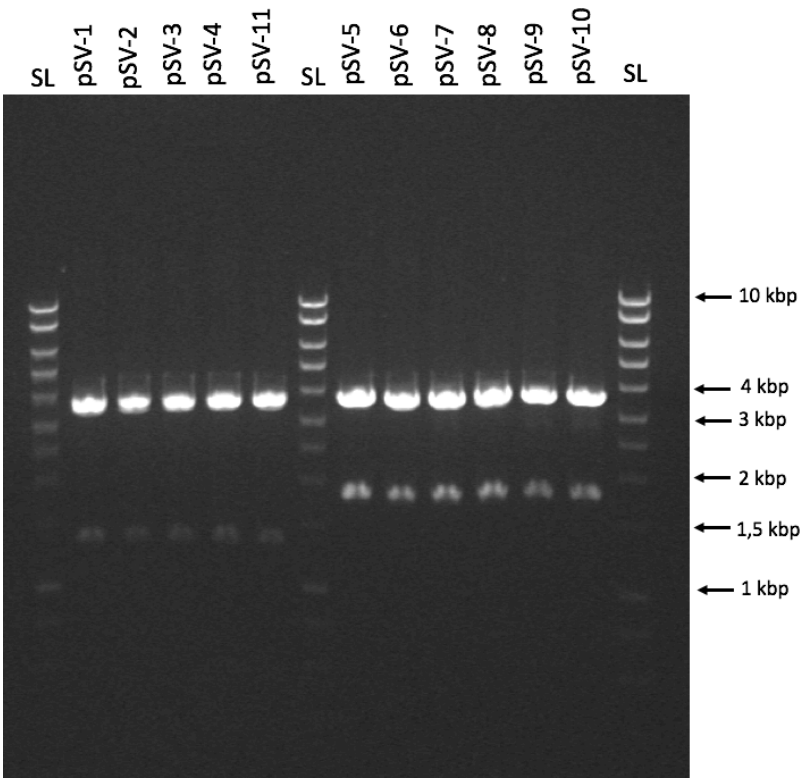

Figure 12: Image of pSV-1 to pSV-11 plasmids with gyrA/*parC* gene inserts From K56-2 CIP^R, K56-70 WT and K56-78 WT, after digestion with *Eco*RI. 1% agarose gel. All digests were consistent with expected fragment sizes. SL; Smart Ladder.

All of the *Eco*RI digestions matched the expected band sizes. This concluded the cloning of the HGR constructs with the WT *gyrA* or *parC* from K56-2 (pSV-13 and pSV-15, respectively). These constructs would later be used to repair the mutated *gyrA* and *parC* genomic targets in K56-2 CIP^R strain. For the remaining constructs it was then necessary to introduce the *gyrA* and *parC* mutations from K56-2 CIP^R.

3.2.1.3 Introduction of *gyrA* and *parC* Point Mutations by ITAC

Small DNA fragments containing the $gyrA_{(S83L\ A119E)}$ or $parC_{(G78D)}$ from K56-2 CIP^R were cloned by ITAC into pSV-2, pSV-3, pSV-5 and pSV-7, replacing the corresponding portion of *gyrA* and *parC* in the WT constructs. ITAC is a very rapid method of molecular cloning (see Section 2.12.3) that combines DNA fragments with overlapping or homologous ends. The resulting plasmid can be transformed into chemically competent cells after the one-hour reaction time and filtration step. The DNA fragments to be cloned by ITAC were prepared by

PCR amplification to add overlapping regions to the fragments ends using primers that contained the complementary regions.

The pSV-2, pSV-3, pSV-5 and pSV-7 plasmids were diluted to 1 ng/µL in sterile Milli-Q water. The plasmid backbones as well as portions of the *gyrA*/*parC* WT genes were PCR amplified in duplicate, using primers #330 #331 for pSV-2 and pSV-3 and #334 #335 for pSV-5 and pSV-7. These primers were designed with a region of 30 bases that matched the sequence surrounding the $gyrA_{(S83L\ A119E)}$ and $parC_{(G78D)}$ mutations in K56-2 CIP^R, which was suitable for cloning by ITAC. After PCR amplification, the products were digested with *Dpn*I. *Dpn*I has a very frequently found recognition site, but will only digest methylated DNA (in this case the original plasmids that were methylated by methylase enzymes in DH5α). This allowed for separation of the template DNA from the PCR products on the agarose gel. The samples were analyzed by electrophoresis, and the correct sized bands (4477 bp for pSV-2 and pSV-3, and 5172 bp for pSV-5 and pSV-7) were extracted from the gel, yielding DNA concentrations between 17,1 ng/µL and 70,7 ng/µL.

Regions where the $gyrA_{(S83L\ A119E)}$ and $parC_{(G78D)}$ mutation were located in K56-2 CIP^R, were amplified in duplicate from pSV-11 (primers #324 #325) and pSV-9 (primers #332 #333). This resulted in PCR products of 356 bp and 112 bp in size that were extracted from the gel after electrophoresis, yielding DNA concentrations of 48,6 and 24,9 ng/µL, respectively.

See Figure A 4, Figure A 5, Figure A 6, Figure A 7 and Figure A 8 in Attachments for gel images after electrophoresis of the plasmid backbone and mutation region PCR products.

ITAC was used to clone the PCR amplified pSV-2 and pSV-3 with the *gyrA* mutation region from pSV-11, and the PCR amplified pSV-5 and pSV-7 with the *parC* mutation region from pSV-9, where 2,5 µL of each fragment to ligate were added to the ITAC reactions. This resulted in four gene constructs with *gyrA* or *parC* from either K56-70 WT or K56-78 WT, containing the *gyrA* or *parC* mutation(s) from K56-2 CIP^R. The reactions were then transformed into DH5-α cells and plated onto LB KM_{50} plates. Four isolated transformants were stored in glycerol freeze stocks and plasmid DNA was isolated, resulting in DNA yields from 92,96 to 301,7 ng/µL. The plasmids were then digested with restriction endonuclease *Eco*RI to identify whether the plasmid vectors where intact and the correct size. The expected digest sizes were 3500 bp + 1333 bp for PCR-Blunt-$gyrA_{(S83L\ A119E)}$ and 3508 bp + 1784 bp for pCR-Blunt-$parC_{(G78D)}$. *Eco*RI digestion resulted in fragments of expected sizes, however

half of the PCR-Blunt-*parC*$_{(G78D)}$ plasmids had additional unexpected bands, but at least one of the tested candidate plasmids looked correct for each plasmid that was cloned (Figure 13). The plasmids pSV-19 to pSV-22 and were selected for further work.

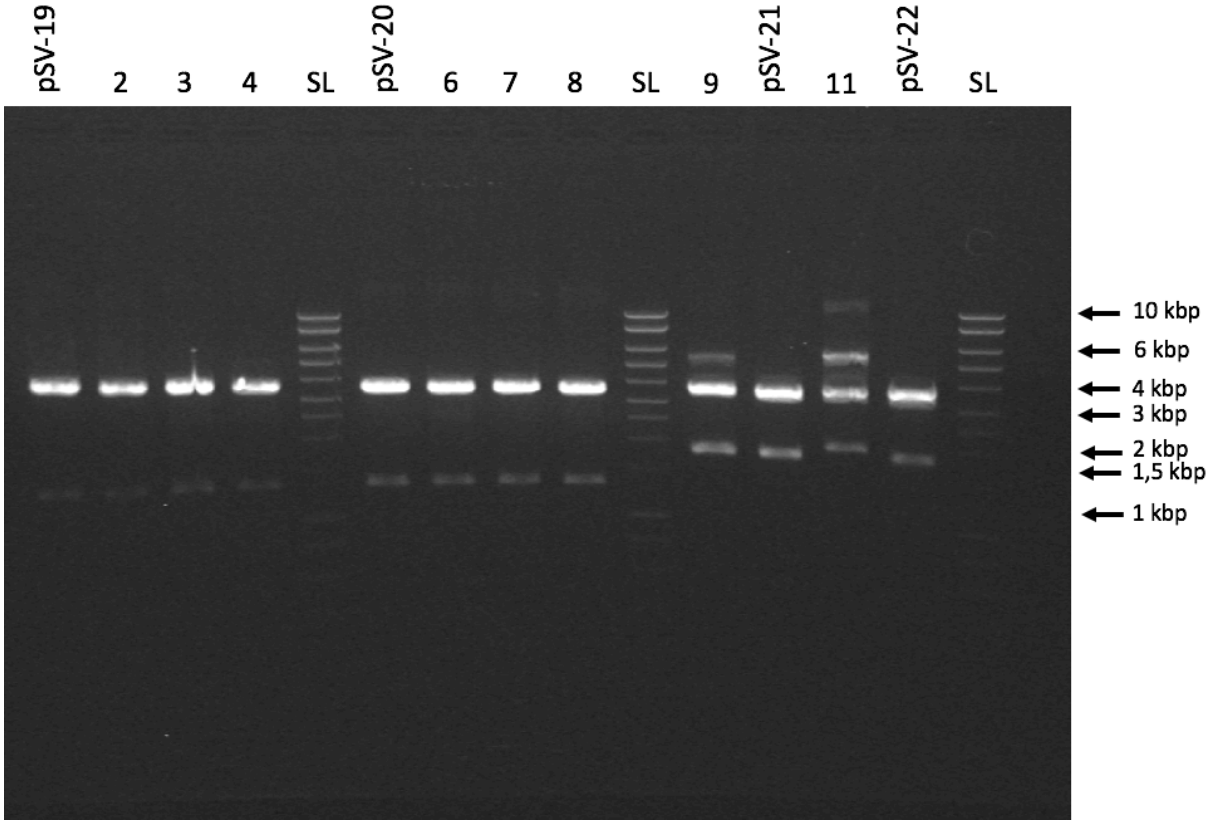

Figure 13: Image of pSV-19 to pSV-22 after *Eco*RI digest. 1% agarose gel. **Lane description:** 2-4: pCR-Blunt-K56-70-WT-*gyrA*$_{(S83L\ A119E)}$ clone #2-4. 6-8: pCR-Blunt-K56-78-WT-*gyrA*$_{(S83L\ A119E)}$ clone #2-4. 9: pCR-Blunt-K56-70-WT-*parC*$_{(G78D)}$ clone #1. 11: pCR-Blunt-K56-78-WT-*parC*$_{(G78D)}$ clone #1. SL; Smart Ladder.

To confirm that the desired *gyrA* and *parC* mutations had been successfully cloned into the WT constructs, each of these four plasmids and the K56-2 WT containing plasmids, pSV-13 and pSV-15, were submitted for sequencing (see Section 2.11). The general plasmid sequencing primers M13 (#300 #301) were used, in addition to internal sequencing primers #324 for pSV-13, pSV-19 and pSV-20, and #333 for pSV-15, pSV-21 and pSV-22 to ensure complete coverage. Using the Sequencher software we aligned the resulting HGR construct sequences to the respective strain WT sequences.

For plasmids pSV-13, pSV-19 and pSV-20, the HGR constructs had the expected DNA sequence (Figure A 13 in Attachments). The sequencing to confirm the gene constructs in the pSV-15, pSV-21 and pSV-22 plasmids did not cover the entire construct. However, based on the initial comparison, we suspected that pSV-22 contained the *parC* gene region from K56-70 WT and not K56-78 WT. Plasmids pSV-15, pSV-21 and pSV-22 where sequenced again, using primers #300, #301 and #332, which allowed for coverage over the entire construct (Figure A 14). We confirmed the sequences of the constructs in pSV-15 and pSV-21. The sequencing results revealed that the construct in pSV-22 was indeed the gene background from K56-70 WT *parC* and not from K56-78 WT *parC,* but the construct did contain the desired *parC* mutation. This was most likely due to a personal error during ligation of the *parC* gene into pCR-Blunt.

3.2.1.4 Repeating pCR-Blunt-K56-78-WT-*parC*$_{(G78D)}$ Construct

Striving to detect where the K56-70 WT *parC* fragment was introduced into the construction of the K56-78 *parC* HGR construct, pSV-8 was sequenced, which confirmed the correct gene background from K56-78 WT *parC*. From this point the ITAC assembly was repeated to introduce the *parC* mutation; the pCR-Blunt backbone and parts of the *parC* construct was amplified from pSV-8 (primers #334 #335) as well as the *parC*$_{(G78D)}$ region in pSV-9 (primers #332 #333). The pSV-8 derived PCR product was digested with *Dpn*I and the correct sized PCR products (5172 bp and 112 bp) were extracted from the gel yielding DNA concentrations of 14,0 ng/µL for pSV-8 and 14,3 ng/µL for pSV-9. See Figure A 9 in Attachments for gel image of pSV-8 PCR product. Then the ITAC reaction and transformation was repeated and resulted in DH5-α transformants on LB KM_{50} plates. Four single colonies were selected, isolated in liquid LB KM_{50} and stored in glycerol freeze stocks. Plasmid isolation resulted in DNA yields of 267,3 to 326,7 ng/µL, and were digested with *Eco*RI. Expected band sizes of 3508 bp + 1784 bp were observed on a gel in three of the four candidates (Figure 14). pSV-23 was chosen, but DNA sequencing of pSV-23 (primers #300, #301, #332, and #333) showed that a single point mutation had occurred.

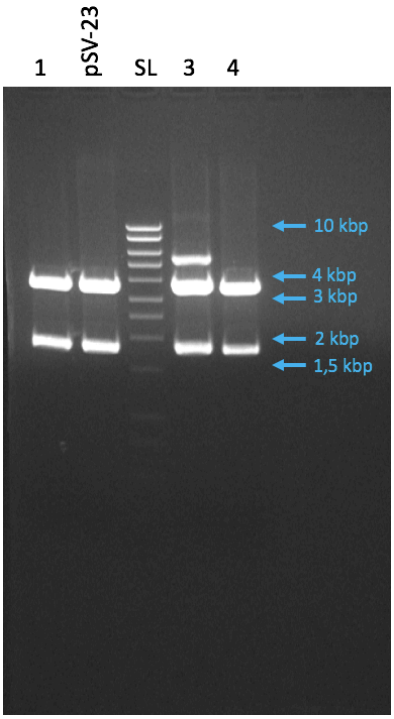

Figure 14: Image of pSV-23 after *Eco*RI digest. 1% agarose gel. **Lane description:** 1, 3, 4: pCR-Blunt-K56-78-WT-parC$_{(G78D)}$ clone #1, #3, #4. SL; Smart Ladder.

We confirmed the sequences of the K56-78 WT *parC* constructs in pSV-17 and pSV-18 (primers #300, #301, #332, and #333). There were no mutations present in these constructs, so the single mutation observed in pSV-23 was likely an error introduced during PCR amplification. pSV-18 was used as the backbone for the third attempt to construct the pCR-Blunt-K56-78-WT-parC$_{(G78D)}$. PCR amplification of the plasmid backbone from pSV-18 was performed as before (primers #334 #335). The PCR product was digested with *Dpn*I and the expected band size (5172 bp) was visualized on an agarose gel. Gel extraction yielded a DNA concentration of 40,6 ng/µL.

This PCR product and the *parC*-mutation region previously amplified from pSV-9, were cloned by ITAC assembly and transformed into DH5-α. Four transformants from the LB KM_{50} plate were isolated and stored in glycerol freeze stocks. The plasmid DNA was extracted, which yielded concentrations between 84,5 and 270,9 ng/µL. Restriction fragment analysis by *Eco*RI digestion resulted in expected fragment sizes (3508 bp + 1784) for all four candidates. The plasmid with the highest yield, pSV-24 was therefore chosen for further

analysis. DNA sequencing of pSV-24 with primers #300, #301, #332, and #333 showed that construct had the correct K56-78 *parC* region sequence with the desired $parC_{(G78D)}$ mutation (Figure A 14 in Attachments).

This concluded the cloning of pSV-19, pSV-20, pSV-21, and pSV-24, which contained the HGR constructs for the $gyrA_{(S83L\ A119E)}$ and $parC_{(G78D)}$ mutations.

3.2.2 Cloning *gyrA* and *parC* Constructs into pDS132 by ITAC

In order to use the HGR constructs to introduce or repair mutations to *gyrA* and *parC* in the ECO-SENS strains, the constructs had to be moved from pSV-13, pSV-15, pSV-19, pSV-20, pSV-21, and pSV-24, into an integrative plasmid. The conjugative plasmid pDS132 was considered suitable for this purpose, since it is non-replicative in the target strains (R6K origin of replication), has selectable (chloramphenicol resistance, *cat*) and counter-selectable (sucrose intolerance, *sacB*) markers. (Figure 15).

Figure 15: Plasmid map of pDS132 (5286 bp). Properties and restriction sites used in this project are indicated.

Our initial strategy was to subclone the HGR constructs into pDS132, using the ITAC method. Plasmid DNA was isolated for pDS132 and pSV-13, pSV-15, pSV-19, pSV-20, pSV-21, and pSV-24, yielding concentrations of 295,8 ng/µL and between 106,4 and 329,7 ng/µL, respectively. The HGR constructs were amplified from each plasmid by PCR and overlapping regions complimentary to the pDS132 vector insertion site were added using primers #348 and #349. The pDS132 vector was linearized by endonuclease digestion with *Xba*I in four reactions digesting 800 ng of pDS132 each. The digested plasmid was then treated with rSAP, to dephosphorylate the ends of the linearized plasmid, preventing it from recircularizing (see Section 2.12.4.1). The PCR fragments and linearized pDS132 were analyzed by electrophoresis (Figure 16 and Figure 17). Correct sized DNA fragments (*gyrA* constructs: 1394 bp, *parC* constructs: 1845 bp, and pDS132: 5286 bp) were excised from the gel and the DNA was extracted. The resulting DNA yields of the *gyrA* constructs were between 70,3 and 99,7 ng/µL and from 23,4 to 33,8 ng/µL for the *parC* constructs. For pDS132, the four resulting gel bands where pooled and the DNA was extracted using one single column. This resulted in a DNA concentration of 9,4 ng/µL.

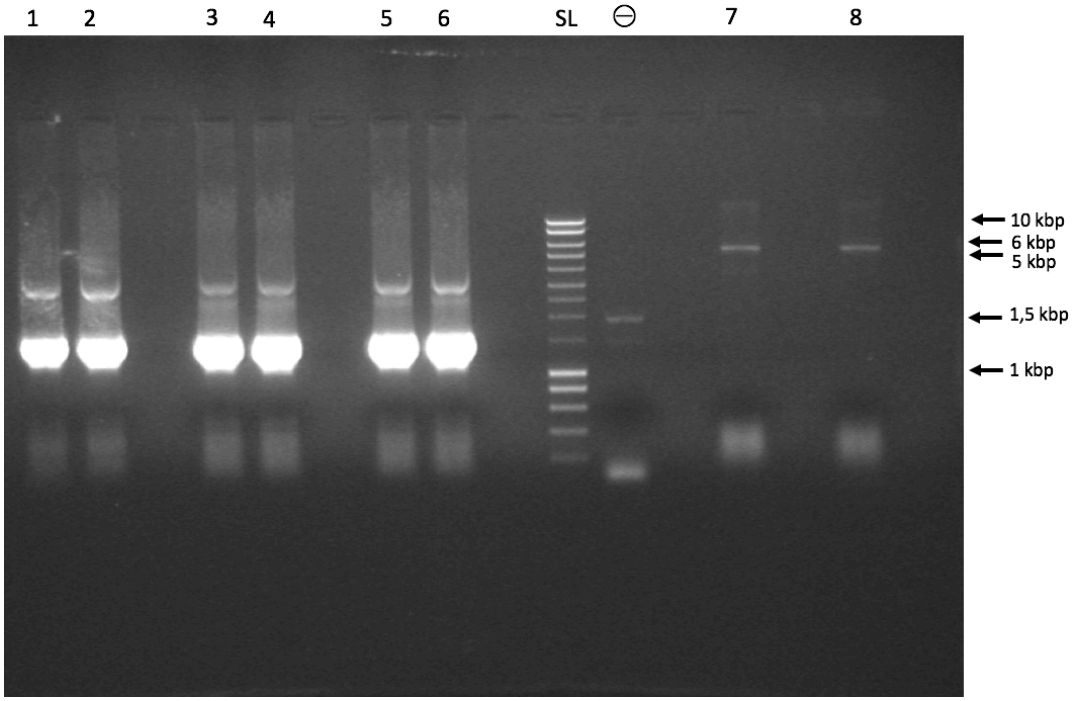

Figure 16: Image of PCR products from plasmids pSV-13, pSV-19 and pSV-20, and pDS132 after digestion with *Xba*I. 1% agarose gel. **Lane description:** 1, 2: PCR products of gene construct from pSV-13. 3, 4: PCR products of gene construct from pSV-19. 5, 6: PCR products of gene construct from pSV-20. 7, 8: pDS132 digested with *Xba*I, parallel #1-2. (–)；negative (PCR master mix), SL; Smart Ladder.

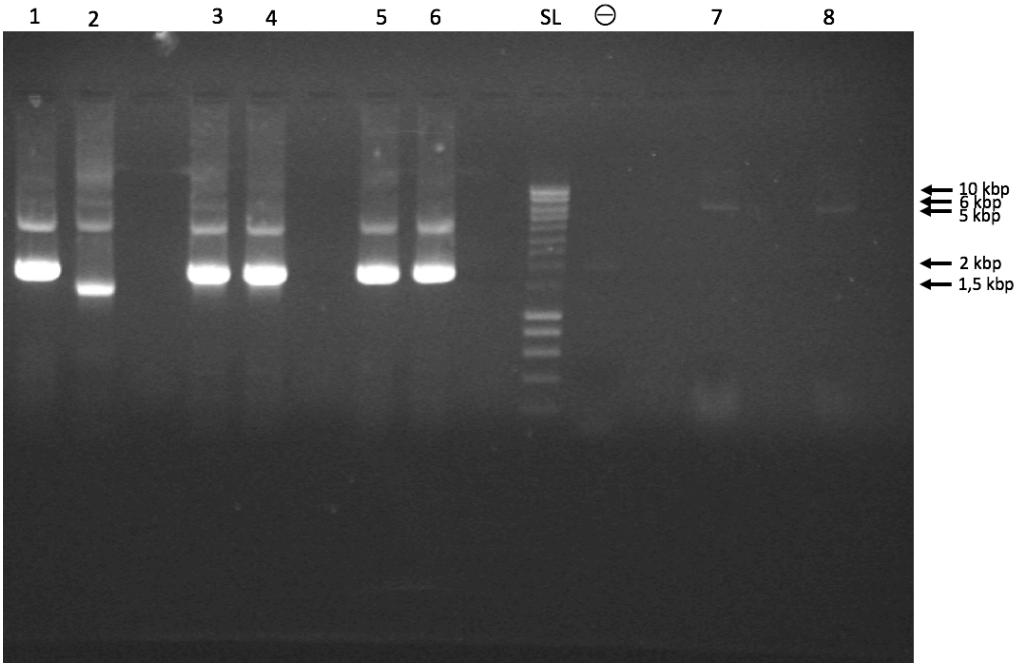

Figure 17: Image of PCR products from plasmids pSV-15, pSV-21 and pSV-24, and pDS132 after digestion with *Xba*I. 1% agarose gel. **Lane descriptions.** 1: PCR product of gene construct from pSV-15. 2: Failed PCR of gene construct from pSV-15. 3, 4: PCR products of gene construct from pSV-21. 5, 6: PCR products of gene construct from pSV-27. 7, 8: pDS132 digested with *Xba*I, parallel #3-4. (−) ; negative (PCR master mix), SL; Smart Ladder.

The ITAC method was used to assemble the HGR construct-PCR products with the linearized, dephosphorylated pDS132. For the *gyrA* constructs, 4 µL of vector DNA and 1 µL of insert DNA was used, and for the *parC* constructs, 3 µL of vector and 2 µL of insert was used. The ITAC reactions were then transformed into chemically competent MFD*pir* cells and spread on LB-agar plates containing DAP_{400} and CHL_{25}.

This approach was not successful, as there was no growth of MFD*pir* transformants, even after 48 hours of incubation. Failure of the ITAC reaction was most likely, so we took the following steps outlined below to improve the chances of successful cloning into pDS132, experimenting only with pSV-13 and pSV-19.

Troubleshooting – Gel Fragment Yields

The gel extraction of the linearized pDS132 resulted in very poor yield (9,4 ng/µL), and our first thought was that there was a problem with the gel extraction method, and that the low yields of the vector caused unsuccessful cloning. The *Xba*I digest and rSAP

dephosphorylation of pDS132 was repeated (Figure A 10 in Attachments), but this did not give higher yields from gel extraction (8,11 ng/µL).

Striving to enhance the yield of the linearized plasmid, two 25 µL digestion reactions were set up where 4 µg of pDS132 was treated with 0,5 µL *Xba*I in a prolonged six-hour digestion. The samples were then treated with rSAP and analyzed on an agarose gel by electrophoresis (Figure A 11, Attachments). The correct sized DNA bands were again eluted on a single silica column during gel extraction. This time, the Monarch® DNA Gel Extraction Kit (NEB) was used. This enlarged digest and the change of gel extraction kit did not enhance DNA yield, which resulted in an even lower plasmid concentration of 6,6 ng/µL.

Troubleshooting – ITAC Ratios

Since we were not able to improve the concentration of the pDS132 vector for ITAC assembly, we decided to try varying the vector:insert ratios. Ideally, there should be one HGR construct for every vector in the ITAC reaction. Using a 1:1 volume:volume ratio, adding 2,5 µL of both vector and insert (at different DNA concentrations) had worked well for the initial ITAC assemblies to construct the pSV-19, pSV-20, pSV-21 and pSV-24 plasmids, but optimization of this ratio could increase the likelihood of a successful cloning. In addition to a 1:1 volume:volume ratio, ratios of 1:3, 2:3, 3:1, 4:1 and 4,5:0,5 between vector and insert were tried, using pDS132 linearized plasmid with concentrations from 6,6-9,4 ng/µL. In addition, a molecular ratio was calculated as indicated in Section 2.12.4, resulting in a 1:1,67 volume:volume ratio. However, in each case, the following transformation into MFD*pir* cells resulted in no colonies on LB KM_{50} DAP_{400} plates.

Troubleshooting – Plasmid Transformation

To rule out the possibility that transformation into the MFD*pir* chemically competent cells was unsuccessful (*e.g.* a reduced ability to obtain a plasmid) a transformation with 5 µL of the uncut pDS132 vector (71,2 ng/µL), was set up. The transformation of 356 ng of uncut pDS132 resulted in growth of approximately 100 colonies of MFD*pir* transformants on LB CHL_{25} DAP_{400} plates, which confirmed an effective transformation protocol.

This experiment did not determine the actual transformation efficiency of our competent cells, as this typically is measured by counting visible colonies after transformation of only 100 pg-1 ng of DNA. Still, yielding only 100 colonies of MFD*pir* transformants after transforming

356 ng was considered low, compared to the expected number of $5x10^8$ colony forming units per µg (CFU/µg) DNA (58).

We could have attempted to optimize the transformation protocol to get the best possible efficiency from our cells (*e.g.* by testing several different heat shock- and recovery times during transformation). If that would not increase the efficiency, we could have made new chemically competent MFD*pir* cells that hopefully would be more competent. But as the transformation of uncut pDS132 gave growth of transformants, (suggesting that if the ITAC reaction was efficient, we could expect transformants), we continued to evaluate the cloning process.

Troubleshooting – ITAC pDS132 Vector Fragment Concentration

Since we only had successful cloning by ITAC when joining two DNA fragments that had been amplified by PCR, and after several unsuccessful attempts on cloning the fragments after linearizing the plasmid by digestion with *Xba*I, we decided to also amplify the pDS132 vector by PCR. The primers for pDS132 (#387 #388) were designed to add regions complementary to the ends of the HGR construct amplicons, functioning as the region of overlap required for ITAC.

PCR amplification of pDS132 resulted in a 5137 bp PCR product (Figure A 12 in Attachments). Gel extraction of the correct sized-band yielded a concentration of 63,7 ng/µL. We set up ITAC reactions using this pDS132 PCR fragment and the HGR construct-PCR products from before. We expected the ITAC reaction to be successful with this enhanced vector concentration, but several attempts with volume:volume ratios of 1:1, 1:1,67, 1:3 and 3:1 (vector:insert) were tested without success, as no colonies were observed on the LB CHL_{25} DAP_{400} plates after transformation into MFD*pir*.

Troubleshooting – ITAC Reaction Efficiency

Since our original ITAC reactions were successful in the construction of pSV-19, pSV-20, pSV-21 and pSV-24, we suspected a problem with our ITAC reactions. A new batch of the ITAC reaction mixture had been made since our first successful experiments, so we evaluated the efficiency of the ITAC reaction. We did this by repeating one of our previously successful ITAC reactions. By storing all PCR-products at -20 °C during this project, we were able to repeat one of the very first ITAC reactions that had been successful, and compared the results

with the new ITAC reagents to the previous results. An ITAC reaction to assemble the pSV-19 plasmid was repeated. The reaction was then transformed into DH5-α, resulting in approximately 25 single colonies of DH5-α transformants from plating the whole transformation (1 mL). This was much fewer transformants than from the original reaction, resulting in 299 single colonies from plating 100 µL of the transformation.

This poor result suggested that at least one step in our ITAC strategy had changed, causing reduced overall efficiency. Since the transformation process into DH5-α had been evaluated previously and was successful, the transformation was unlikely to be the issue, as the protocol was thoroughly followed using DH5-α cells from the same batch. The latest prepared ITAC buffer was likely to have been less efficient than the one previously used, and a new batch should have been prepared. However, due to costs and the latency to receive the necessary reagents, we could not test this. We determined that the purification of the ITAC reactions before transformation was the only step we could optimize in the ITAC protocol.

Troubleshooting – DNA Purification Step

According to the ITAC method, following the ITAC reaction itself, the samples were to be purified with sterile Milli-Q water by drop dialysis (Section 2.12.3.1). Another method to purify such a sample is to use a kit for general DNA fragment purification, *e.g.* a PCR clean-up kit. During most DNA purification steps, some of the sample is lost. We wondered if during the drop dialysis filtration step we lost more of the DNA than with an alternative method, and that the lack of transformants was due to a loss of our sample before transformation.

We compared two DNA purification methods, drop dialysis and sample purification with a PCR clean-up kit. The same ITAC reaction that was used to investigate ITAC efficiency (assembling pSV-19) was again repeated in triplicate. Of the three resulting samples, one was not purified, one was filtered by drop dialysis, and the last was purified using the QIAquick PCR Purification Kit (Qiagen, Hilden, Germany) following manufacturer's guidelines. Each reaction was then transformed into chemically competent DH5-α cells and plated onto LB KM_{50} plates for 24 hours.

The sample purified with the PCR clean-up kit yielded the fewest transformations, with only one colony (Table 10). The ITAC followed by drop dialysis resulted in the same amount of

growth as the earlier repetition (approximately 25 colonies of DH5-α transformants from the entire 1 mL transformation), but the transformation carried out without any purification step resulted in approximately 60 colonies of DH5-α transformants, the most of the three approaches.

Table 10: Results from ITAC purification optimization. Using no filtration of ITAC products yielded the most colonies of transformants, while using a PCR Purification Kit yielded fewest colonies of transformants.

ITAC reaction to assemble pSV-19	Purification step	Number of visible colonies
Original ITAC	Drop dialysis	299 colonies (100 µL transformation)
Repeated ITAC	Drop dialysis	~ 25 colonies (1 mL transformation)
Second repetition #1	Drop dialysis	~ 25 colonies (1 mL transformation)
Second repetition #2	PCR Purification Kit	1 colony (1 mL transformation)
Second repetition #3	No purification	~ 60 colonies (1 mL transformation)

For the PCR clean up kit, some of the DNA was either bound to the silica column and not released during elution, or was not initially bound to the column and the DNA was washed away alongside contaminants during the washing step. During the drop dialysis, DNA might be lost by diffusion into the water, or loss of some of the sample could occur when pipetting off of the filter.

Nevertheless, the rationale for purifying the samples is to get rid of excess reaction residues, and clean DNA is considered optimal for the transformation process. But since we had the greatest success without cleanup of the ITAC reaction, we made another attempt to join the PCR amplified pDS132 vector and the PCR amplified HGR constructs. Again we used different ratios of the pDS132 vector to the construct inserts, but without any filtration step before transformation of the samples into MFD*pir*. The ratios tested were 1:1, 1:1,67, 1:3 and 2:3, however none of these reactions yielded transformants on LB CHL_{25} DAP_{400} plates.

Remaining Variables

While we were able to optimize and eliminate a number of variables to improve the ITAC reaction and transformation procedure, our initial approach to move the gene constructs from pSV-13, pSV-15, pSV-19, pSV-20, pSV-21, and pSV-24 into pDS132 by ITAC, was not successful. See Figure 18 for illustration of the trouble shooting process and cloning attempts with the pDS132.

Ultimately, the inefficiency of the ITAC could have been due to partial overlapping regions elsewhere in the plasmid. Deciding on a different region of overlap where the HGR constructs were to be inserted in pDS132, could improve the success of this method. We were unable to eliminate two major sources of reduced efficiency that should be further investigated: the new ITAC reaction buffer yielded over 100 fold fewer transformants (25 vs 2990 colonies per 1 mL transformation in DH5-α cells) and the low efficiency of transformation into chemically-competent MFD*pir* cells.

If we were to continue attempts to move the HGR constructs into the vector by ITAC, our next approach would have been to produce new ITAC buffer. Amongst other cautions, keeping the enzymes in the ITAC buffer at cool temperatures at all times is key in order for the enzymes in the reaction buffer to remain active.

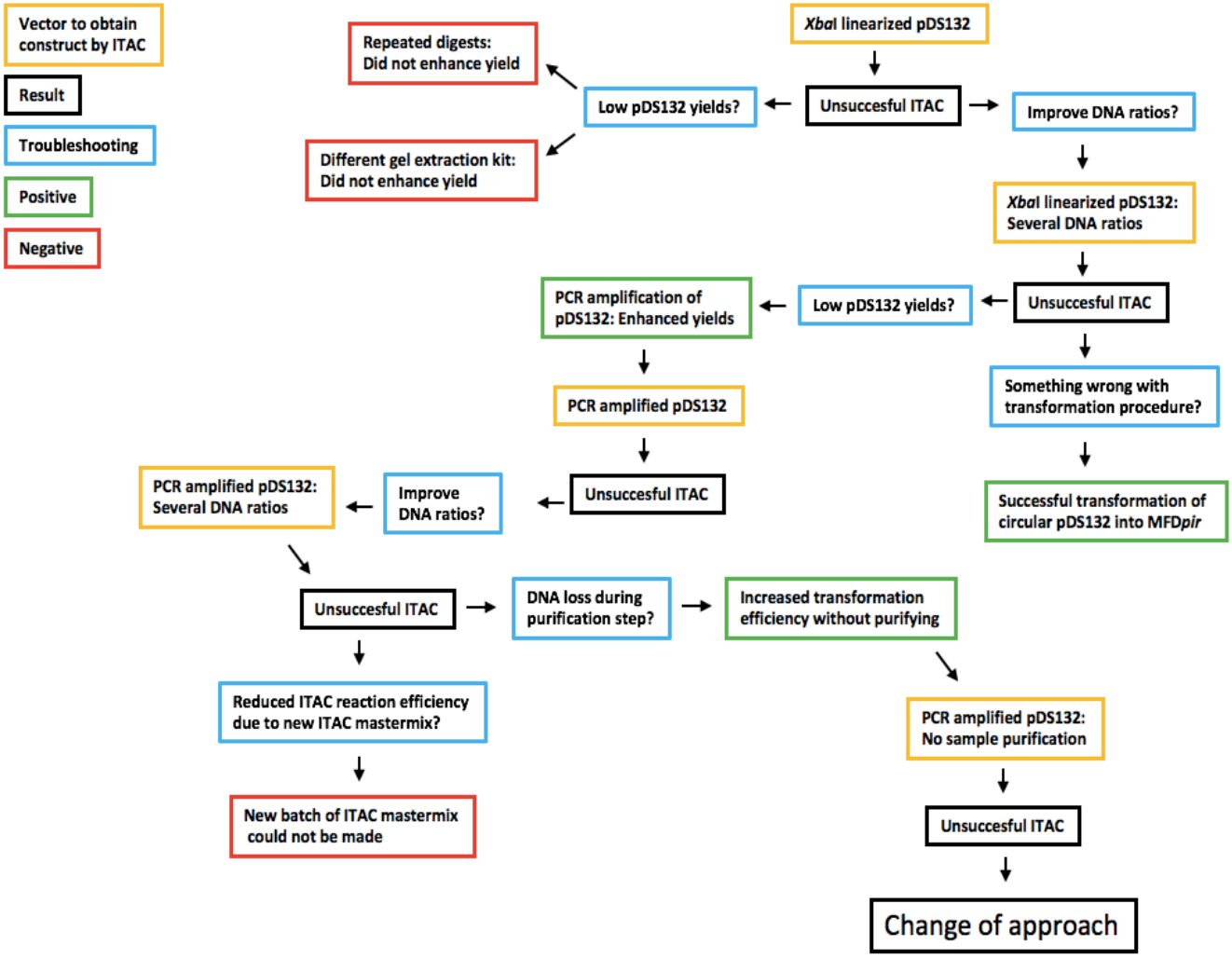

Figure 18: Flow chart of attempts made to clone HGR constructs into pDS132 by ITAC. After several attempts to optimize the ITAC procedure, we decided to change approach.

3.2.3 Molecular Cloning of *gyrA* and *parC* Constructs into pEX6K

We decided to use more traditional methods to move the HGR constructs into pDS132. Cutting both vector and insert with one restriction endonuclease would result in compatible ends on the fragments that can be joined by DNA ligation.

However, the restriction recognition sites available on pDS132 and the sites surrounding the HGR constructs were incompatible, meaning that no known endonucleases could cut both pDS132 and the inserts for ligation. The pDS132 plasmid contained only a few restriction sites in the multiple cloning region, which greatly limited the choices for cloning into this vector.

An alternative approach would be to cut both the vector and insert with incompatible endonucleases and process the resulting ends so that both fragments have blunt ends. However, this approach was avoided in this project because of the low efficiencies of both the blunting reaction and blunt-end ligation. Instead we decided to subclone HGR constructs into another vector, pGEM®-T Easy (Figure 5), and to further clone them into an alternative conjugative plasmid, pEX6K (Figure 19), that contains compatible restriction sites with pGEM®-T Easy.

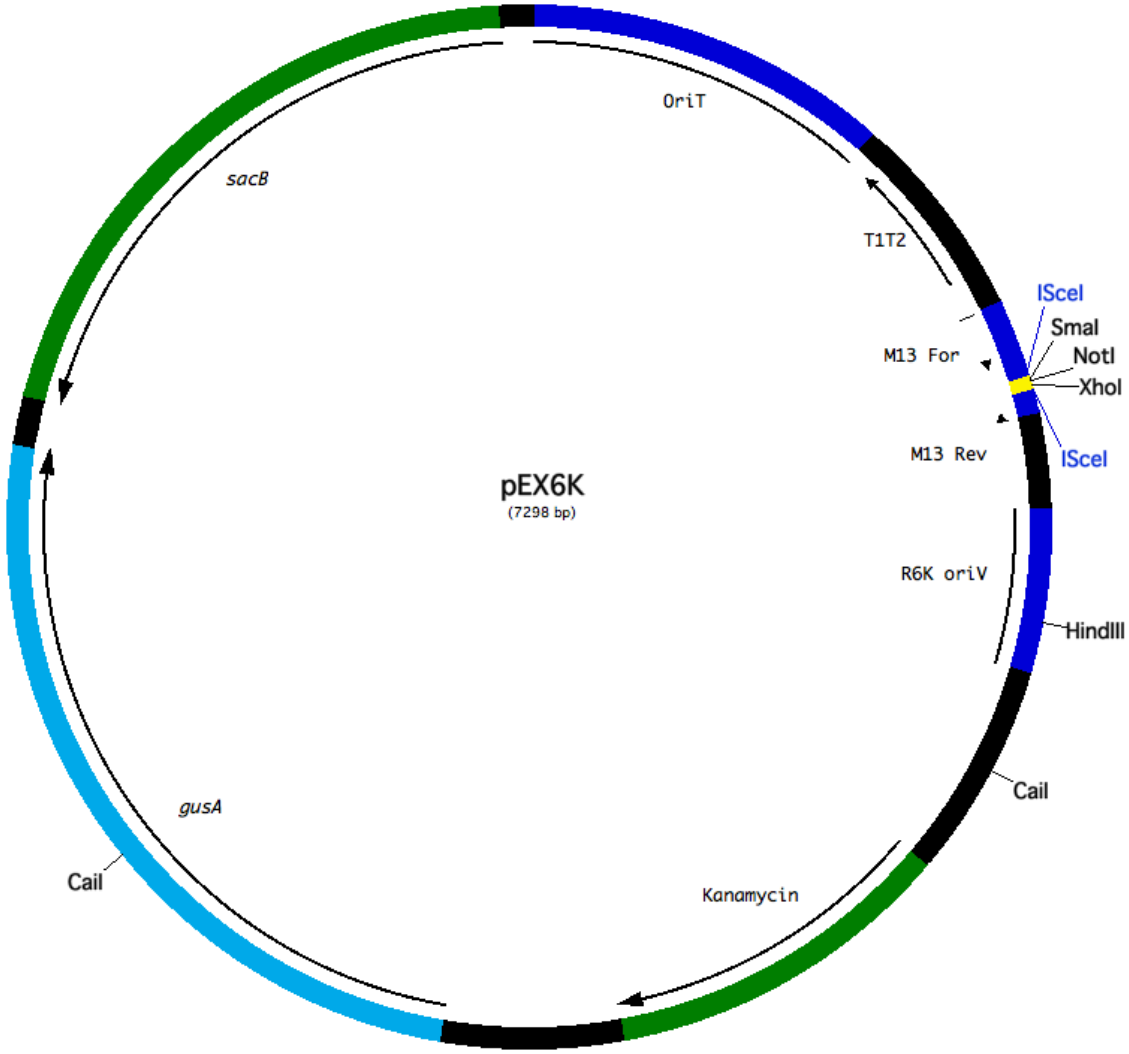

Figure 19: Plasmid map of pEX6K (7298 bp). Properties and restriction sites used in this project are indicated.

The HGR constructs were subcloned into the linearized pGEM®-T Easy vector, which contains 3´ T overhangs. For successful cloning, inserts needed to contain an extra A base in

the 5′ ends, a so called A-tail. Each of the six HGR construct-PCR products previously amplified with primers #342 and #343, were given a 5′ A-tail by incubating the samples with adenine and Dream Taq DNA polymerase (Section 2.12.2.1).

The compatible HGR constructs were ligated into the pGEM®-T Easy vector (Section 2.12.2) and then transformed into chemically competent DH5-α. The transformations were plated on LB-Agar plates with AMP_{100}, $XGal_{50}$ and $IPTG_{0,5\ mM}$. Each of the six ligations yielded single white colonies, but also blue colonies that contained the empty vector. The ligation reaction was very efficient and white colonies were observed even when plating a 1:10 dilution of the transformation.

For each ligation, four single white colonies were selected, struck for isolation on AMP_{100}, $XGal_{50}$ and $IPTG_{0,5\ mM}$ plates to confirm the lack of blue color, and grown in liquid culture with AMP_{100} the following day. Isolates were stored in glycerol freeze stocks, and plasmid DNA was isolated from the remaining liquid culture for two of the parallels, using the Monarch® Plasmid Miniprep Kit (NEB). Plasmid isolation resulted in DNA concentrations ranging from 91,0 ng/µL to 336 ng/µL. The parallel with the highest DNA concentration was selected to continue work with, plasmids pSV-25 to pSV-30.

To clone the HGR constructs from the pGEM-T Easy background into pEX6K, 1000 ng of DNA from the pSV-25 to pSV-30 plasmids was digested with *Not*I. DNA digests were then analyzed by electrophoresis (Figure 20). DNA was extracted from desired *Not*I-digested construct bands (*gyrA* constructs: 1391 bp, *parC* constructs: 1842 bp) yielding between 5,6 ng/µL and 7,3 ng/µL of DNA.

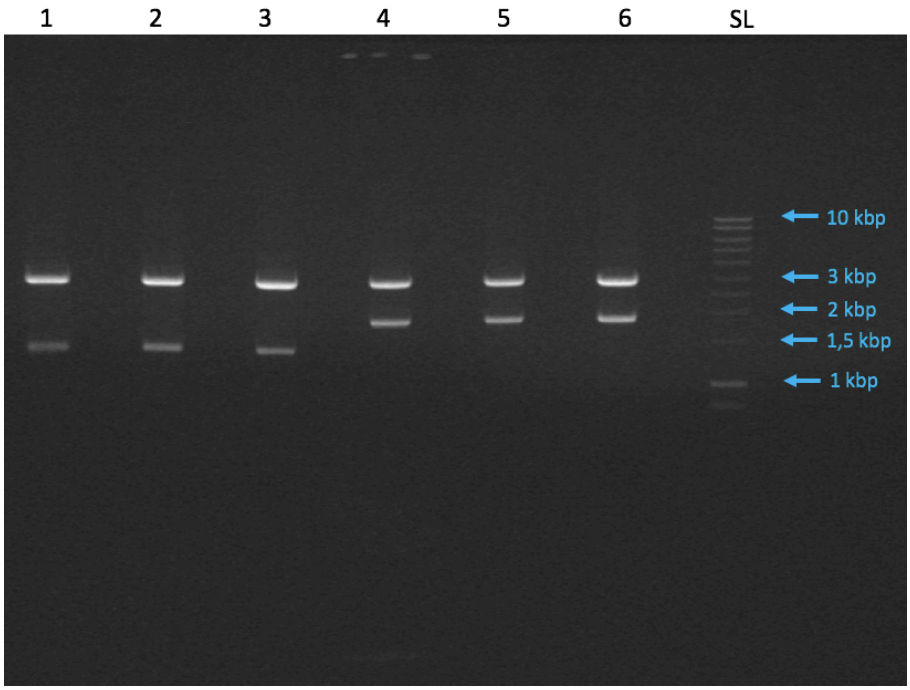

Figure 20: Image of pSV-25 to pSV-30 after digestion with *NotI* 1% agarose gel. Undigested plasmid: 2981 bp. **Lane description.** 1: pSV-25-construct. 2: pSV-26-construct. 3: pSV-27-construct. 4: pSV-28-construct. 5: pSV-29-construct. 6: pSV-30-construct. SL; Smart Ladder.

To ensure high plasmid yield, six 5 mL liquid cultures of MFD*pir* (LB KM_{50} DAP_{400}) containing the pEX6K plasmid were grown overnight and plasmid DNA was extracted. The pEX6K DNA was extracted on a single column, which resulted in a plasmid DNA concentration of 213,7 ng/µL. To linearize the plasmid and make the ends compatible with the HGR construct inserts, the pEX6K vector was also digested with *Not*I. Triplicates of 800 ng pEX6K were digested followed by dephosphorylation of the ends with rSAP. The linearized plasmid was not analyzed by electrophoresis as the uncut plasmid would be of almost the same size. The linearized plasmid was instead purified after the digestion reaction by using the gel extraction kit, yielding a plasmid concentration of 59,7 ng/µL.

The *Not*I treated pEX6K vector and HGR constructs were fused together by ligation (Section 2.12.4), and transformed into MFD*pir* before plating on LB KM_{50} DAP_{400}. Tiny colonies of MFD*pir* transformants had grown after overnight incubation. Four colonies from each ligation were isolated by plating on LB KM_{50} DAP_{400} and grown in liquid the following day, before being stored in glycerol freeze stocks. Remains of the liquid cultures from two of the four parallels were used for plasmid isolation. Plasmid isolation of the transformants yielded very little plasmid DNA with concentrations ranging from 3,4-13,2 ng/µL. However for

pEX6K-K56-78-WT-*gyrA*$_{(S83L\ A119E)}$ parallel #2 (pSV-32), plasmid isolation resulted in a much higher DNA concentration of 298,3 ng/µL. The plasmids with the highest yield were chosen, pSV-31 to pSV-36.

Because plasmid yields from pSV-31, pSV-33 to pSV-36 were so low, it was possible that the transformants did not contain the correct plasmid. The colonies of MFD*pir* transformants after ligation with pEX6K were tiny and we were suspicious of whether the small colony growth could be contamination of the plates. A clean LB KM_{50} DAP_{400} was incubated overnight, but nothing grew on the plate, suggesting that no contamination had occurred when pouring the plates.

The ligations of the HGR constructs with pEX6K should have been repeated for pSV-31, and pSV-33 to pSV-36, but we decided to proceed with pSV-32 that yielded high plasmid concentration after isolation.

To confirm successful ligation of the *gyrA* construct into pEX6K in pSV-32, the plasmid DNA was sequentially digested with *Sma*I, *Xho*I and a third endonuclease to confirm the orientation of the insertions, *Hind*III. The pEX6K-*parC* derivatives were supposed to be digested with *Cai*I. However, only pSV-32 could be digested, as the plasmid concentrations after isolation from MFD*pir* were too low to setup the DNA digestions (it would not be possible to visualize the DNA bands after digestion).

Digestions with *Sma*I, *Xho*I and *Hind*III were setup of pSV-32, pEX6K and the pEX6K predecessor, pEXKm5 (Figure 21). These digestions resulted in expected fragment sizes from pEXKm5 (7767 bp + 11bp), but not the expected fragment sizes from pEX6K (6752 bp + 535 bp + 11 bp). The pEX6K digest resulted in fragments of approximately 3500 bp + 2000 bp + 1500 bp + 650 bp, which suggested that the content of the pEX6K vector was different than expected.

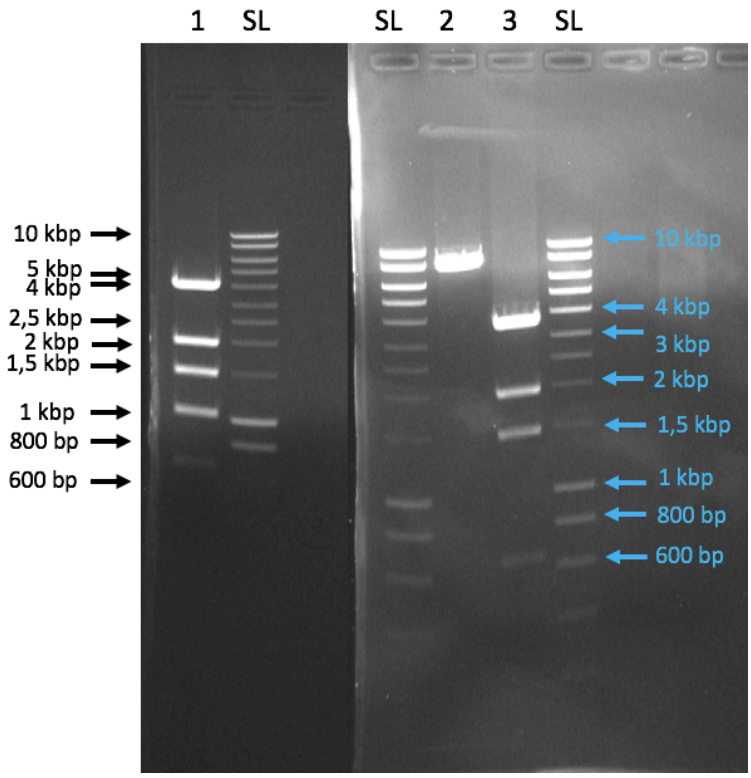

Figure 21: Image of pSV-32, pEXKm5 and pEX6K after sequential digestion with *Sma*I, *Xho*I and *Hind*III. 1% agarose gel. **Lane description.** 1: pSV-32. 2: pEXKm5. 3: pEX6K. SL; Smart Ladder.

Digestion of pSV-32 did not result in the expected fragment sizes either, and the gel image showed the same fragment sizes as for pEX6K, but with an additional fragment of approximately 1000 bp. This suggested that our insert was likely present in the pEX6K background, but that the pEX6K plasmid was not digesting as we expected.

3.3 Conjugation of pEX6K-derivatives into ECO-SENS Strains

We assumed that the K56-78-*gyrA*$_{(S83L\ A119E)}$ construct for HGR was correctly cloned into pEX6K, pSV-32. The next step was to mobilize the pSV-32 plasmid from the conjugation donor strain MFD*pir,* into the K56-WT ECO-SENS strain by conjugation.

Liquid cultures of MFD*pir* containing pSV-32 and the K56-78 WT ECO-SENS were grown overnight, representing the donor and recipient strains, respectively. The overnight cultures of both donor and recipient were inoculated together (conjugation) and individually, on one LB

DAP_{400} plate (Section 2.14). After conjugation, the MFD*pir* donor strain, the WT ECO-SENS recipient strain, and the mated cells were plated on LB KM_{50}. Only the recipient that had gained the plasmid with the KM^R marker should grow under the selective pressure, since the MFD*pir* donor strain is DAP auxotroph, and the WT ECO-SENS recipient should not be KM^R. However, plating of the strains on individual KM_{50} plates, resulted in growth of both the conjugated/mated cells (195 colonies) and the K56-78 WT ECO-SENS recipient (128 colonies).

The ECO-SENS strains used in this study are part of a pan-susceptible panel of clinical *E. coli* isolates, however, susceptibility testing of the WT ECO-SENS strains with KM had not been done previously in the MicroPop lab. We suspected that the K56-78 WT ECO-SENS strain might be resistant to KM_{50}.

3.3.1 Susceptibility Testing of WT ECO-SENS Strains

A macrobroth dilution experiment was set up to determine the rough MIC of kanamycin to inhibit growth of K56-2 WT, K56-70 WT and K56-78 WT ECO-SENS strains. Liquid cultures of LB KM_{50}, KM_{100}, KM_{200}, KM_{300} and KM_{400} with the three different strains (applied from glycrol freeze stock) were grown overnight. There was not growth in any of the cultures, except for K56-78 WT in LB KM_{50}. This suggested that plates of LB KM_{50} lacked a high enough concentration of KM to prevent growth of the K56-78 WT ECO-SENS strain following conjugation. LB KM_{100} plates were prepared and the conjugation of pSV-32 between MFD*pir* and the K56-78 WT ECO-SENS was repeated. Incubation on LB DAP_{400} and spreading of the cells on KM_{100} the following day, again resulted in growth of the K56-78 WT strain.

We suspected that the macrobroth dilution method had not resulted in accurate MIC values, so we decided to determine the MIC of KM by using a more standardized microbroth dilution method (Section 2.15). The drug concentrations which inhibited at least 90% of the growth, IC_{90}, was determined based on OD_{600} measurements with a plate-reader after incubation. The IC_{90} was calculated to be 2 µg/mL KM for all the WT ECO-SENS strains (K56-2, K56-70 and K56-78), and also for the ATCC strain, which was within the expected range for the control strain (1-4 µg/mL, (26)).

Since the strains were susceptible to KM at much lower concentrations than the LB KM_{100} plates, and the plates were made with same KM stock that was used in the microbroth assay, we suspected that a step in the conjugation method might induce KM^R in the WT ECO-SENS strains. Experiments to evaluate the effects of the washing steps, as well as plating on DAP_{400}, were set up. Liquid cultures of the K56-2, K56-70 and K56-78 WT ECO-SENS strains were grown in LB, and 30 µL of the cultures were directly spotted on both LB and LB DAP_{400} plates (without washing with $MgSO_4$). After 24 hours of incubation, the strains were washed with liquid LB according to the conjugation protocol, and the solutions were spread on KM_{100} plates. This resulted in growth of all the strains, both those that were spotted on LB and those spotted on LB DAP_{400}. From this result, we ruled out the possibility that the $MgSO_4$ washing step or spotting on LB DAP_{400} would induce KM^R in the ECO-SENS strains.

Chapter 4: Concluding Remarks and Future Aspects

The aim of this project was to develop a HGR approach to generate mutants carrying defined AMR mutations. Specifically, we aimed to study the effect of defined point mutations known to cause CIP resistance. While we were able to create HGR constructs with the desired *gyrA*$_{(S83L\ A119E)}$ or *parC*$_{(G78D)}$ mutations from the K56-2 CIP^R strain, we encountered a lot of difficulty cloning the HGR constructs into a suitable plasmid (either pDS1332 or pEX6K). Ultimately we were not able to generate CIP^R mutants by HGR, and various aspects of the protocol have yet to be optimized.

The ITAC buffer was likely to have reduced efficiency, and a new batch should be prepared. In addition, new chemically competent MFD*pir* donor cells should also be made. Further investigation to determine if there is a step in the plating of ECO-SENS strains that introduces or selects for KM^R is required if KM is to be used as resistance marker on the integrative plasmid. Designing and developing HGR approaches requires a lot of time and effort, but once established, HGR is a valuable tool to evaluate effects of defined mutations.

In the future, successful conjugation of the integrative plasmid containing the HGR constructs, and confirmation that the HGR constructs indeed have replaced the target sequence in the recipient ECO-SENS strains, will allow us to study the effects of the *gyrA*$_{(S83L\ A119E)}$ or *parC*$_{(G78D)}$ mutations. The resulting mutants can then be tested to detect changes and differences in antimicrobial susceptibility caused by these mutations. The K56-2 CIP^R containing the *gyrA*$_{(S83L\ A119E)}$ or *parC*$_{(G78D)}$ mutations displays collateral sensitivity towards different antimicrobials than the K56-70 CIP^R and K56-78 CIP^R. It will be interesting to finally investigate to what extend the *gyrA*$_{(S83L\ A119E)}$ or *parC*$_{(G78D)}$ are responsible for collateral effect changes. This work will ultimately expand our understanding of collateral susceptibility networks, and the factors that affect them, which is of importance if treatment strategies based on this phenomenon are to be introduced.

References

1. Muto A, Osawa S. The guanine and cytosine content of genomic DNA and bacterial evolution. Proceedings of the National Academy of Sciences of the United States of America. 1987;84(1):166-9.
2. Gordon DM. The ecology of *Escherichia coli*. 2013:3-20.
3. Chattopadhyay S, Sokurenko EV. Evolution of pathogenic *Escherichia coli*. 2013:45-71.
4. Nicolle LE. Epidemiology of urinary tract infections. Clinical Microbiology Newsletter. 2002;24(18):135-40.
5. Spurbeck RR, Mobley HLT. Uropathogenic *Escherichia coli*. 2013:275-304.
6. Helsedirektoratet. Cystitt: Helsedirektoratet; 2015 [updated November 9, 2015. 2.1:[Available from: http://www.antibiotikaiallmennpraksis.no/index.php?action=showtopic&topic=vXmA4Spa&j=1.
7. Helsedirektoratet. Pyelonefritt: Helsedirektoratet; 2016 [updated December 1, 2016. 1.3:[Available from: http://www.antibiotikaiallmennpraksis.no/index.php?action=showtopic&topic=hpwDhzb5&j=12Ish.
8. Helsedirektoratet. Nasjonal faglig retningslinje for bruk av antibiotika i sykehus 2013. Available from: https://helsedirektoratet.no/retningslinjer/antibiotika-i-sykehus/seksjon?Tittel=urinveier-5 - øvre-urinveisinfeksjon,-uvi-(pyelonefritt).
9. Statens Legemiddelverk. Preparatomtale Ciprofloxacin: Statens Legemiddelverk; 2015. Available from: https://www.legemiddelsok.no/_layouts/15/Preparatomtaler/Spc/2001-05768.pdf.
10. Reseptregisteret. Ciprofloxacin: omsetning i DDD: Folkehelseinstituttet; 2017. Available from: http://www.reseptregisteret.no/.
11. Jami M-S, Barreiro C, García-Estrada C, Martín J-F. Proteome Analysis of the Penicillin Producer *Penicillium chrysogenum*: CHARACTERIZATION OF PROTEIN CHANGES DURING THE INDUSTRIAL STRAIN IMPROVEMENT. Molecular & Cellular Proteomics : MCP. 2010;9(6):1182-98.
12. Wright GD. Q&A: Antibiotic resistance: where does it come from and what can we do about it? BMC Biology. 2010;8:123-.
13. Walsh C. Molecular mechanisms that confer antibacterial drug resistance. Nature. 2000;406(6797):775-81.
14. Green DW. The bacterial cell wall as a source of antibacterial targets. Expert Opin Ther Targets. 2002;6(1):1-19.
15. Goering RV, Dockrell HM, Zuckerman M, Roitt IM, Chiodini PL. Mims' Medical Microbiology. 5th ed. London, United Kingdom: Elsevier Health Sciences; 2013.
16. Choi SM, J.B. Folate Status: Effects on Pathways of Colorectal Carcinogenesis. The Journal of Nutrition [Internet]. 2002; 132(8):[2413S-8S pp.]. Available from: http://jn.nutrition.org/content/132/8/2413S.full.
17. Rossi M, Amaretti A, Raimondi S. Folate production by probiotic bacteria. Nutrients. 2011;3(1):118-34.
18. Liu T, Wang B, Guo J, Zhou Y, Julius M, Njire M, et al. Role of folP1 and folP2 Genes in the Action of Sulfamethoxazole and Trimethoprim Against Mycobacteria. J Microbiol Biotechnol. 2015;25(9):1559-67.
19. Bruce Alberts, Dennis Bray, Karen Hopkin, Alexander D. Johnson, Julian Lewis, Martin Raff, et al. Essential Cell Biology. New York: Garland Science Pub; 2010.

20. Chopra I, Roberts M. Tetracycline antibiotics: mode of action, applications, molecular biology, and epidemiology of bacterial resistance. Microbiol Mol Biol Rev. 2001;65(2):232-60 ; second page, table of contents.
21. Ruiz J. Mechanisms of resistance to quinolones: target alterations, decreased accumulation and DNA gyrase protection. J Antimicrob Chemother. 2003;51(5):1109-17.
22. Hooper DC. Mechanisms of fluoroquinolone resistance. Drug Resistance Updates. 1999;2(1):38-55.
23. Kohanski MA, Dwyer DJ, Collins JJ. How antibiotics kill bacteria: from targets to networks. Nature reviews Microbiology. 2010;8(6):423-35.
24. Helsedirektoratet. Antibiotikaresistens: Fra akademisk kuriositet til folkehelseproblem 2013 [cited 2017 April 1]. Available from: http://www.helsebiblioteket.no/retningslinjer/antibiotikabruk-tannhelse/antibiotikaresistens.
25. Reller LB, Weinstein M, Jorgensen JH, Ferraro MJ. Antimicrobial Susceptibility Testing: A Review of General Principles and Contemporary Practices. Clinical Infectious Diseases. 2009;49(11):1749-55.
26. EUCAST. Breakpoint tables for interpretation of MICs and zone diameters: The European Committe on Antimicrobial Susceptibility Testing; 2017 [Available from: http://www.eucast.org/fileadmin/src/media/PDFs/EUCAST_files/Breakpoint_tables/v_7.1_Breakpoint_Tables.pdf].
27. EUCAST. Antmicrobial wild type distributions of microorganisms: The European Committe on Antimicrobial Susceptibility Testing; 2017 [Available from: https://mic.eucast.org/Eucast2/].
28. Rice LB. Mechanisms of resistance and clinical relevance of resistance to beta-lactams, glycopeptides, and fluoroquinolones. Mayo Clin Proc. 2012;87(2):198-208.
29. Randall CP, Mariner KR, Chopra I, O'Neill AJ. The Target of Daptomycin Is Absent from *Escherichia coli* and Other Gram-Negative Pathogens. Antimicrobial Agents and Chemotherapy. 2013;57(1):637-9.
30. Poole K. Efflux-mediated multiresistance in Gram-negative bacteria. Clinical Microbiology and Infection. 2004;10(1):12-26.
31. Elkins CA, Mullis LB. Substrate competition studies using whole-cell accumulation assays with the major tripartite multidrug efflux pumps of *Escherichia coli*. Antimicrob Agents Chemother. 2007;51(3):923-9.
32. Pietsch F, Bergman JM, Brandis G, Marcusson LL, Zorzet A, Huseby DL, et al. Ciprofloxacin selects for RNA polymerase mutations with pleiotropic antibiotic resistance effects. J Antimicrob Chemother. 2016.
33. Bennett PM. Plasmid encoded antibiotic resistance: acquisition and transfer of antibiotic resistance genes in bacteria. Br J Pharmacol. 2008;153 Suppl 1:S347-57.
34. Griffiths AJF, Gelbart WM, Miller JH, Lewontin RC. Modern Genetic Analysis 1999. Available from: https://www.ncbi.nlm.nih.gov/books/NBK21322/.
35. Laxminarayan R, Duse A, Wattal C, Zaidi AKM, Wertheim HFL, Sumpradit N, et al. Antibiotic resistance—the need for global solutions. The Lancet Infectious Diseases. 2013;13(12):1057-98.
36. Woegerbauer M, Jenni B, Thalhammer F, Graninger W, Burgmann H. Natural Genetic Transformation of Clinical Isolates of *Escherichia coli* in Urine and Water. Applied and Environmental Microbiology. 2002;68(1):440-3.
37. Nikaido H. Multidrug resistance in bacteria. Annu Rev Biochem. 2009;78:119-46.
38. Grohmann E, Muth G, Espinosa M. Conjugative Plasmid Transfer in Gram-Positive Bacteria. Microbiology and Molecular Biology Reviews. 2003;67(2):277-301.

39. Food and Agriculture Organization of the United Nations. Antimicrobial Resistance (Animal Health) [Available from: http://www.fao.org/antimicrobial-resistance/key-sectors/animal-health/en/].
40. Eraker H, Kasnes EB, Kumano-Ensby AL. Fabrikkene skaper resistente bakterier: Norsk Rikskrinkastning (NRK); 2016 [updated March 15, 2016. Available from: https://www.nrk.no/dokumentar/xl/_-fabrikkene-skaper-resistente-bakterier-1.12853101].
41. Eliassen KE, Fetveit A, Hjortdal P, Berild D, Lindbæk M. Nye retningslinjer for antibiotikabruk i primærhelsetjenesten [New guidelines for antibiotic use in primary health care]. Tidsskriftet Den Norske Legeforening. 2008;128(20):2330-4.
42. Durante-Mangoni E, Signoriello G, Andini R, Mattei A, De Cristoforo M, Murino P, et al. Colistin and Rifampicin Compared With Colistin Alone for the Treatment of Serious Infections Due to Extensively Drug-Resistant *Acinetobacter baumannii*: A Multicenter, Randomized Clinical Trial. Clinical Infectious Diseases. 2013;57(3):349-58.
43. Brown EM, Nathwani D. Antibiotic cycling or rotation: a systematic review of the evidence of efficacy. Journal of Antimicrobial Chemotherapy. 2005;55(1):6-9.
44. Szybalski W, Bryson V. GENETIC STUDIES ON MICROBIAL CROSS RESISTANCE TO TOXIC AGENTS I.,: Cross Resistance of *Escherichia coli* to Fifteen Antibiotics. Journal of Bacteriology. 1952;64(4):489-99.
45. Imamovic L, Sommer MO. Use of collateral sensitivity networks to design drug cycling protocols that avoid resistance development. Sci Transl Med. 2013;5(204):204ra132.
46. Lazar V, Pal Singh G, Spohn R, Nagy I, Horvath B, Hrtyan M, et al. Bacterial evolution of antibiotic hypersensitivity. Mol Syst Biol. 2013;9:700.
47. Madyagol M, Al-Alami H, Levarski Z, Drahovska H, Turna J, Stuchlik S. Gene replacement techniques for *Escherichia coli* genome modification. Folia Microbiol (Praha). 2011;56(3):253-63.
48. Kahlmeter G. The ECO•SENS Project: a prospective, multinational, multicentre epidemiological survey of the prevalence and antimicrobial susceptibility of urinary tract pathogens—interim report. Journal of Antimicrobial Chemotherapy. 2000;46(suppl_1):15-22.
49. Kahlmeter G, Poulsen HO. Antimicrobial susceptibility of *Escherichia coli* from community-acquired urinary tract infections in Europe: the ECO-SENS study revisited. International Journal of Antimicrobial Agents. 2012;39(1):45-51.
50. Ferrières L, Hémery G, Nham T, Guérout A-M, Mazel D, Beloin C, et al. Silent Mischief: Bacteriophage Mu Insertions Contaminate Products of *Escherichia coli* Random Mutagenesis Performed Using Suicidal Transposon Delivery Plasmids Mobilized by Broad-Host-Range RP4 Conjugative Machinery. Journal of Bacteriology. 2010;192(24):6418-27.
51. Messing J. [2] New M13 vectors for cloning. Methods in Enzymology. 1983;101:20-78.
52. Philippe N, Alcaraz J-P, Coursange E, Geiselmann J, Schneider D. Improvement of pCVD442, a suicide plasmid for gene allele exchange in bacteria. Plasmid. 2004;51(3):246-55.
53. Untergasser A, Cutcutache I, Koressaar T, Ye J, Faircloth BC, Remm M, et al. Primer3—new capabilities and interfaces. Nucleic Acids Research. 2012;40(15):e115-e.
54. Lehnman IR. DNA Ligase: Structure, Mechanism, and Function. Science. 1974;186(4166):790.

55. Gibson DG, Young L, Chuang RY, Venter JC, Hutchison CA, 3rd, Smith HO. Enzymatic assembly of DNA molecules up to several hundred kilobases. Nat Methods. 2009;6(5):343-5.
56. NEB. Overview of the Gibson Assembly Cloning Method [Available from: https://www.neb.com/products/e5510-gibson-assembly-cloning-kit.
57. Inoue H, Nojima H, Okayama H. High efficiency transformation of *Escherichia coli* with plasmids. Gene. 1990;96(1):23-8.
58. Hanahan D. Studies on transformation of *Escherichia coli* with plasmids. Journal of Molecular Biology. 1983;166(4):557-80.

Attachments

Table A 1: Antimicrobials and chemicals added to growth media.

Antimicrobial	Final Concentration	Selection for
Kanamycin	50 µg/mL	pCR®-Blunt, pEX6K
Chloramphenicol	25 µg/mL	pDS132
Ampicillin	100 µg/mL	pGEM®-T Easy
XGal	50 µg/mL	pGEM®-T Easy
IPTG	0,5 mM	pGEM®-T Easy
DAP	400 µg/mL	MFD*pir*

Table A 2: Table of plasmids constructed in this project

Plasmid name	Descriptive plasmid name	Description of DNA content	Resistance and requirements
pSV-1	pCR-Blunt-K56-70-WT-*gyrA*-3	pCR®-Blunt (3500 bp) + K56-70-WT *gyrA* PCR product (1321 bp, primers #326+ 327) clone #3 orientation 2	KM_{50}
pSV-2	pCR-Blunt-K56-70-WT-*gyrA*-4	pCR®-Blunt (3500 bp) + K56-70-WT *gyrA* PCR product (1321 bp, primers #326 #327) clone #4 orientation 2	KM_{50}
pSV-3	pCR-Blunt-K56-78-WT-*gyrA*-1	pCR®-Blunt (3500 bp) + K56-78-WT *gyrA* PCR product (1321 bp, primers #326 #327) clone #1 orientation 1	KM_{50}
pSV-4	pCR-Blunt-K56-78-WT-*gyrA*-2	pCR®-Blunt (3500 bp) + K56-78-WT *gyrA* PCR product (1321 bp, primers #326 #327) clone #2 orientation 2	KM_{50}
pSV-5	pCR-Blunt-K56-70-WT-*parC*-1	pCR®-Blunt (3500 bp) + K56-70-WT *parC* PCR product (1772 bp, primers #328 #329) clone #1	KM_{50}

		orientation 1	
pSV-6	pCR-Blunt-K56-70-WT-*parC*-4	pCR®-Blunt (3500 bp) + K56-70-WT *parC* PCR product (1772 bp, primers #328 #329) clone #4 orientation 2	KM_{50}
pSV-7	pCR-Blunt-K56-78-WT-*parC*-1	pCR®-Blunt (3500 bp) + K56-78-WT *parC* PCR product (1772 bp, primers #328 #329) clone #1 orientation 1	KM_{50}
pSV-8	pCR-Blunt-K56-78-WT-*parC*-3	pCR®-Blunt (3500 bp) + K56-78-WT *parC* PCR product (1772 bp, primers #328 #329) clone #3 orientation 2	KM_{50}
pSV-11	pCR-Blunt-K56-2-CIP^R-*gyrA*-1	pCR®-Blunt (3500 bp) + K56-2-CIP^R *gyrA* PCR product (1321 bp, primers #326 #327) clone #1 orientation 1	KM_{50}
pSV-12	pCR-Blunt-K56-2-CIP^R-*gyrA*-2	pCR®-Blunt (3500 bp) + K56-2-CIP^R *gyrA* PCR product (1321 bp, primers #326 #327) clone #2 orientation 1	KM_{50}
pSV-9	pCR-Blunt-K56-2-CIP^R-*parC*-3	pCR®-Blunt (3500 bp) + K56-2-CIP^R *parC* PCR product (1772 bp, primers #328 #329) clone #3 orientation 1	KM_{50}
pSV-10	pCR-Blunt-K56-2-CIP^R-*parC*-4	pCR®-Blunt (3500 bp) + K56-2-CIP^R *parC* PCR product (1772 bp, primers #328 #329) clone #4 orientation 1	KM_{50}
pSV-13	pCR-Blunt-K56-2-WT-*gyrA*-1	pCR®-Blunt (3500 bp) + K56-2-WT *gyrA* PCR product (1321 bp, primers #326 #327) clone #1 orientation 1	KM_{50}
pSV-14	pCR-Blunt-K56-2-WT-*gyrA*-2	pCR®-Blunt (3500 bp) + K56-2-WT *gyrA* PCR product (1321 bp, primers #326 #327) clone #2 orientation 2	KM_{50}
pSV-15	pCR-Blunt-K56-2-WT-*parC*-2	pCR®-Blunt (3500 bp) + K56-2-WT *parC* PCR product (1772 bp, primers #328 #329) clone #2 orientation 2	KM_{50}
pSV-16	pCR-Blunt-K56-2-WT-*parC*-4	pCR®-Blunt (3500 bp) + K56-2-WT *parC* PCR product (1772 bp, primers #328 #329) clone #4 orientation 2	KM_{50}
pSV-17	pCR-Blunt-K56-78-WT-*parC*-2	pCR®-Blunt (3500 bp) + K56-78-WT *parC* PCR product (1772 bp, primers #328 #329) clone #3 orientation 1	KM_{50}

pSV-18	pCR-Blunt-K56-78-WT-*parC*-4	pCR®-Blunt (3500 bp) + K56-78-WT *parC* PCR product (1772 bp, primers #328 #329) clone #3 orientation 1	KM_{50}
pSV-19	pCR-Blunt-K56-70-WT-*gyrA*$_{(S83L\ A119E)}$	PCR products of pCR-Blunt-K56-70-WT-*gyrA*-portion from pSV-2 (4477 bp, primers #330 #331) + *gyrA*$_{(S83L\ A119E)}$ from pSV-11 (356 bp, primers #324 #325) clone #1	KM_{50}
pSV-20	pCR-Blunt-K56-78-WT-*gyrA*$_{(S83L\ A119E)}$	PCR products of pCR-Blunt-K56-78-WT-*gyrA*-portion from pSV-3 (4477 bp, primers #330 #331) + *gyrA*$_{(S83L\ A119E)}$ from pSV-11 (356 bp, primers #324 #325) clone #1	KM_{50}
pSV-21	pCR-Blunt-K56-70-WT-*parC*$_{(G78D)}$	PCR products of pCR-Blunt-K56-70-WT-*parC*-portion from pSV-5 (5172 bp, primers #334 #335) + *parC*$_{(G78D)}$ from pSV-9 (112 bp, primers #332 #333) clone #2	KM_{50}
pSV-22	pCR-Blunt-K56-"78"-WT-*parC*$_{(G78D)}$-(70 WT)	PCR products of pCR-Blunt-K56-78-WT-*parC*-portion from pSV-7 (5172 bp, primers #334 #335) + *parC*$_{(G78D)}$ from pSV-9 (112 bp, primers #332 #333) clone #2	KM_{50}
pSV-23	pCR-Blunt-K56-78-WT-*parC*$_{(G78D)}$-SNP	**(Repetition)** PCR products of pCR-Blunt-K56-78-WT-*parC*-portion from pSV-7 (5172 bp, primers #334 #335) + *parC*$_{(G78D)}$ from pSV-9 (112 bp, primers #332 #333) clone #2	KM_{50}
pSV-24	pCR-Blunt-K56-78-WT-*parC*$_{(G78D)}$	**(2. Repetition)** PCR products of pCR-Blunt-K56-78-WT-*parC*-portion from pSV-7 (5172 bp, primers #334 #335) + *parC*$_{(G78D)}$ from pSV-9 (112 bp, primers #332 #333) clone #4	KM_{50}
pSV-25	pGEM-T-Easy-K56-70-WT-*gyrA*$_{(S83L\ A119E)}$	pGEM®-T Easy (3015 bp) + A-tailed PCR product of K56-70-WT-*gyrA*$_{(S83L\ A119E)}$ gene construct from pSV-19 (1357 bp)	AMP_{100}
pSV-26	pGEM-T-Easy-K56-78-WT-*gyrA*$_{(S83L\ A119E)}$	pGEM®-T Easy (3015 bp) + A-tailed PCR product of K56-78-WT-*gyrA*$_{(S83L\ A119E)}$ gene construct from pSV-20 (1357 bp)	AMP_{100}
pSV-27	pGEM-T-Easy-K56-70-WT-*parC*$_{(G78D)}$	pGEM®-T Easy (3015 bp) + A-tailed PCR product of K56-70-WT-*parC*$_{(G78D)}$ gene construct from pSV-21 (1808 bp)	AMP_{100}

pSV-28	pGEM-T-Easy-K56-78-WT-*parC*$_{(G78D)}$	pGEM®-T Easy (3015 bp) + A-tailed PCR product of K56-78-WT-*parC*$_{(G78D)}$ gene construct from pSV-24 (1808 bp)	AMP_{100}
pSV-29	pGEM-T-Easy-K56-2-WT-*gyrA*	pGEM®-T Easy (3015 bp) + A-tailed PCR product of K56-2-WT-*gyrA* gene construct from pSV-13 (1357 bp)	AMP_{100}
pSV-30	pGEM-T-Easy-K56-2-WT-*parC*	pGEM®-T Easy (3015 bp) + A-tailed PCR product of K56-2-WT-*parC* gene construct from pSV-25 (1808 bp)	AMP_{100}
pSV-31	pEX6K-K56-70-WT-*gyrA*$_{(S83L\ A119E)}$	*Not*I-treated pEX6K (7298 bp) + K56-70-WT-*gyrA*$_{(S83L\ A119E)}$ gene construct released from pSV-25	KM_{50}, requires DAP_{400}
pSV-32	pEX6K-K56-78-WT-*gyrA*$_{(S83L\ A119E)}$	*Not*I-treated pEX6K (7298 bp) + K56-78-WT-*gyrA*$_{(S83L\ A119E)}$ gene construct released from pSV-26	KM_{50}, requires DAP_{400}
pSV-33	pEX6K-K56-70-WT-*parC*$_{(G78D)}$	*Not*I-treated pEX6K (7298 bp) + K56-70-WT-*parC*$_{(G78D)}$ gene construct released from pSV-27	KM_{50}, requires DAP_{400}
pSV-34	pEX6K-K56-78-WT-*parC*$_{(G78D)}$	*Not*I-treated pEX6K (7298 bp) + K56-78-WT-*parC*$_{(G78D)}$ gene construct released from pSV-28 by	KM_{50}, requires DAP_{400}
pSV-35	pEX6K-K56-2-WT-*gyrA*	*Not*I-treated pEX6K (7298 bp) + K56-2-WT-*gyrA* gene construct released from pSV-30	KM_{50}, requires DAP_{400}
pSV-36	pEX6K-K56-2-WT-*parC*	*Not*I-treated pEX6K (7298 bp) + K56-2-WT-*parC* gene construct released from pSV-30	KM_{50}, requires DAP_{400}

Table A 3: Primers (oligonucleotides) used in this project.

#	Name	Sequence (5´-3´)	T_M (°C)	T_A (°C)	Extension time (sec)	Amplicon size (bp)
326	*gyrA*-F	CACAACCGACATCGAGCAC	65,7	64	40	1321
327	*gyrA*-R	GCAACTGGGTCTGGGAGTAG	63,7	64	40	1321
324	*gyrA*-K56-2 CIP-F	ACCGGTCAACATTGAGGAAG	63,9	62	15	356
325	*gyrA*-K56-2 CIP-R	CCAGACGGATTTCCGTATAAC	62,0	62	15	356
330	pCR-Blunt-*gyrA*-ITAC-F	CATCGACGGCGACTCTGCGGCGGAA ATGCGTTATACGGAAATCCGTCTGG	92,2	62	140	4477
331	pCR-Blunt-*gyrA*-ITAC-R	TCGCATAATCCAGATAGGAGCTCTT CAGCTCTTCCTCAATGTTGACCGGT	85,2	62	140	4477
328	*parC*-F	CTATCTTGATGCCCGACGAG	64,6	64	55	1772
329	*parC*-R	GCAAGATGACGCAGTTTCAG	63,6	64	55	1772
332	*parC*-K56-2 CIP-F	TACCGTCGGTGACGTACTGG	65,9	64	15	112
333	*parC*-K56-2 CIP-R	ACCATCAACCAGCGGATAAC	63,7	64	15	112
334	pCR-Blunt-*parC*-ITAC-F	TGGTCCTGATGGCGCAGCCGTTCTC TTACCGTTATCCGCTGGTTGATGGT	91,0	64	160	5172
335	pCR-Blunt-*parC*-ITAC-R	AGGCACTATCGTCGTGCGGATGGTA TTTACCCAGTACGTCACCGACGGTA	87,4	64	160	5172
348	pCRBlunt-Ins-ITAC-F	AGGTATATGTGATGGGTTAAAAAGGATCG ATCCTCTAGCGAGCTCGGATCCACTAGTAA	83	66	42/56	1394/1845
349	pCRBlunt-Ins-ITAC-R	CCGGGAGAGCTCGATATCGCATGCGGTA CCTCTAGGCCAGTGTGATGGATATCTGC	90	66	42/56	1394/1845
342	pCRB-Ins-F	CGAGCTCGGATCCACTAGTAA	63,2	66	41/54	1357/1808

343	pCRB-Ins-R	GCCAGTGTGATGGATATCTGC	64,4	66	41/54	1357/1808
388	pDS132+pCRB-Ins-ITAC-F	CTGAATTCTGCAGATATCCATCACA CTGGCGTTATCCGCTCACAATTCCA	86,4	61	154	5137
389	pDS132+pCRB-Ins-ITAC-F	TGGCGGCCGTTACTAGTGGATCCGA GCTCGCGATCCTTTTTAACCCATCA	89,7	61	154	5137
300	M13-F	GTAAAACGACGGCCAGT	58,7	50	240	Variable
301	M13-R	AACAGCTATGACCATG	48,6	50	240	Variable

Table A 4: Restriction endonucleases and corresponding buffers. All endonucleases and buffers are from NEB, except *Cai*I (Thermo Fisher Scientific).

Restriction Endonuclease	**Buffer**	**Temperature °C**
*Sac*I	Buffer 1.1.	37
*Eco*RI	Special *Eco*RI buffer	37
*Eco*RV	CutSmart	37
*Dpn*I	(No buffer used)	37
*Xba*I	CutSmart	37
*Not*I	CutSmart	37
*Sma*I	CutSmart	25
*Xho*I	CutSmart	37
*Hind*III	CutSmart	37
*Cai*I	Tango	37

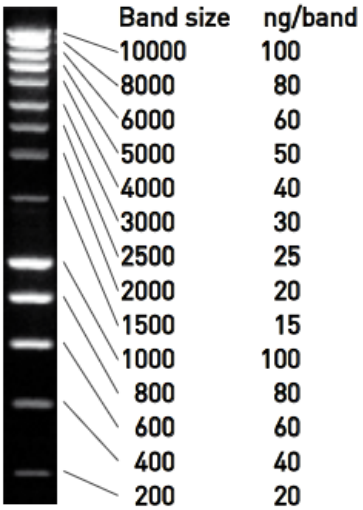

Figure A 1: Smart Ladder *MW-1700-10*, from Eurogentec (Seraing, Belgium). Band sizes in bp.

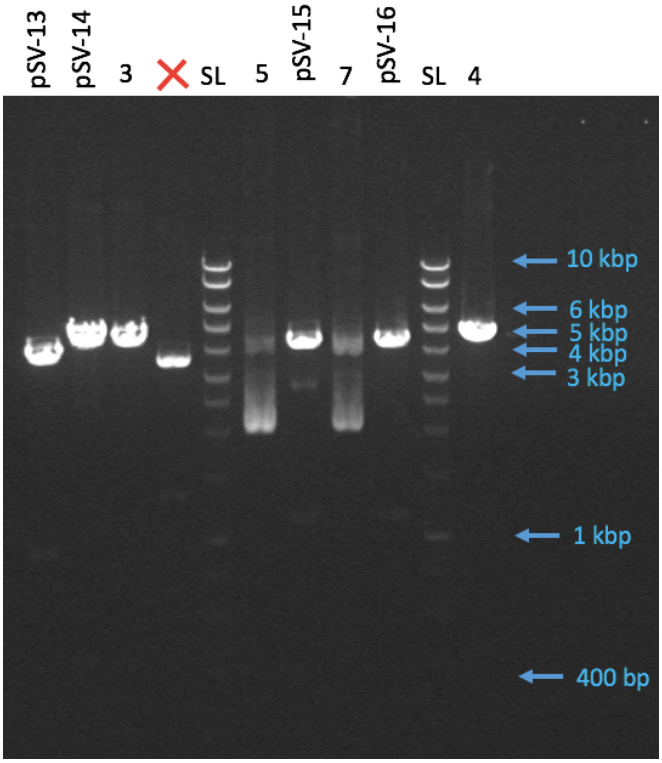

Figure A 2: Image of pCR-Blunt-*gyrA* and pCR-Blunt-*parC* plasmids with gene inserts from K56-2 WT, after digestion with *Sac*I (plasmid w/*gyrA*) and *Eco*RV (plasmid w/*parC*). (1% agarose gel.) 3, 4: pCR-Blunt-K56-2-WT-*gyrA* clone #3 and #4. 5, 7: Unsuccessful digest of pCR-Blunt-K56-2-WT-*parC* clone #1 and #3. SL; Smart Ladder

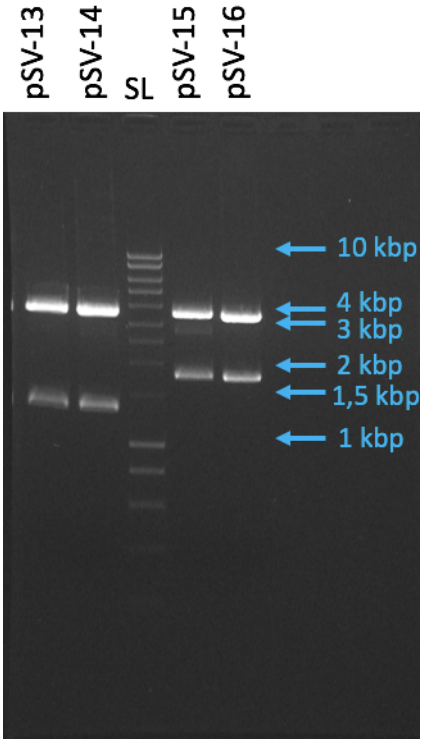

Figure A 3: Image of pSV-13 to pSV-16 plasmids with *gyrA*/parC gene inserts from K56-2 WT, after digestion with *Eco*RI. (1 % agarose gel.) The digest showed expected fragment sizes in all of the cases. SL; Smart Ladder.

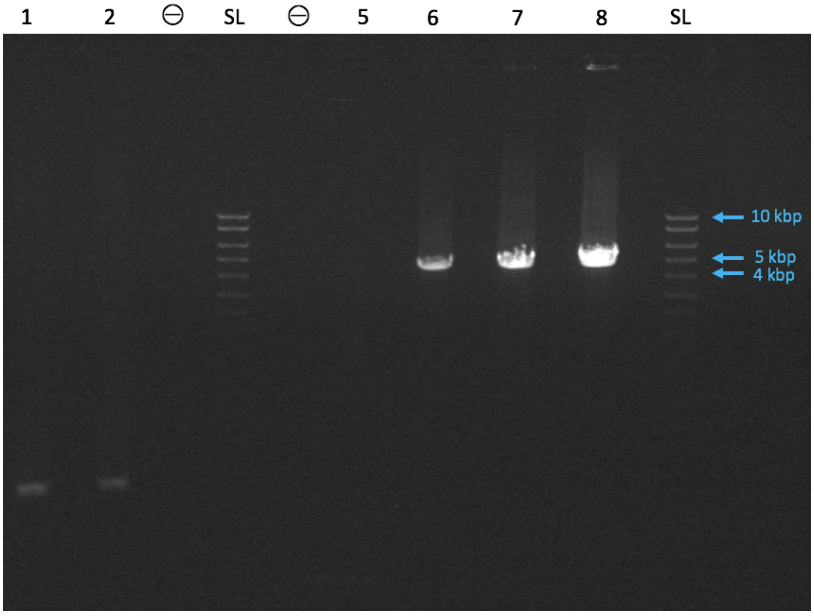

Figure A 4: Image of PCR products from plasmids pSV-11, pSV-2, pSV-3. (1 % agarose gel.) **Lane descriptions.** 1, 2: PCR products of $gyrA_{(S83L\ A119E)}$ from pSV-11. 5: Failed PCR K56-70-WT-*gyrA*-portion from pSV-2. 6: PCR product K56-70-WT-*gyrA*-portion from pSV-2. 7, 8: PCR products K56-78-WT-*gyrA*-portion from pSV-3. (−); negative (PCR master mix), SL; Smart Ladder.

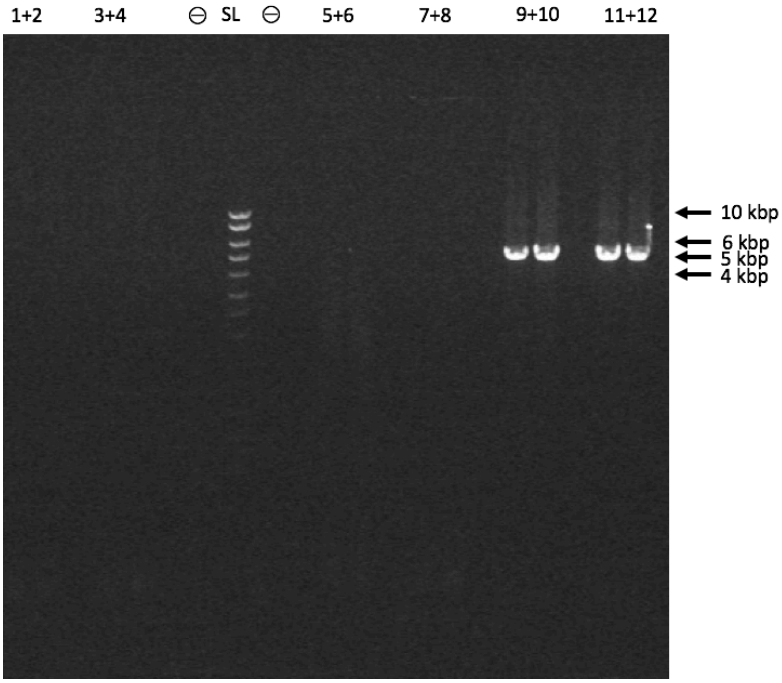

Figure A 5: Image of PCR products from plasmids pSV-11, pSV-2, pSV-3. (1 % agarose gel.) **Lane descriptions.** 1, 2: PCR products of *gyrA*$_{(S83L\ A119E)}$ from pSV-11. 5: Failed PCR K56-70-WT-*gyrA*-portion from pSV-2. 6: PCR product K56-70-WT-*gyrA*-portion from pSV-2. 7, 8: PCR products K56-78-WT-*gyrA*-portion from pSV-3. (−); negative (PCR master mix), SL; Smart Ladder.

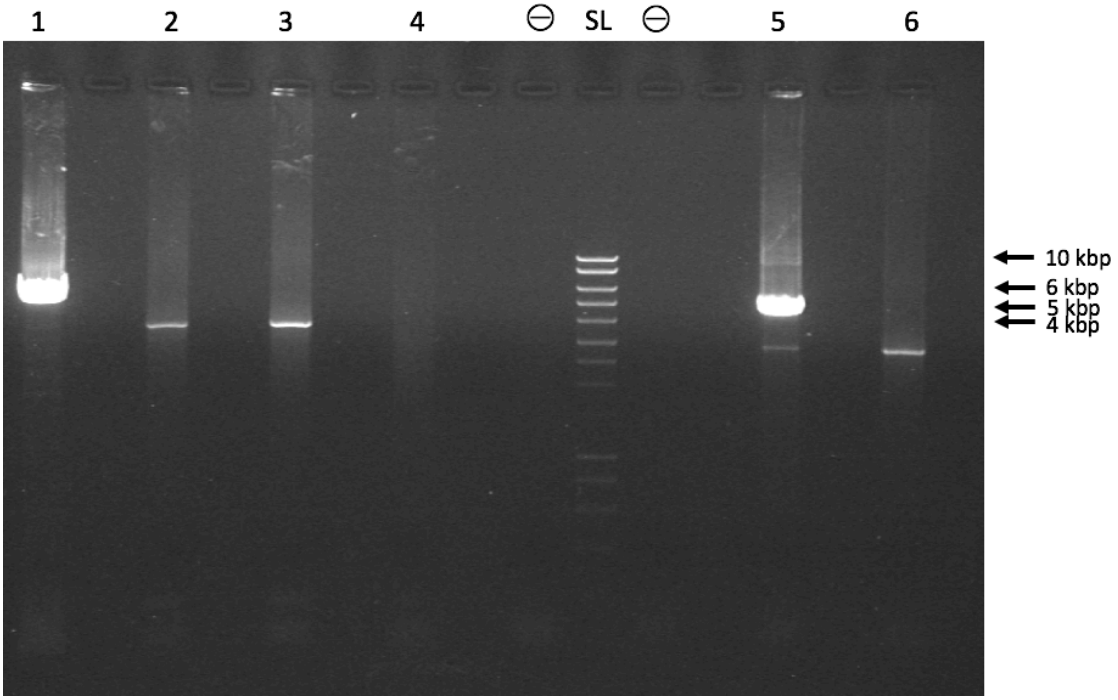

Figure A 6: Image of PCR products from plasmids pSV-5, pSV-7, and (repeated) pSV-2 (1 % agarose gel). **Lane description:** 1: PCR product K56-70-WT-*parC*-portion from pSV-5. 2: Failed PCR from pSV-5. 3, 4: Failed PCR from pSV-7. 5: PCR product K56-70-WT-*gyrA*-portion from pSV-2. 6: Failed PCR from pSV-2. (−); negative (PCR master mix), SL; Smart Ladder.

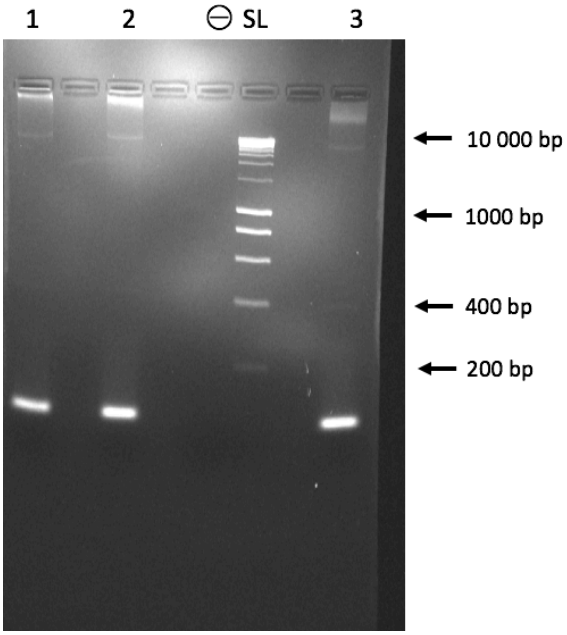

Figure A 7: Image of PCR products from plasmids pSV-9. (2 % agarose gel.) **Lane descriptions:** 1, 2, 3: PCR product of *parC*$_{(G78D)}$ from pSV-9. (−); negative (PCR master mix), SL; Smart Ladder.

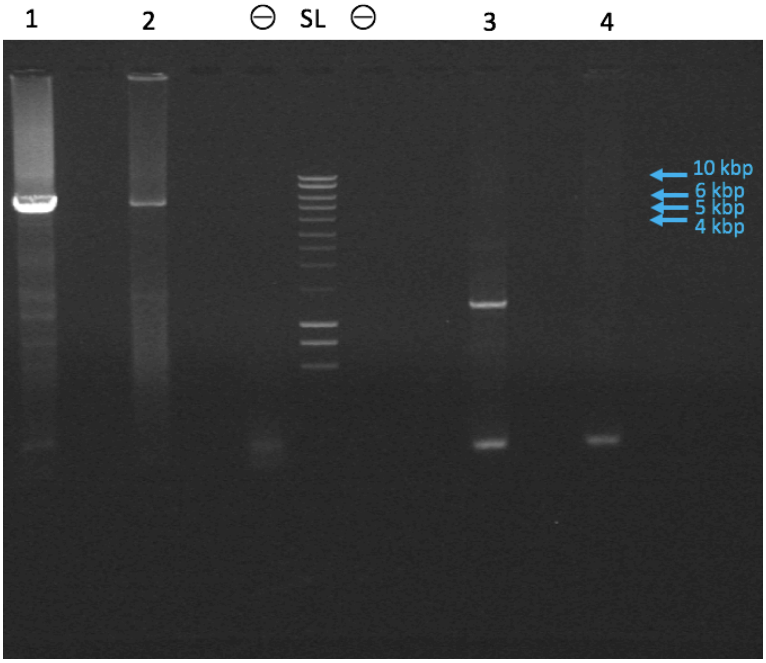

Figure A 8: Image of PCR products from plasmids pSV-7 and pSV-9. (1 % agarose gel.) **Lane descriptions:** 1, 2: PCR products of K56-78-WT-*parC*-portion from pSV-7. 3, 4: PCR product of *parC*$_{(G78D)}$ from pSV-9. (−); negative (PCR master mix), SL; Smart Ladder.

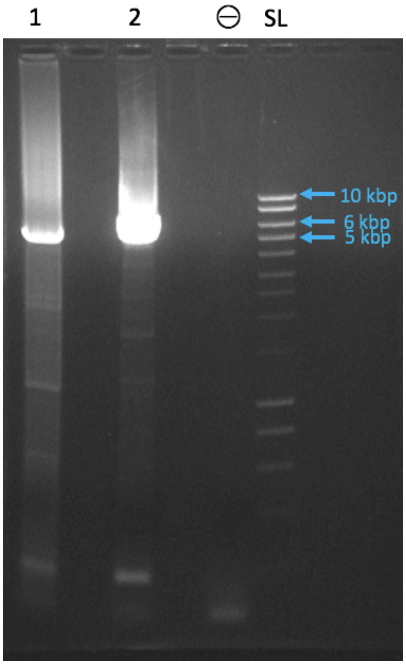

Figure A 9: Image of PCR products from plasmid pSV-8. (1 % agarose gel.) **Lane description:** 1, 2: PCR products K56-70-WT-*parC*-portion from pSV-8. (−); negative (PCR master mix), SL; Smart Ladder.

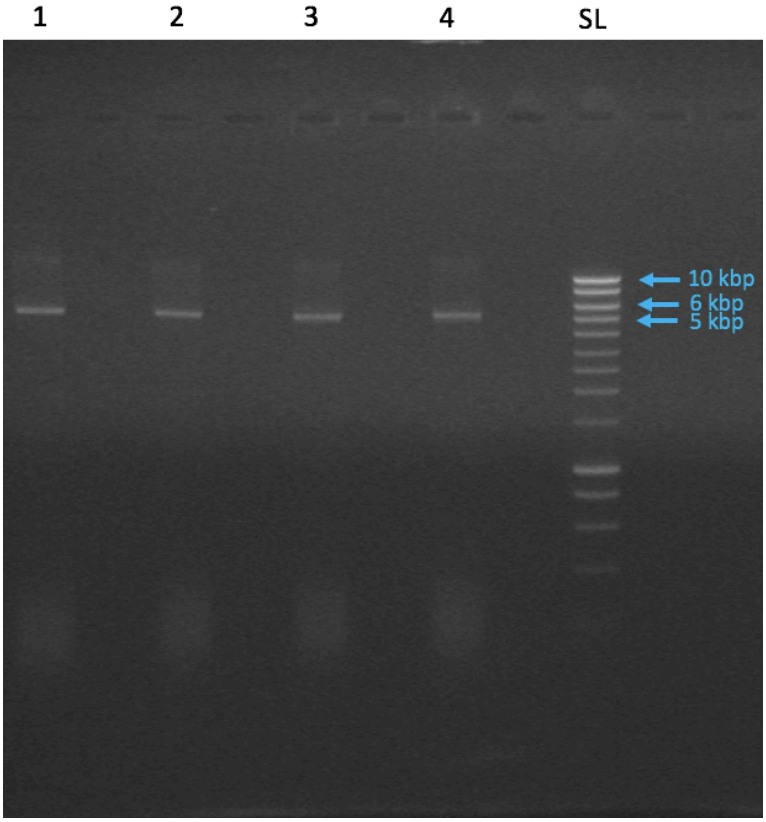

Figure A 10: Image of pDS132 after repeated digestion with *Xba*I. (1 % agarose gel.) **Lane description:** 1-4: pDS132 digested with *Xba*I, parallels #1-4. SL; Smart Ladder.

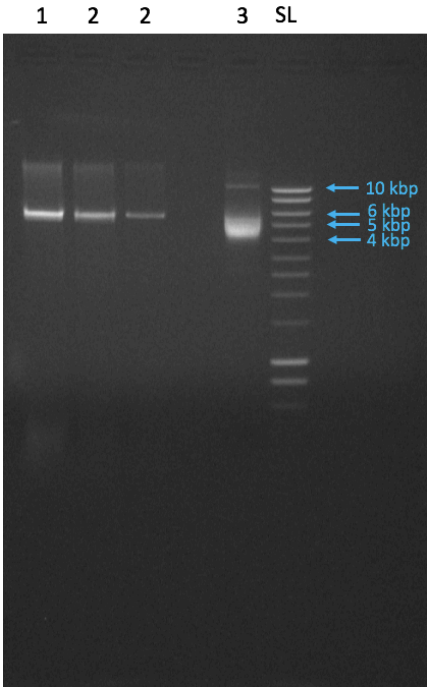

Figure A 11: Image after electrophoresis of expanded *Xba*I digest 4 µg plasmid and 6 hours incubation time. (1 % agarose gel.) **Lane description:** 1: *Xba*I-treated pDS132, parallel #1. 2: *Xba*I-treated pDS132, parallel #2. 3: Uncut pDS132. SL; Smart Ladder.

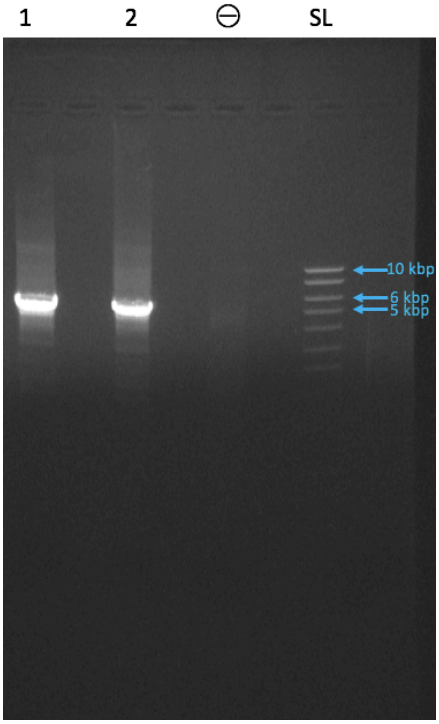

Figure A 12: Image of PCR products of pDS132. (1 % agarose gel.) **Lane description:** 1, 2: PCR products of pDS132, parallel #1 and #2. (−); negative (PCR master mix), SL; Smart Ladder.

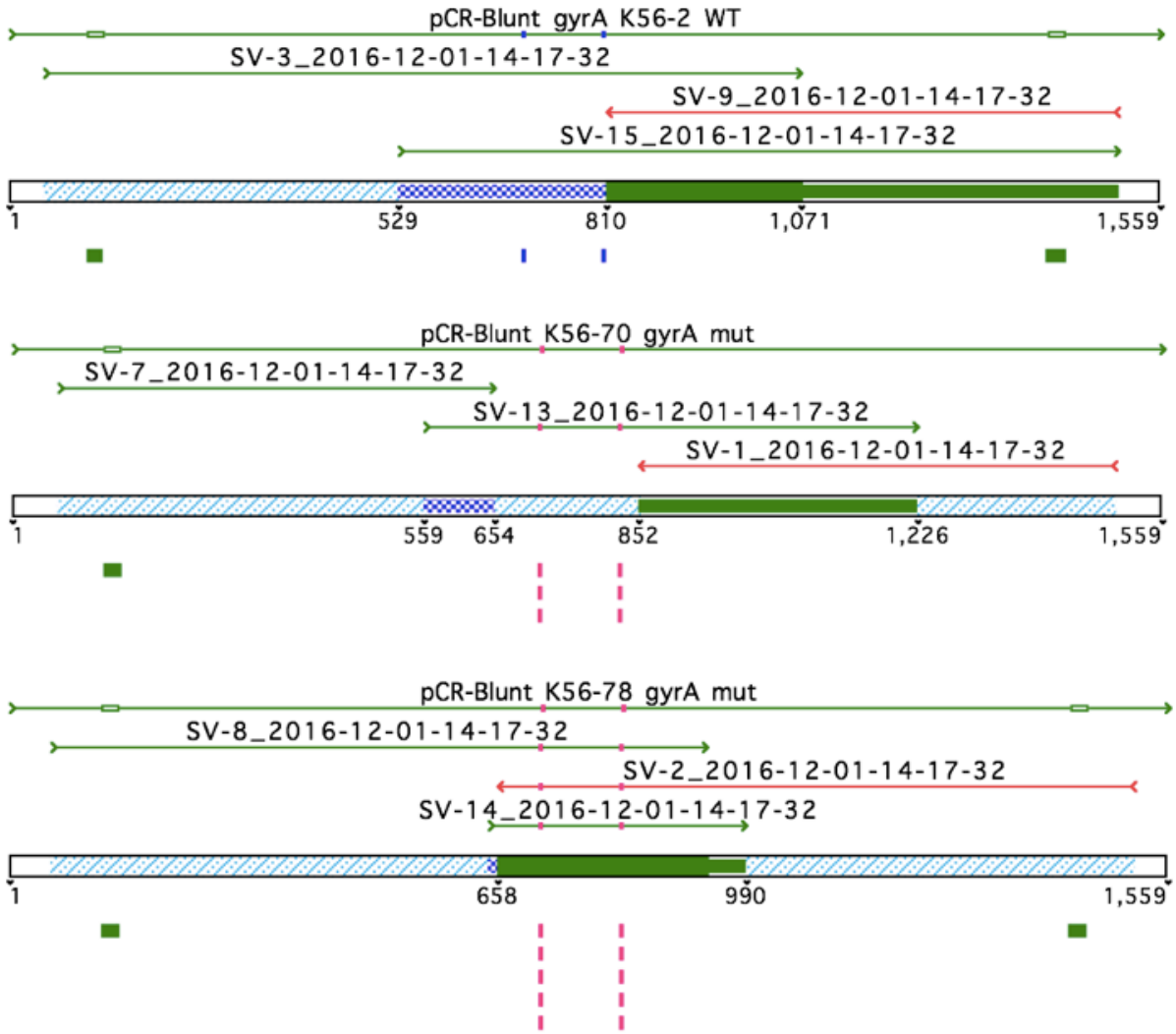

Figure A 13: Sequence results from pSV-13, pSV-19 and pSV-20. pCR-Blunt *gyrA* K56-2 WT: pSV-13, pCR-Blunt K56-70 *gyrA* mut: pSV-19, pCR-Blunt K56-78 *gyrA* mut: pSV-20. Analyzed with Sequencher software.

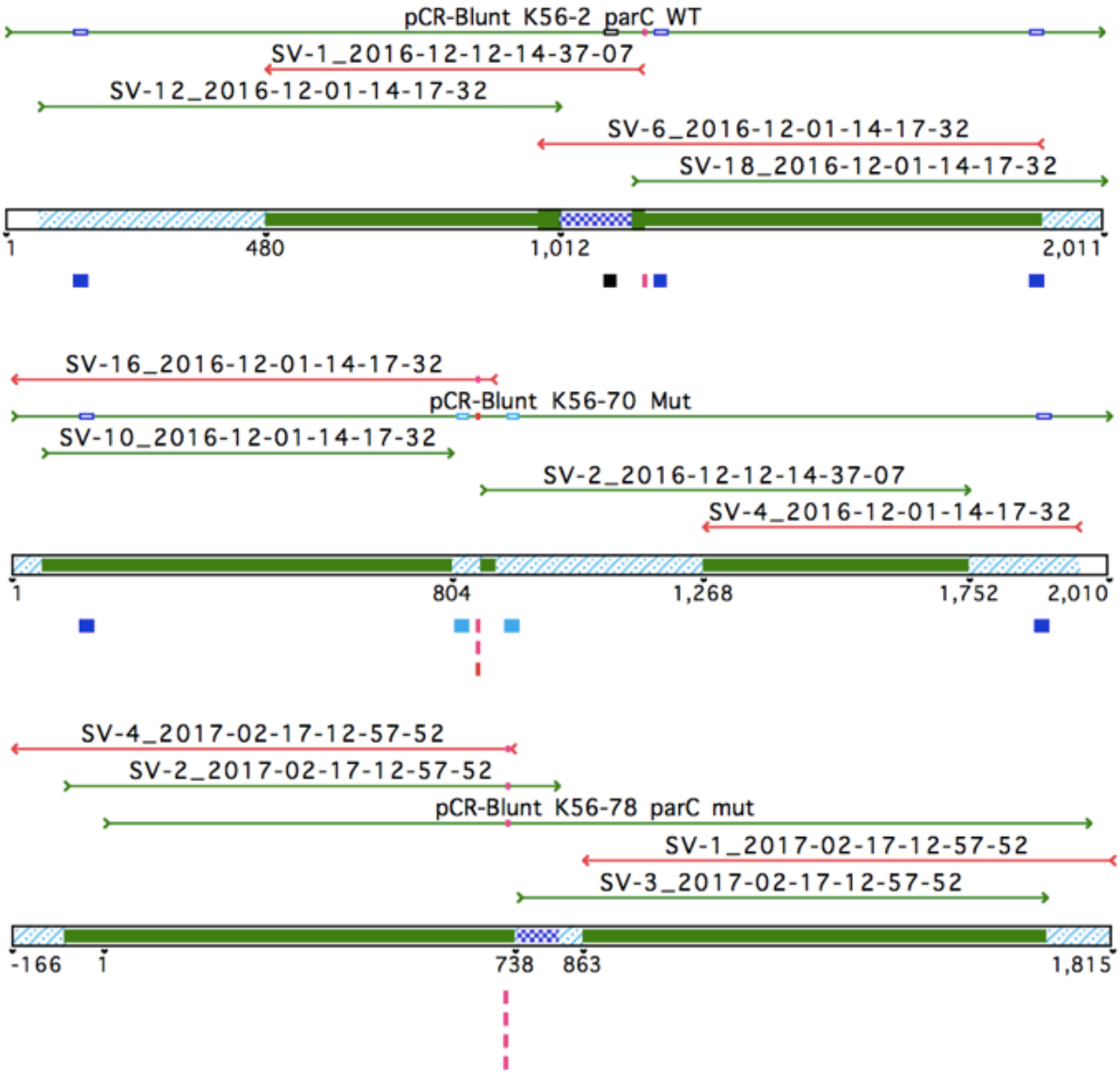

Figure A 14: Sequence results from pSV-15, pSV-21 and pSV-24. pCR-Blunt *parC* K56-2 WT: pSV-15, pCR-Blunt K56-70 *parC* mut: pSV-21, pCR-Blunt K56-78 *parC* mut: pSV-24. Analyzed with Sequencher software.